Fifth International Symposium on
Explosion, Shock Wave and High-strain-rate Phenomena
(ESHP 2016)

Conference Proceedings

25-28 September 2016, Beijing, China

Objective

The objective of the triennial international ESHP conferences is to create a forum where people involved in scientific research or industrial applications related to explosion, shock waves and high-strain-rate phenomena can meet and discuss results and ideas. The symposium is comprised of invited lectures and contributed presentations. Oral and poster presentations are arranged for the contributed presentations.

Topics

The symposium is planned to discuss the recent progress of theoretical, numerical and experimental researches on explosion, shock waves and high-strain-rate phenomena. The symposium covers the following general topics but the category is not limited: deflagration, detonation, and shock chemistry of energetic and reactive materials; shock wave and related phenomena in condensed and gaseous phases; response of materials and structures under high strain rates; production of materials by shock and detonation waves (shock induced phase transition and chemical reactions, explosive welding, shock modification,etc); innovative application of high-energy-rate phenomena. Additional contributions from related research areas are also welcome. The organizers of ESHP2016 would also like to organize three special sessions:

- **Session 1:** Shock Processing and Production of Materials,
  Organizers: Prof. Pengwan Chen & Prof. Kazuyuki Hokamoto
- **Session 2:** Numerical Simulation of Explosion and Impact,
  Organizers: Prof. Cheng Wang, Prof. Xiaowei Chen & Prof. Zoran Ren
- **Session 3:** Dynamic Behavior of Materials at High Strain Rates,
  Organizers: Prof. Yulong Li & Prof. Daniel Rittel
- **Workshop:** High Pressure Food Processing (HPFP),
  Organizers: Prof. Shigeru Itoh & Prof. Motonobu Goto

Organized by

State Key Laboratory of Explosion Science and Technology, Beijing Institute of Technology, China

Supporting Organizations

Explosive Mechanics Division, Chinese Society of Theoretical and Applied Mechanics, China

Explosion and Safety Division, China Ordnance Society, China

Collaborative Innovation Center of Safety and Protection, Beijing Institute of Technology, China

The National Natural Science Foundation of China (Grant 11221202), China

Institute of Pulsed Power Science, Kumamoto University, Japan

Section of Explosion and Impulsive Processing, Japan Explosive Society, Japan

Committee of the High-Energy-Rate Forming, Japan Soc. for Technol. of Plastic

The International Society of Multiphysics, Japan

Honorary Chairs

Shigeru Itho, Okinawa National College of Technology, Japan

Fenglei Huang, Beijing Institute of Technology, China

Co-chairs

Pengwan Chen, Beijing Institute of Technology, China

Kazuyuki Hokamoto, Kumamoto University, Japan

International Advisory Committee

Ang, H.G. (Singapore)	Balagansky, I. (Russia)	Ben-dor, G. (Israel)
Buchar, J. (Czech)	Deribas, A. (Russia)	Chen, X.W. (China)
Katayama, M. (Japan)	Kim, S.J. (Korea)	Li, X. (China)
Li, Y.L. (China)	Lu F.Y.(China)	Mamalis, A.G.(Greece)
Meng, Q.G. (China)	Moatamedi,M.(Norway)	Molinari, A. (France)

Orgnazing Committee

Scientific Committee

CONTENTS

ID001: Liquid Phase Explosive Fabrication of Superconducting MgB_2 Composites

A. Peikrishvili[1,3] , G. Mamniashvili[2], B. Godibadze[3]. T. Gegechkori[2], E.Chagelishvili[3]

[1]F.Tavadze Institute of Metallurgy and Materials Science, 15 kazbegi Av. 0130, Tbilisi, Georgia.

[2]Andronikashvili Institute of Physics Ivane Javakhishvili Tbilisi State University,
6, Tamarashvili St., 0177, Tbilisi, Georgia

[3]G.Tsulukidze Mining Institute, 7, Mindeli St., 0186, Tbilisi, Georgia,

E-mail: akaki.peikrishvili@stcu.int,

Abstract: An original two-stage liquid phase hot explosive compaction (HEC) procedure of Mg-B precursors above 900o C provides the formation of superconductivity MgB2 phase in the whole volume of billets with maximal Tc=38.5 K without any further sintering.

The liquid-phase HEC strongly solid-state reaction rate due to the high penetrating capability of shock-waves in a whole volume of cylindrical billets and to consolidate superconductive MgB_2 composites near to theoretical density. There were established that the structure and the superconductive characteristics of fabricated MgB2 billets strongly depends on consolidation temperature and intensity of loading.

The above mentioned and other features of structure/property relationship as well as experimental conditions will be presented and considered too.

Keywords: HTSC, MgB_2, Liquid-phase, Shock-assisted consolidation, Magnetometer.

ID002: Metal Jet Generation of the High-speed Oblique Collision for Similar/Dissimilar Metals

Mingdong Li[1] , Akihisa Mori[2, a] , Shigeru Tanaka[3], Kazuyuki Hokamoto[3]

[1]Graduate School of Engineering, Sojo University, Ikeda 4-22-1, Nishi-ku, Kumamoto 860-0082, Japan

[2]Sojo University, Ikeda 4-22-1, Nishi-ku, Kumamoto 860-0082, Japan

[3]Institute of Pulse Power Science, Kumamoto University, Kurokami 2-39-1, Chuo-ku, Kumamoto 860-8555, Japan

[a]makihisa@mec.sojo-u.ac.jp

Abstract: Explosive welding is known well as the method to weld strongly for the similar and dissimilar metal combinations. It is necessary to know the behavior of metals collided in this method, such as the metal jet generation and the welded interface, to achieve the good welding of difficult-to-weld materials. In the present work, the phenomena of the high-speed oblique collision which is same as the explosive welding were observed by using a single-stage powder gun and high speed video camera. It was succeeded to photograph a metal jet clearly with changing the collision angle and the collision velocity for the oblique collision of the similar and dissimilar metals, as shown Fig. 1.

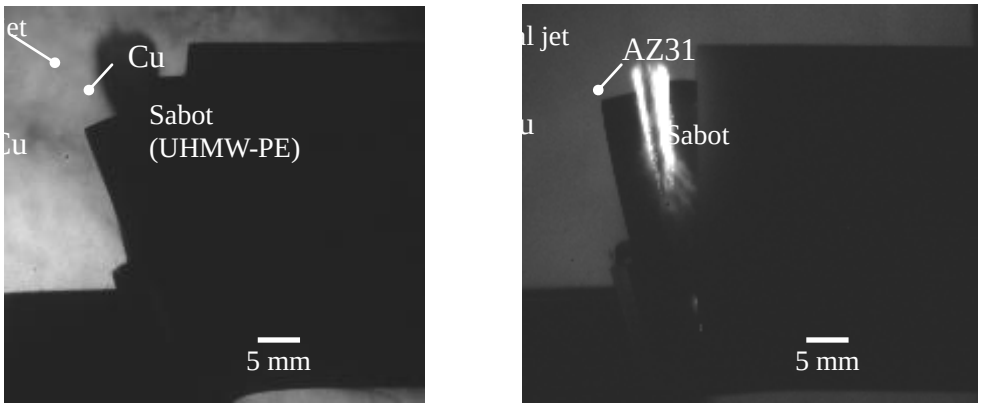

(a) Cu/Cu, V_p=627.1ms^{-1}, α = 20 ° (b) AZ31/Cu, V_p=530.1ms^{-1}, α = 15 °

Fig.1 Metal jet generation (5mm-thick and 32mm-diameter discs) (t = 8μs)

ID003: Consolidation of Cu–W Composites Combining SHS and HEC Technologies

B. Godibadze[1], S.V. Aydinyan[3,2], H.V. Kirakosyan[3], S.L. Kharatyan[3,2], A. Peikrishvili[1], G. Mamniashvili[4], E.Sh. Chagelishvili[1], D.R. Lesuer[5], M. Gutierrez.[6]

[1] G.Tsulukidze Mining Institute, Tbilisi, Georgia

[2]Yerevan State University, A. Manukyan str., 1, 0025, Yerevan, Armenia

[3]A.B. Nalbandyan Institute of Chemical Physics NAS RA, P. Sevak str., 5/2, 0014, Yerevan, Armenia,

[4] Jazvakhishvili Tbilisi State University, Andronikashvili Institute of Physics

[5] Lawrence Livermore National Laboratory, Livermore, CA, USA

[6]Technalia Research Institute, San Sebastian.

Spain Corresponding author e-mail: sofiyaaydinyan25@gmail.com

Abstract: The alloys of W-Cu have been growing industrial interest for superior thermal managing and as microwave materials due to the high thermal conductivity of copper and the low thermal expansion coefficient of tungsten [1]. W–Cu alloy parts are generally fabricated by Cu infiltration into W skeleton or liquid phase sintering of W–Cu powder mixtures [2]. However, because of the W–Cu system exhibits mutual insolubility, W–Cu powder compacts show very poor sinter ability [3]. The Physical-mechanical properties of the composite largely depend on both microstructure and composition relating to fabrication methods and synthesis conditions.

In this work a new approach for the preparation of Cu-W composite materials was proposed, the essence of which is the joint reduction of tungsten and copper oxides by energy saving combustion synthesis or self-propagating high-temperature synthesis (SHS process) method [4] using Mg+C mixture as combined reducer. The latter will allow controlling the reaction temperature in a wide range, and performing complete reduction of both oxides synthesizing W-Cu composite powders in a controllable combustion mode. The combustion experiments in the CuO-WO_3-xMg-yC quaternary system were performed based on the preliminary thermodynamic calculations made for that system, as well as considering the experimental results of binary and ternary systems. It was shown that at certain amount of reducers and slow propagation of combustion wave, it becomes possible the joint and complete reduction of both oxides. According to XRD analysis results, at optimal conditions combustion products contain only - W, Cu and MgO. After

the acid treatment (10%wt. HCl) of the product obtained at optimal conditions, it represents a desired W-Cu composite with particles submicron sizes. EDS analysis certifies the homogeneity of obtained W-Cu composite material with similar distribution of both metals.

W-Cu precursors developed by CS process were subjected to consolidation into cylindrical rods using hot explosive consolidation (HEC) technology and hot vacuum compaction (HVC) process. The consolidation temperature was changed up to 1000 ℃ at the shock wave loading intensity under 10 GPA. The investigations showed that fine W-Cu precursors obtained by combustion-coreduction process and their further explosive consolidation allows to fabricate high dense cylindrical billets near to theoretical density without cracks and uniform distribution of consisting phases. The consolidated samples are characterized with good integrity, which depends on the distribution and size of the W and Cu particles. It was further established that the electrical properties (resistance and dependence of the susceptibility) of the consolidated W-Cu composites are changed depending on phase content and density of the consolidated samples.

It was demonstrated that combination of CS and HEC undoubtedly has advantages compared to other technologies and may be considered as an alternative way to fabricate novel Cu–W composites with enhanced properties.

References

[1] Copper and Copper Alloys, By Joseph R. Davis, *ASM International*, 2001, p. 621.

[2] A. Ghaderi Hamidi, H. Arabi, S. Rastegari, *Int. J. Ref. Met. & Hard Mater.,* 29, 2011, 538–541.

[3] M. Amirjan, N. Parvin, K. Zangeneh-Madar, *Mat. Sci. & Eng. A*, 527, 2010, 6922–6929.

[4] A.G. Merzhanov, Mukasyan A.S., Combustion of solid flame, *Tonus Press*. Moscow. 2007.

ID004: Numerical Investigation of the Influence of Axial Length on Liquid-fuel Continuous Rotating Detonation Engine

Baoxing Li[1, a] , Chunsheng Weng[1, b]

[1]National Key Lab of Transient Physics, Nanjing University of Science and Technology, Nanjing ,210094, China

[a]bestlibaoxing@163.com, [b]wengcs@126.com

Abstract: The application of detonations for propulsion has received widespread attention recently. Compared with the conventional combustion mode, detonation is an extremely efficient combustion process, it contributes to higher strength, faster propagation speed, and higher thermal efficiency. Various ways have been used to control detonations in detonation-based engines, among which the continuous rotating detonation engine (CRDE) may be the most suitable for space launch due to its unique advantages compared to other detonation engines. In order to Two-dimensional Conservation Element and Solution Element(CE/SE) method is deduced to calculate the detonation process of continuous rotating detonation engines using gasoline as fuel, the effects of the axial length of combustor on the flow field and propulsive performance of CRDE are numerically investigated. Results show that the CE/SE method is quite efficient to capture discontinuities such as detonation waves, the flow field structure of the combustor (shown in Fig. 1) is qualitatively consistent with the experimental results of kerosene/air/oxygen mixture detonation. With the increase of axial length, the length of oblique shock wave increases, the fluctuation at exit is reduced, the peak values and average values of the exit pressure and exit density decline, while the peak values of the axial velocity first increase and then decline, the average values of the axial velocity increase. The centrifugal force leading to vibration is generated by the circumferential velocity at exit, thus the performance of CRDE is lost. With the increase of axial length, the circumferential velocity decreases, then the vibration weakens and the lost of the CRDE performance declines. In addition, the mass flux remains constant and is not influenced by the axial length of combustor. When the axial length increases, the flow field needs more time to reach quasi-steady state, the specific impulse first increases and then remains constant. Through the numerical investigation, the detonation process of the liquid-fuel CRDE may be better understood, and the numerical results provide guidance for experimental study.

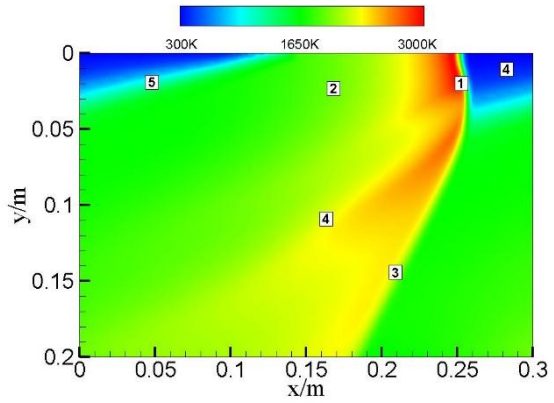

(a) Computational result

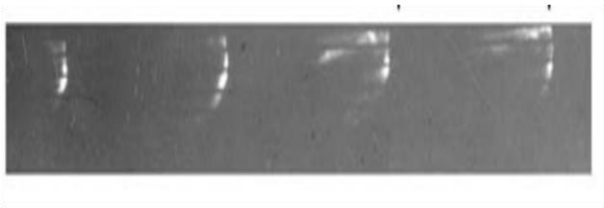

(b) Experimental result

Fig.1 The flow field structure of CRDE;1)is the detonation wave, 2) detonated products, 3) oblique shock wave, 4) the discontinuity between freshly detonated products and older products, 5) fresh mixture layer, 6).contact surface between fresh mixture and detonated products.

ID005: Experimental and Numerical Study on the Shock Response of a Cylindrical Shell under Pyroshock Loading

Bingwei Li[1, a], Xuejun Zhu[1], Xinzhong Fan[1], Yan Xia[1], Zijun Nangong[1]

[1]China Academy of Launch Vehicle Technology, Beijing 100076, China

[a]bingwei_li@yahoo.com

Abstract: The aerospace structures and equipment experience severe shock loading during the inter-stage separation, which is conducted by the high energy explosion of the pyroshock devices. Therefore, it is important to determine the shock response of the cabin structure, which is typically a cylindrical shell, under separation shock loading. The separation experiment of a cylindrical shell is performed, and the shell is cut into two parts along the circumferential direction by the flexible linear shaped charges. The influences of the charge amount and the distance from the explosive source on the response of the structure are investigated. The transient problem of the cylindrical shell under shock loading is also modeled and simulated numerically, using LS-DYNA. This research is helpful for the prediction of the shock response and the damage estimation of the shell structures under pyroshock loading.

ID006: Optical Method for Studying the Corner Turning Performance of TATB Based Polymer Bonded Explosive at Different Temperatures

Wei Cao, Yong Han, Xiangli Guo*, Jianlong Ran, Luchuan Jia, Xiaojun Lu

Institute of Chemical Materials, China Academy of Engineering Physics, Miangyang 621999, Sichuan, China

Abstract: To study the effect of temperature on propagation laws of detonation waves of explosives, the corner turning performance of TATB (triaminotrinitrobenzene) based polymer bonded explosive (PBX) was studied by mushroom test apparatus at three different temperatures.The breakout image was recorded by a high-speed rotating mirror streak camera, the first breakout angles, failure angles and delay times of hemispherical explosive were obtained. Results show that the first breakout angle, failure angle and delay time varied with the ambient temperature. The delay time was lower at lower ambient temperature. The temperature will influence the chemical reaction rate of hemispherical charge at the initiation stage.

Keywords: corner turning performance, temperature, optical method, TATB based PBX

* Corresponding author, email:guoxl@caep.cn

ID007: Preparation of ZirConium Dioxide Nanoparticles by Electrical Wire Explosion in the Air

Chucai Peng, Jinxiang Wang[a], Fujia Lu

Science and Technology on Transient Physics Laboratory, Nanjing University of Science and Technology, Nanjing, Jiangsu 210094, China

[a]wjx@njust.edu.cn

Abstract: Zirconium dioxide is an important ceramic with a variety of excellent properties including high melting point, high resistivity, high refractive index, low thermal expansion coefficient, etc. [1]. So it can be used to enhance the electrochemical stability of lithium ion battery [2], manufacture high-quality semiconductor [3] and improve the strength of hydroxyapatite bone cement [4]. Therefore, it is meaningful to search a high quality and efficiency preparation method for the broad application prospects and development potential of nanosized zirconium dioxide.

Electrical wire explosion (EWE) method is recently applied to produce nanosized powders, which is categorized in the gas phase methods [5]. There are studies on the dependences of the particle properties, productivity, and product yield of Zr upon the explosion conditions to optimize their selection in a device with a simpler separation system [6]. However, most of the researchers were focused on the stage after explosion. The process before explosion and the influence of deposited energy on particle properties were rarely discussed.

In this research, Zirconium dioxide nanoparticles were generated by electrical explosion of zirconium wire in the air. The current, voltage and deposited energy waveforms of wire explosion process were used to analyse the dynamics of particle formation. It was analysed that the arc discharge resulted in an explosion and stopped the energy deposition in wire. The oxidation reaction was completed in the stage of explosion expansion. The morphologies of synthesized nanoparticles were nearly spherical with diameters ranging from 1 nm to 100 nm, which were obtained by scanning electron microscopy and transmission electron microscope. The phase compositions of crystallites determined by the x-ray diffraction shows that the ratio of the tetragonal and monoclinic phases increase with the increasing charging energy of storage capacitor.

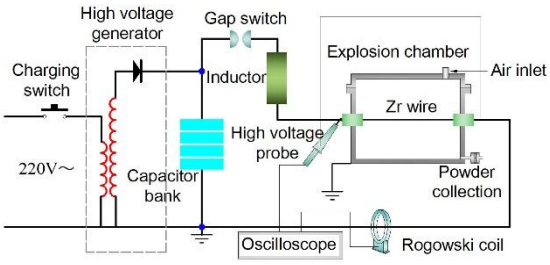

Fig. 1 Schematic diagram of the experimental setup

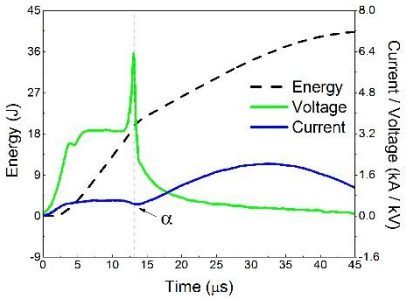

Fig. 2 Typical voltage, current and deposited energy waveforms across a Zr wire during explosion

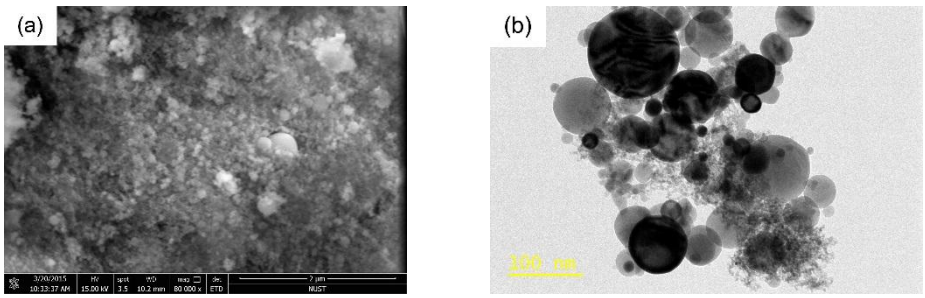

Fig. 3 (a) SEM and (b) TEM images for samples obtained by zirconium wire explosion in the air

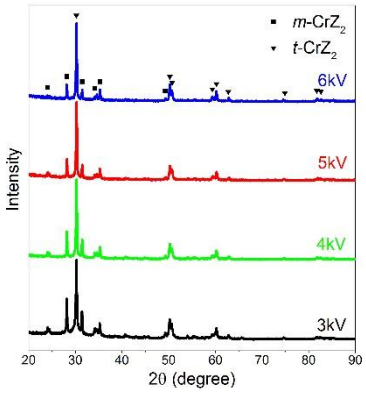

Fig. 4 XRD patterns for samples obtained with zirconium wire explosion in the air

Table 1 Phase composition and average crystalline size of explosion products

Charging voltage (kV)	Phase composition (Mass %)		Average Size (nm)	
	m-ZrO_2	*t*-ZrO_2	*m*-ZrO_2	*t*-ZrO_2
3	38.9	61.1	62.7	30.6
4	32.2	67.8	66.7	35.8
5	26.6	73.4	67.3	36.2
6	21.1	78.9	69.4	43.5

Acknowledgments

This work was supported by the National Natural Science Foundation of China (11272158) and the Natural Science Foundation of Jiangsu Province (BK20151353)

References

[1] X. Li, Y. Yu and Y. Meng: *ASC Appl. Mater. Inter.* Vol. 5 (2013), pp1414

[2] Z. Li, T. Chen and Y. Liao: *Ionics* Vol. 21 (2015), pp2763

[3] K. Tang, J. Zhang, W. Yan, Z. Li, Y. Wang, W. Yang, Z. Xie, T. Sun and F. Harald: *J. Am. Chem. Soc.* Vol. 130 (2008), pp2676

[4] W. Yu, X. Wang, J. Zhao, Q. Tang, M. Wang and X. Ning: *Ceram. Int.* Vol. 41 (2015), pp10600.

[5] C.H. Cho, S.H. Park, Y.W. Choi and B.G. Kim: *Surf. Coat. Tech.* Vol. 201 (2007), pp4847

[6] A.V. Bagazeev, Yu.A. Kotov, A.I. Medvedev, E.I. Azarkevich, T.M. Demina, A.M. Murzakaev and O.R. Timoshenkova: *Nanotechnologies in Russia* Vol. 5 (2010), pp656

ID008: Analysis on the Ballistic Trajectory of Normal Penetration of a Rigid Projectile into Concrete Targets Based on Meso-scopic Model

Yongjun Deng[1,2, a] , Xiaowei Chen[1,2 b] , Yong Yao[2], Tao Yang[2]

[1]Institute of Systems Engineering, China Academy of Engineering Physics, P.O.Box 919-416, Mianyang 621999, Sichuan, China

[2]School of Civil Engineering and Architecture, Southwest University of Science and Technology, Mianyang 621000, Sichuan, China

[a]516341369@qq.com, [b]chenxiaoweintu@yahoo.com

Abstract: Due to the high strength and excellent durability, concrete has been wildly used in many fundamental constructions.The concrete structure would bear not only the static and earthquake loading but also the anti-penetration and blasting effects in the war and terrorist attack. Penetration process is a problem of transient contact that projectile interact with target. Nowadays, many studies have been conducted by means of the theoretical, simulation and experiment analysis [1-5]. In the present study, the random model of three-phase heterogeneous composite was used in the modeling of concrete, which consists of aggregate, cement hydrates and the Interfacial Transition Zone (ITZ) around aggregates [6]. Both the uniform model and mesoscopic model of concrete was used in the numerical simulation to analyze the normal penetration mechanism of rigid projectile（Fig.1）. And the ballistic trajectory deflexion was studies by the mesoscopic composition analysis.

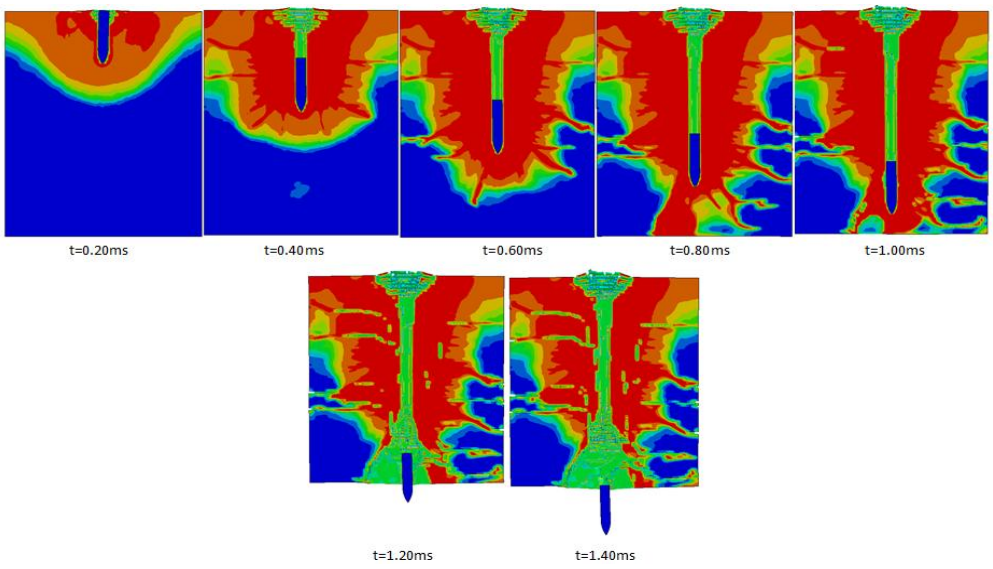

(a) Concrete target with uniform model

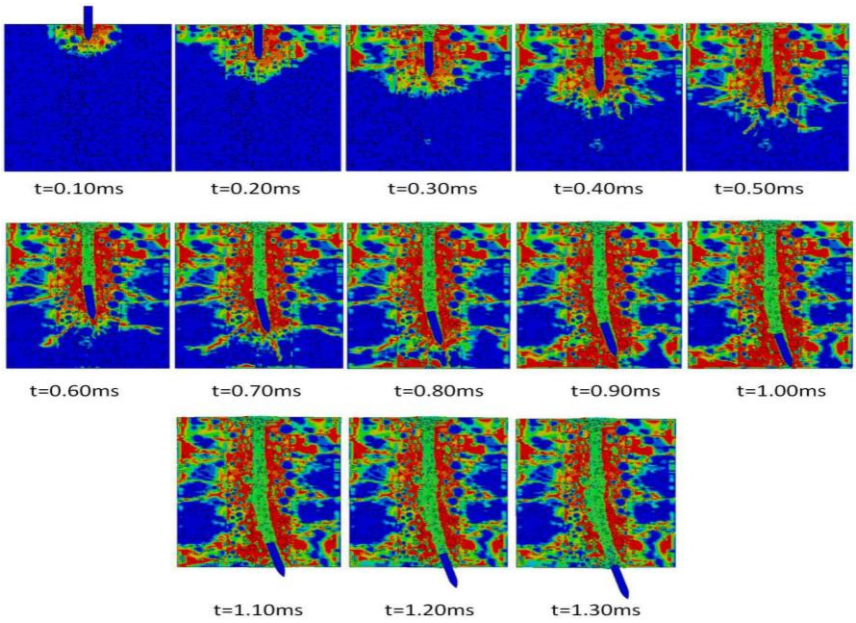

(b)Concrete target with mesoscopic model

Fig.1 Comparision of penetration process of uniform model and mesoscopic model

References

[1] Backmann ME, Goldsmith W. The mechanics of Penetration of projectiles into targets[J]. Int J Engng Sci, 1978, 16: 1-99

[2] Goldsmith W. Review: Non-ideal projectile impact on targets[J]. Int J Impact Engng, 1999, 22: 95-395

[3] Li, QM, Reid SR, Wen HM, Telford A R. Local impact effects of hard missiles on concrete targets[J]. Int J Impact Engng, 2005, 32(1-4): 224-284

[4] Forrestal MJ, Frew DJ, Hickerson JP, et al. Penetration of concrete targets with deceleration-time measurements[J]. Int J Impact Engng, 2003, 28(5):479-497

[5] Chen Xiao-wei. Advances in the penetration/ perforation of rigid projectiles[J].Advance in mechanics. 2009, 39(3): 316-351

[6] Wang ZM, Kwan AKH, Chan HC. Mesoscopic study of concrete I: Generation of random aggregate structure and finite element mesh[J]. Computers and Structures, 1999, 70: 533-544

[7] He Xiang,Xu Xiang-yun.etc.Experimental investigation on projectiles' high-velocity penetration into concrete targets[J].Explosion and Shock Waves. 2010, 30(1):1-6

[8] Li Zhi-kang, Huang Feng-lei.A dynamic spherical cavity-expansion theory for concrete materials[J].Explosion and Shock Waves.2009, 29(1):95-100

ID009: Effects of Solution Temperature on Dynamic Mechanical Properties and Adiabatic Shear Sensitivity of Ti-5Mo-5V-8Cr-3Al

Ding Wang[1, ,2, a], Lin Wang[1, 2, b], Huaxiang Dai[1, 2], Haiming Tao[3]

[1]National Key Laboratory of Science and Technology on Materials under Shock and Impact, Beijing Institute of Technology, Beijing 100081, China

[2]School of Materials Science and Engineering, Beijing Institute of Technology, Beijing 100081, China

[3]Powder Metallurgy and Special Materials Research Department, Beijing General Research Institute for Non-ferrous Metals, Beijing 100088, China

[a]st901127@163.com, [b]linwang@bit.edu.cn

Abstract: Titanium alloy was widely used in the aerospace industry owing to its low density, high strength and corrosion resistance [1,2]. Metastable β titanium alloy Ti-5Mo-5V-8Cr-3Al was used in solid rocket engine shell, pressure vessels, star-shaped connectors and rivets, screws [3]. However, it was inevitable for titanium alloy being subjected to impact loads in their serving conditions. Given this, the dynamic responses including dynamic mechanical properties of titanium alloy under high strain rate became very important. Recently, the investigations on Ti-5Mo-5V-8Cr-3Al alloy were extensively in certain aspects. But the influence of heat treatment on the dynamic mechanical has not been studied in details. Therefore, the influence of heat treatment on the dynamic properties of Ti-5Mo-5V-8Cr-3Al titanium alloy was systemically investigated in this work.

The Ti-5Mo-5V-8Cr-3Al alloy plates was aging treated in this study. The value of Mo equivalent was 22.2. The beta-transus temperature determined by differential scanning calorimetry (DSC) was 1027 K. The alloy was solution treated at 973 K, 1003 K, 1073 K and 1093 K for 30 mins, followed by air cooling. Then, each sample was aging treated at 813 K for 480 mins, followed by air cooling. The results of dynamic compression tests which using Split Hopkinson Pressure Bar (SHPB) indicated that, the dynamic strength of Ti-5Mo-5V-8Cr-3Al alloy improved when the solution temperature was lower than 1073 K. The results of dynamic shear tests showed that, the adiabatic shear sensitivity decreased with the solution temperature increased when the solution temperature was lower than 1073 K, the sample of 1073 K solution and aging treated presented the best

resistance of adiabatic shear.

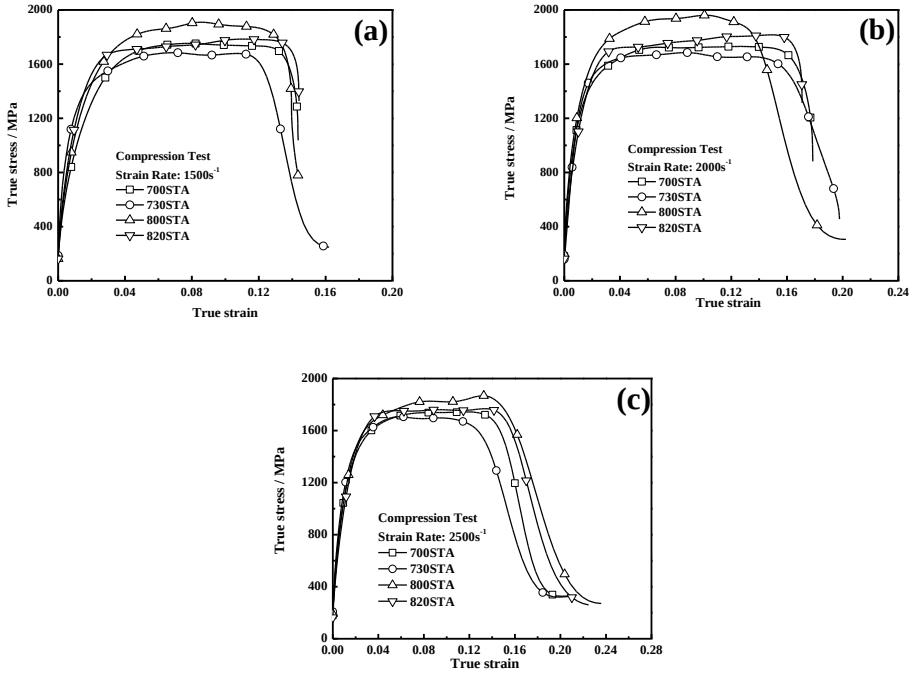

Fig.1 Typical dynamic true stress-strain curves for Ti-5Mo-5V-8Cr-3Al alloy under compression loading: (a) 1500s^{-1}; (b) 2000s^{-1}; (c) 2500s^{-1}

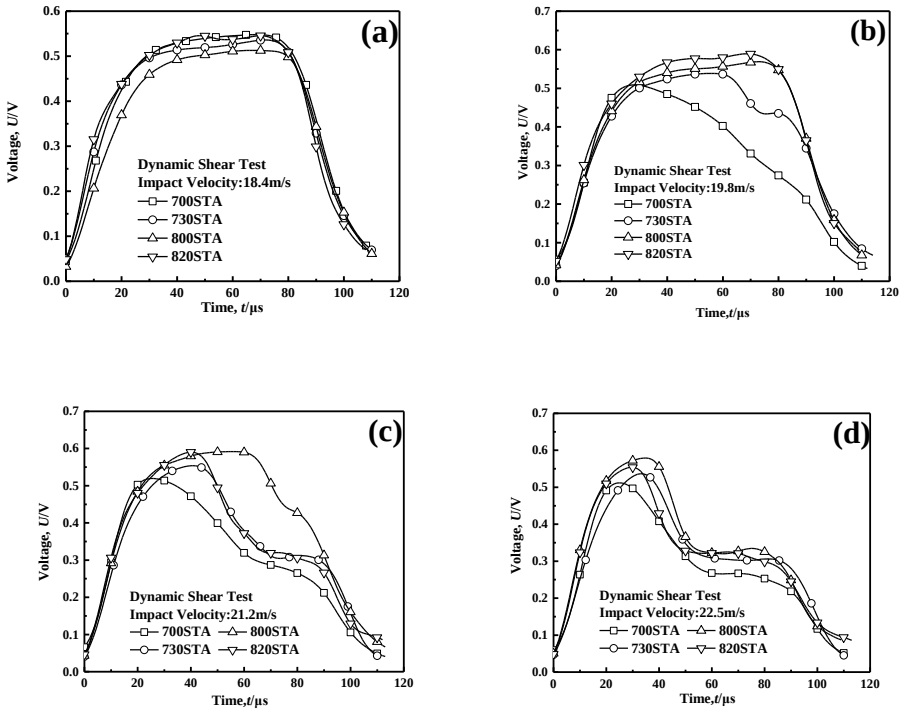

Fig.2 Typical voltage-time curves of dynamic shear test for Ti-5Mo-5V-8Cr-3Al alloy under compression loading: (a) 18.4 m/s; (b) 19.8 m/s; (c) 22.2 m/s; (d) 22.5 m/s

References

[1] R. Boyer and R. Briggs. *Journal of Materials Engineering and Performance* 14, (2005), pp681-685.

[2] W. Brewer, R. Bird, and T. Wallace. *Materials Science and Engineering A* 243, (1998), pp299-304.

[3] D. Yang, Y. Fu, S. Hui, W. Ye, Y. Yu and E. Liang. *Chinese Journal of Rare Metals* 35, (2011), pp575-580.

ID010: Effect of Post Weld Heat Treatment on Al 5052-SS 316 Explosive Cladding with Different Interlayers

E. Elango[1*], S. Saravanan[1], K.Raghukandan[2]

[1]Department of Mechanical Engineering, Annamalai University, Tamilnadu, India.

[2]Department of Manufacturing Engineering, Annamalai University, Tamilnadu, India.

[1*]eelango69@gmail.com,[1]ssvcdm@gmail.com,[2]raghukandan@gmail.com

Abstract: In explosive cladding, the chemical energy released from an explosive pack is employed to develop a metallurgical bond between two similar or dissimilar metals. This study focuses on effect of post weld heat treatment (PWHT) on interfacial and mechanical properties of Al 5052-SS 316 explosive clad at varied loading ratios and inclination angles. The use of interlayer is proposed for the control of kinetic energy loss to alleviate the formation of intermetallic compounds at the interface. Vickers hardness variation along the thickness of the sample was measured and type of intermetallic compounds formed at the interface is investigated by optical microscope (OM) and Scanning electron microscope (SEM). The post clad Al 5052-SS 316 clads are subjected to PWHT of 300^0C-450^0C and the results are presented. Increase in PWHT temperature enhances the tensile strength of the composite, whereas, the tensile strength decreases at elevated temperatures due to the diffusion of Al and Fe elements and the formation of detrimental intermetallic compounds.

Keywords: Explosive cladding, dissimilar metals, PWHT, intermetallic, strength

Corresponding author: E.Elango
Research Scholar, Department of Mechanical Engineering,
Annamalai University, Tamilnadu, India
Email: eelango69@gmail.com

ID011: Improving the Scent of Citrus Junos Tanaka (Yuzu) Juice Using Underwater Shockwave Pretreatment

Eisuke Kuraya[1*], Atsushi Yasuda[2,3], Akiko Touyama[1], and Shigeru Itoh[1]

[1] National Institute of Technology, Okinawa College, Japan

[2] Graduate School of Science and Technology, Kumamoto University, Japan

[3] Osaka Sanitary Co. Ltd., Japan

[*]Corresponding author: kuraya@okinawa-ct.ac.jp

Citrus fruits are widely cultivated in regions between the tropical and temperate zones, and they are some of the most important commercial crops. *Citrus junos* Tanaka (yuzu), a sour fruit, is cultivated mainly in Japan and Korea. In Japan, its annual production amounted to approximately 25,000 ton in 2009. Yuzu has a strong characteristic aroma compared to that of other citrus fruits, and its juice is widely used in Japanese foods. In the standard juicing process, high pressure is applied to the flavedo and/or albedo of the yuzu fruit, resulting in the extraction of ascorbic acid and flavanone glycosides into the juice. Owing to the high pressures employed, over-extraction of the bitter components (e.g., naringin, neohesperidin, and limonoids) often occurs; therefore, the pressure must be carefully controlled.

In shockwave-treated plants, the cell structures are split and crushed, resulting in multiple cracks generating on the cell walls through spalling destruction [1]. The effect of the instantaneous high pressure produced by the conventional mixer blending extraction method contributes to increased yields of the tomato saponin, esculeoside A, from tomatoes [2] and increased extraction efficiency of lipophilic gingerols and shogaols from ginger [3]. In a recent study, we showed that multiple cracks generated by underwater shockwaves acted as a permeation pathway, increasing the extraction ratio of essential oils in steam distillation processes [1]. This observation indicated that the implementation of an underwater shockwave treatment as a preprocessing step was useful in the extraction of functional components from food materials. In this presentation, we introduce a novel application of this pretreatment process, resulting in the improvement of the scent of yuzu fruit juice. We also evaluated the contents of volatile compounds present in the juice to determine whether such a pretreatment method affected its characteristics.

The processing equipment for the pretreatment of the yuzu fruit using underwater shockwaves was developed, consisting of a pressure vessel, high voltage power supply unit, and a high voltage regulator. The high voltage power supply generated energy up to 6.4 kJ; an underwater shockwave was generated instantaneously within the vessel by electrical discharge. A whole yuzu fruit was placed in a silicone tube, which was separated from the source of shockwave generation, and subjected to the instantaneous high-pressure load produced by the underwater shockwave. This processing equipment continuously produced an instantaneous high-pressure impulse force, which crushed the cell walls within the yuzu sample. Based on prior study [4], pressure produced by the shockwave generator at 4.9 kJ was 40 MPa. The samples were subjected to the high pressure produced by the underwater shockwave discharge of 2.5 kJ or 4.9 kJ.

The materials were subjected to shock wave pretreatment or left untreated before squeezing, and the juice was extracted by hand pressing using a hand-operated citrus juicer. The volatile compounds in the juice were analyzed by head-space gas-chromatography-mass spectrometry, and identified by the peak areas and mass spectrometry libraries. We identified 20 compounds in the juice, and the major compounds detected were limonene (72.5%), γ-terpinen (14.7%), β-phellandrene (4.1%), myrcene (1.9%), β-pinene (1.8%), α-pinene (1.1%), and linalool (1.1%).

Employing shock wave pretreatment at 4.9 kJ resulted in an increase in the contents of the most abundant compounds in the juice, compared to those obtained from the untreated yuzu, by a factor of 10.6. Moreover, contents of trace compounds such as β-phellandrene, myrcene, and α-pinene also increased, along with the major compounds. This treatment could also improve the beneficial properties of the juice, as determined by the analysis of the functional compounds such as ascorbic acid and flavanon glycosides. These results suggested that the flavor of the juice could be extracted more effectively through underwater shockwave preprocessing treatments.

Acknowledgements

This study was part of the project “A Scheme to Revitalize Agriculture and Fisheries in Disaster Area through Deploying Highly Advanced Technology” by the Ministry of Agriculture, Forestry and Fisheries, Japan.

References

[1] E. Kuraya, Y. Miyafuji, A. Takemoto, and S. Itoh: *Transaction of the Materials Research Society of Japan* 39 (2014), pp447-449.

[2] H. Manabe, A. Takemoto, H. Maehara, M. Ohno, Y. Murakami, S. Itoh, and T. Nohara: *Chemical and Pharmaceutical Bulletin* 59 (2011), pp1406-1408.

[3] H. Maehara, T. Watanabe, A. Takemoto, and S. Itoh: *Materials Science Forum* 673 (2011), pp215-218.

[4] O. Higa, R. Matsubara, K. Higa, Y. Miyafuji, T. Gushi, Y. Omine, K. Naha, K. Shimojima, H. Fukuoka, H. Maehara, S. Tanaka, T. Matsui, and S. Itoh: *International Journal of Multiphysics* 6 (2012), pp89-98.

ID012: Numerical Simulation of CL-20 Underwater Explosion Performance of Shock Waves and Pulsating Bubble Phenomena

Song Feng, Guoning Rao, Jinhua Peng

Department of Safety Engineering, School of Chemical Engineering, Nanjing University of Science and Technology, 200 Xiaolingwei St., Nanjing 210094, Jiangsu, China
E-mail: fs8500@126.com

Abstract: This paper describes numerical methodology to model and investigates the shock waves and bubble dynamics produced by an underwater explosion when it happens under limited waters. The nonlinear dynamics results were calculated by ANSYS-AUTODYN explicit software. CL-20 was studied as basic research object in underwater test. It was shown that pressure and impulse histories for simulation are in good correspondence with the data calculated by empirical formula. The results calculated by empirical formula and AUTODYN was compared in order to corroborate the accuracy of numerical results.

Keywords: AUTODYN, CL-20, underwater explosion, shock waves, bubbles.

ID013: Fabrication of Carbon Encapsulated ZrC Nanoparticles by Electrical Explosion Method

Fujia Lu, Jinxiang Wang[a], Chucai Peng

Science and Technology on Transient Physics Laboratory, Nanjing University of Science & Technology, Nanjing 210094, Jiangsu, China

[a]wjx@njust.edu.cn

Abstract: Carbon-coated nanomaterials have broad application prospects in the field of energy, magnetic storage, chemical catalysis and bio-medical. Generally, carbon-coated nanomaterials can be fabricated by different methods such as arc discharge [1], pyrolysis [2], CVD [3] and detonation [4] et al. In this paper, the method of electrical explosion of metal wire in organic liquid was adopted to prepare carbon encapsulated nanoparticles. In the medium of absolute ethyl alcohol, under the high-voltage pulse current (HVPC), the high purity zirconium wire became fusion, gasification, expansion and explosion and then nanoparticles will form. The energy, voltage and current in the experiments were measured to analyze the influence of them on the products. The products were analyzed by X-ray diffraction technique (XRD), transmission electron microscopy (TEM) and high power transmission electron microscopy (HTEM). The results show that the carbon encapsulated Z_rC nanoparticles were fabricated successfully. The diameter range between 10nm-150nm. For the voltage of 4kv, 8kv and 12kv, the average size of the products is 24.9nm, 41.4nm and 43.9nm, respectively.

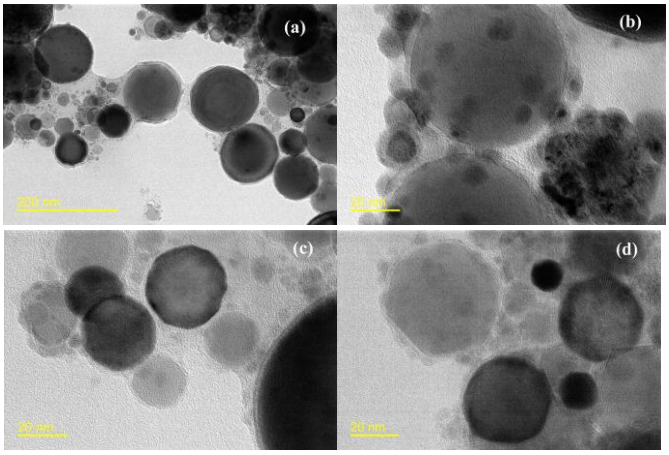

Fig. 1 (a) the TEM image that zirconium wire exploded at 8kv voltage . (b), (c), (d) is the HRTEM images that zirconium wire exploded at 4kv, 8kv and 12kv voltage, respectively.

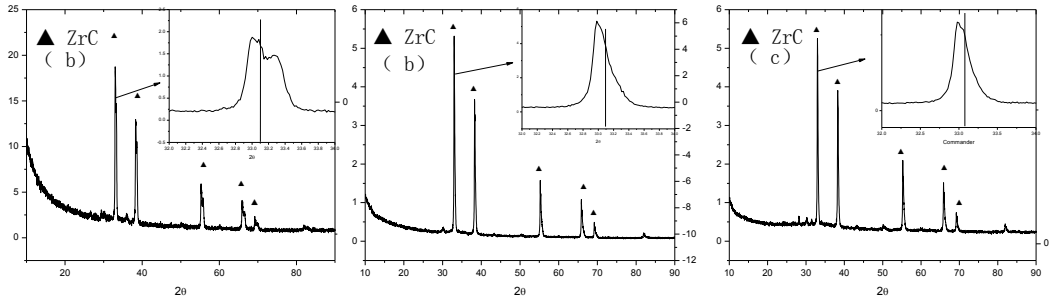

Fig. 2. (a), (b), (c) is the XRD spectrums of products fabricated under 4kv, 8kv and 12kv voltage, respectively.

Acknowledgments

This work was supported by the National Natural Science Foundation of China (11272158) and the Natural Science Foundation of Jiangsu Province (BK20151353)

References

[1] Shi G M, Zhang Z D, Yang H C: *Journal of Alloys & Compounds*, 384(2004), pp296-299

[2] Nong, Deng, Wang: *Chinese Chemical Letters*, 18(2007), pp487-490

[3] Lei Zhongxing, Liu Jing, Li Xuanke: *Magnetic Material and Equipment*, 34(2003), pp4-6

[4] Sun Guilei, Li Xiaojie, Yan Honghao. *The Eighth National Conference of Explosion*.2007

ID014: Dynamic Shear Response and Evolution Mechanisms of Adiabatic Shear Band in Ultrafine-grained Fe and Austenite-ferrite Duplex Steel

Fuping Yuan[1, a] , Xiangde Bian[1] , Ping Jiang[1], Muxin Yang[1], Xiaolei Wu[1, b]

[1]State Key Laboratory of Nonlinear Mechanics, Institute of Mechanics, Chinese Academy of Sciences, No. 15, North 4th Ring, West Road, Beijing 100190, China

[a]fpyuan@lnm.imech.ac.cn, [b]xlwu@imech.ac.cn

Abstract：The dynamic properties of an ultrafine-grained (UFG) Fe and an intercritically annealed 0.2C5Mn steel with UFG austenite-ferrite duplex structure were studied under dynamic shear loading. The formation and evolution mechanisms of adiabatic shear band (ASB) were then investigated using interrupted experiments at different shear displacements and the subsequent microstructure observations. The evolutions of ASB in both materials were found to be a two-stage process, namely an initiation stage followed by a thickening stage. The shear bands in both materials consist of two regions at the thickening stage: a core region and two transition layers. The increased micro-hardness in ASB and TEM observations inside ASB for UFG Fe indicate that grains in the shear band are further refined. The dynamic shear plastic deformation of the 0.2C5Mn steel was observed to have three stages: the strong linear hardening stage followed by the plateau stage, and then the strain softening stage associated with the evolution of ASB. High impact shear toughness was found in this 0.2C5Mn steel, which is due to the following two aspects: the strong linear strain hardening by martensite transformation at the first stage, and the suppressing for the formation of shear band by the continuous deformation in different phases through the proper stress and strain partitioning at the plateau stage. When the adjoining matrix is localized into the transition layers for the 0.2C5Mn steel, the grains are refined along with increasing fraction of austenite phase by inverse transformation. However, when the transition layers are transformed into the core region for the 0.2C5Mn steel, the fraction of austenite phase is decreased and almost disappeared due to martensite transformation again. These interesting observations in the core region and the transition layers should be attributed to the competitions of the microstructure evolutions associated with the non-uniformly distributed shear deformation and the inhomogeneous adiabatic temperature rise in the different regions of shear band. The 0.2C5Mn TRIP steel reported here can be considered as an excellent candidate for energy

absorbers in the automotive industry.

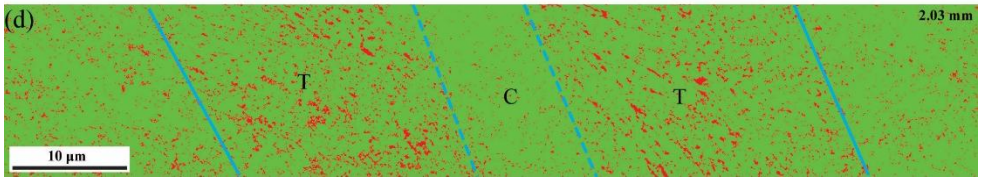

Fig.1 The phase distribution maps by EBSD within ASB for the 0.2C5Mn steel. The red area is for austenite phase and the rest area is for ferrite and martensite phases. "C" denotes the core region and "T" denotes the transition layers.

References

[1] F.P. Yuan, P. Jiang, and X.L. Wu: *International Journal of Impact Engineering* 50 (2012) pp1-8

[2] F.P. Yuan, X.D. Bian, P. Jiang, M.X. Yang and X.L. Wu: *Mechanics of Materials* 89 (2015), pp47-58

ID015: Numerical Study on Influence of Block Material on Lateral Effect of PELE

Gan Li[1, a] , Zhijun Wang[1, b]

[1]School of Mechanical and Electrical Engineering, North University of China, Taiyuan 030051, China

[a]xinren1210@163.com

[b]wzj@nuc.edu.cn

Abstract：PELE (Penetrator with Enhanced Lateral Effect) is a new type of ammunition based on physical effects [1-2], it is mainly used for light armored targets and concrete works. Large diameter PELE is used to carry out the opening of the brick wall, concrete and reinforced concrete and infantry can from the opening into the interior to suppress enemy during the street-fighting. This paper make a primary study on progress of PELE penetrating concrete target, explore the influence of materials on process of PELE penetration into concrete target, and provide some reference for the practical work of PELE. The method of numerical simulation is adopted in this paper.

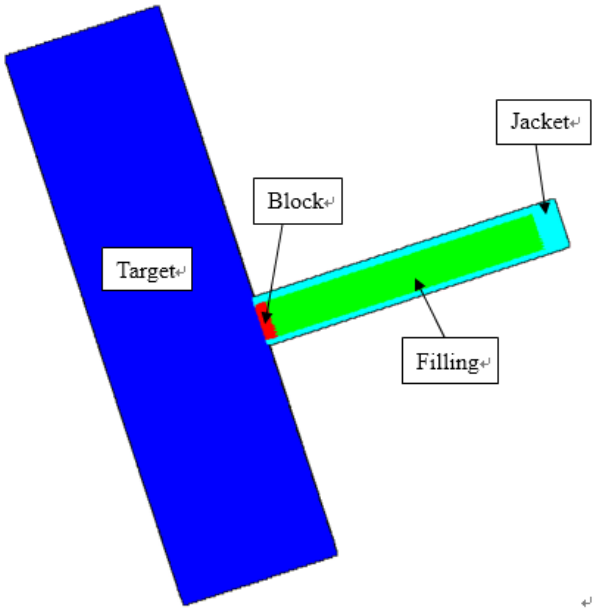

Fig.1 Numerical model for the AUTODYN simulation

References

[1] Paulus G, Schirm V: *International Journal of Impact Engineering*, 33(2006), pp566-579

[2] Jimmy Verreault: *International Journal of Impact Engineering*, 76(2015), pp196-206

[3] YIN Jian ping, WANG Zhi jun, WEI Ji yun: *Journal of Ballistics*, Vol.22 No.1(2010), pp79-82

[4] ZHU Jian sheng, ZHAO Guo zhi, DU Zhong hua, WANG Xian zhi: *Explosive and Shock Waves*, Vol.29, No.3 (2009), pp281-288

[5] YE Xiao jun, DU Zhong hua, HU Chuan hui, TANG You hui, ZHANG Yue-lin: *Chinese Journal of Explosives & Propellants*: Vol.35 No.4 (2012), pp86-90

[6] YE Xiao-jun，DU Zhong-hua，YAO Fang-tang: *Journal of Energetic Material*: Vol.22 No.5 (2014), pp612-616.

[7] FAN Shaobo, CHEN Zhigang, GUO Guangquan, HOU Xiucheng, CHEN Dongmei: *Ordnance Material Science and Engineering*: Vol.35 No.5 (2012), pp47-50.

[8] XU Li-zhi, DU Zhong-hua, WANG De-sheng, WEN Rui-qing, HU Yun-chao: *Journal of Ballistics*: Vol.28 No.1 (2016), pp70-75.

ID016: Assessment of Ballistic Performance of Silicon Carbide Tiles Against Tungsten Alloy Long Rod Projectile

Goh Wei Liang[1,2,a], Luo Boyang[1,b], Zeng Zhuang[1], Tan Eng Beng Geoffrey[2], Ng Kee Woei[2] and Yuan Jianming[1]

1 Temasek Laboratories, Nanyang Technological University, 50 Nanyang Drive, Singapore 637553, Singapore

2 School of Materials Science and Engineering, Nanyang Technological University, Singapore 639798, Singapore

[a]gohwl@ntu.edu.sg,

[b]byluo@ntu.edu.sg

Abstract： Four different grades of Silicon Carbides (SiC) from 3M were investigated with respect to their ballistic performance against tungsten alloy long rod projectile using module test method. This study provided a comparison of the ballistic performance of different SiC tiles under actual armour application conditions, i.e. a finite thickness backing, lateral confinement, and a thin cover plate. The metal-encapsulated ceramic armour modules were tested against 96g tungsten alloy long rod projectiles at a nominal velocity of 1250 m/s. A witness block was placed behind the test module. The ballistic performance was compared using the measurement of depth-of-penetration (DOP) in the witness blocks. The grades of SiC assessed were Grade F, Grade F-plus, Grade T, and Grade T-plus respectively where the F series were solid state sintered to achieve higher hardness while T series were liquid phase sintered to achieve higher fracture toughness. The plus indicated that the ceramics were post hot isostatic pressed (HIP) to achieve further densification and increased bending strength. The F series SiC performed better than T series while the post-HIP SiC performed better than their non-post HIP counterparts. The results showed that the increase in hardness and flexural strength of SiC enhanced the ballistic performance.

ID017: Experimental Study on the Failure Behaviors of Polyethylene Reinforced Cross-ply Laminates Impacted by a Conical-head Projectile

Guangyan Huang[1,*], Wei Zhu[1], Guangyan Liu[2], Shunshan Feng[1]

[1]State Key Laboratory of Explosion Science and Technology, Beijing Institute of Technology, Beijing 100081, China

[2]School of Aerospace Engineering,Beijing Institute of Technology, Beijing 100081, China

[1]huanggy@bit.edu.cn,

[2]gliu@bit.edu.cn,

[1]ju16wave@163.com

Abstract: Ultra-high molecular weight polyethylene (UHMWPE) fiber reinforced polymer matrix composites have been widely employed into anti-ballistic armor systems because of their high ratio of longitudinal strength to density [1]. Failure mechanisms of the composites impacted by a sphere projectile have been studied, including indirect tension and membrane stretching [2]. In this study, Dyneema® UHMWPE fiber reinforced cross-ply laminates (HB26) with four kinds of thickness ranging from 2 to 8 mm were impacted by a 12 mm diameter, 90 ° conical-head projectile. The ballistic limits for these laminates decreased in order: 8 mm, 2 mm, 6 mm, and 4 mm. The unconventionally high ballistic limit for 2 mm laminates was attributed to much more serious plastic bulging because of membrane stretching, compared with the thicker laminates. However, the absorbed energy for the laminates impacted at projectile velocities higher than the ballistic limits basically increased with the panel thickness. Ply lateral displacement and perforations with ‘round-star’ shape were observed. These failure characteristics were consistent with the low penetration resistance of the laminates impacted by the conical-head projectile compared with that impacted by other blunter-head projectiles. The laminates showed higher penetration resistance impacted obliquely compared with the normally impact results at similar initial velocities, which provided an alternative way to design high-performance composite armors with UHMWPE laminates.

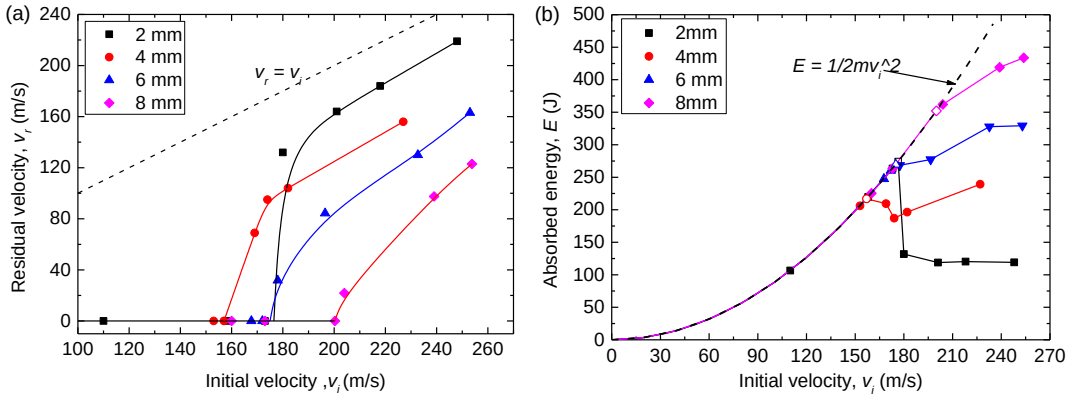

Fig.1 (a) The residual velocity and (b) the absorbed energy for differ-thickness HB26 laminates plotted as functions of the initial velocity of the projectile.

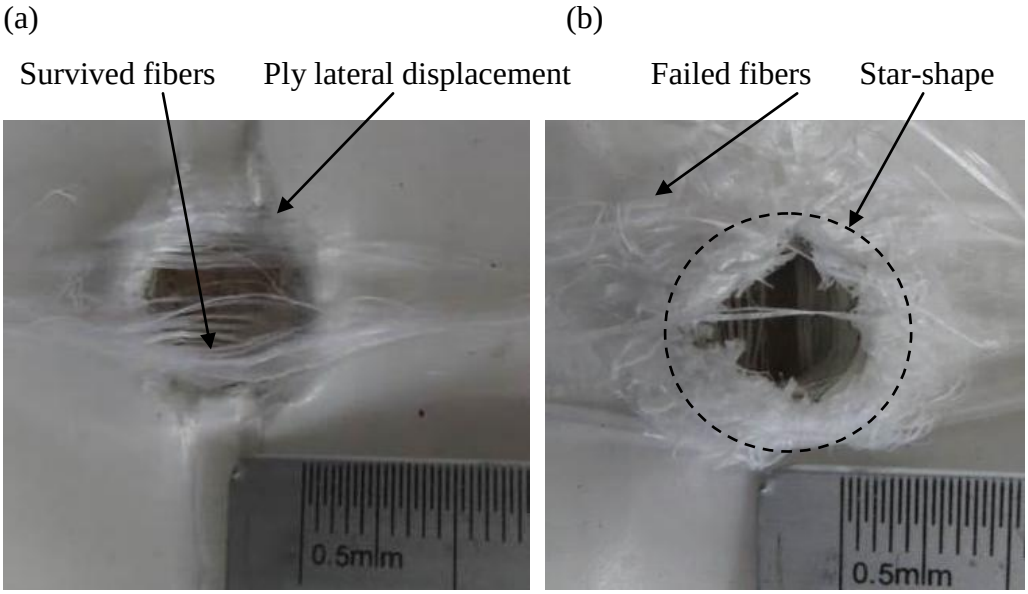

Fig.2 The (a) front view and (b) back view of the perforation in a 4mm thick HB26 laminate impacted at the initial velocity of 169 m/s

References

[1] L. Iannucci, D. Pope. High velocity impact and armor design [J]. EXPRESS Polymer Letters, 2011, 5 (3): 262-272.

[2] M. R. O' Masta a, V. S. Deshpande. Mechanisms of penetration in polyethylene reinforced cross-ply laminates [J]. International Journal of Impact Engineering, 2015, 86: 249-264.

ID018: Synthesis of WC1-x in Liquid Paraffin Using Metal Wire Explosion with Process Measurements

H. Oda[1a], N.Yokota[1], S.Tanaka[2], and K.Hokamoto[2]

[1]Graduate School of Science and Technology, Kumamoto University, 2-39-1 Kurokami, Chuo-ku, Kumamoto 860-8555, Japan

[2]Institute of Pulsed Power Science, Kumamoto University, Kumamoto, Japan

[a]164d8509@st.kumamoto-u.ac.jp

Abstract: Tungsten carbide is widely used in industries as a cutting tool because, it has high melting point, high hardness, high modulus elasticity and wear resistance. WC_{1-x} also considered as a good superconducting material and electrode catalyst [1]. Therefore in the present study, a novel method is proposed to synthesize WC_{1-x} using wire explosion technique.

In the current investigation, WC_{1-x} was synthesized in liquid paraffin as a source of carbon using wire explosion. When a high rate energy was injected by a pulse with high current, tungsten will get superheated and evaporates with an explosion. This phenomenon makes tungsten to react with carbon easily. In this study, energy of 10kJ is added to tungsten wire from a condenser. Tungsten wire of diameter 0.3mm having lengths of 100mm and 200mm also, diameter of 0.5mm having lengths of 100mm and 200mm were used in the study.

The experimental results indicate that WC_{1-x} can be synthesized under liquid paraffin. To analyze the synthesized WC_{1-x}, X-ray diffraction (XRD) and Scanning Electron Microscope (SEM) were used. In order to look at the phenomena, optical observation was carried out by using high speed video camera and voltage measurement was also done at the same time. The energy which it was given during the tungsten explosion was clarified.

Reference

[1] Yang Gao, Xiaoyan Song, Xuemei Liu, Chongbin Wei, Habin Wang, Guangsheng Guo: On the formation of WC1-x in nanocrystalline cemented carbides, Scripta Materialia 68(2013), pp108-110

ID019: Numerical Simulation of Explosive Forming Using Detonating Fuse

Hirofumi Iyama[1, a] , Yoshikazu Higa[2, b] , Masatoshi Nishi[1], Shigeru Itoh[3]

[1]Dept. of Mech. and Intel. Sys. Eng., Natl. Inst. of Tech., Kumamoto Col., 2627 Hirayamashin-machi, Yatsushiro, Kumamoto 866-8501 Japan.

[2]Dept. of Mech. Sys. Eng., Natl. Inst. of Tech., Okinawa Col., 905 Henoko, Nago, Okinawa 905-2192, Japan.

[3]Prof. Emeritus, Kumamoto Univ. & Natl. Inst. of Tech., Okinawa Col.

[a]eyama@kumamoto-nct.ac.jp,

[b]y.higa@okinawa-ct.ac.jp

Abstract: In National Institute of Technology in Japan, the food processing device using the underwater shock wave has developed [1]. The processing mechanism is crushing with the spalling phenomenon of shock wave. The effect is extraction improving, softening, sterilizing etc. with non-heating. The pressure vessel for crushing for the processing of the variety foods has been designed and manufactured. We need a pressure vessel for food processing by underwater shock wave. We propose making the pressure vessel by the explosive forming. Only a few of these pressure vessels will be made. One design suggestion of the pressure vessel made of stainless steel was considered. The pressure vessel is needed that the length, thickness and depth of it were 500mm, 8mm and 200mm, respectively. It is possible that a metal plate is formed with simple supporting parts. However, the forming shape is depend on the shock pressure distribution acting on the metal plate. This pressure distribution is able to change by the shape of explosive, mass of explosive and the shape of pressure vessel. The numerical simulation was carried out. Two kinds of numerical simulation models are considered. One is a model to compare with pressure profile by an experiment. Another is the explosive forming model. The explosive was detonating fuse (is described as ‘DF’). The distance between DF and the stainless steel plate was 50mm. We know the special quality about the explosion of DF. An equation of state of the pressure and the specific volume which can often indicate its special quality is used. The equation of state (is described as EOS) was JWL (Jones-Wilkins-Lee) EOS [2]. All models were calculated as plane strain and symmetrically. Basement of simulation method was ALE (Arbitrary Laglangian-Eulerian) method [3], because on the numerical simulation is able to solved the interaction between

liquid and structure. Mie-Grüneisen EOS [4] was used as the equation of state which can solve the shock properties of water. Because the metal plate is involved high strain rate, Johnson-Cook Equation as material model [5] included the effect of strain rate was applied in this simulation.

References

[1] K. Shimojima, Y. Miyafuji, K. Naha, O. Higa, R. Matsubara, K. Higa, Y. Higa, T. Matsui, A. Takemoto, S. Tanaka, H. Maehara, and S. Itoh: *The International Journal of Multiphysics*, Vol.6, No. 4(2012), pp.355-364.

[2] E. Lee, M. Finger, and W. Collins: *Lawrence Livermore National Laboratory report* UCID-16189(1973).

[3] N. Aquelet, M. Souli, and L. Olovsson: *Application to slamming problems, Computer methods in applied mechanics and engineering*, 195(2006), pp. 110-132.

[4] G. McQueen, S. P. Marsh, J. W. Taylor, J. N. Fritz, and W. J. Carter: *High-Velocity-Impact Phenomena* (1970), p.230.

[5] M. A. Meyers: *Dynamic Behavior of Materials*(1994),pp. 327-328.

ID020: Research on the Synthesis of Carbon-coated Cu Nanoparticles by Gaseous Detonation Method

Honghao Yan[1], Bibo Zhao[1], Tiejun Zhao[1], Xiaojie Li[1,a], Yang Wang

[1]State Key Laboratory of Structural Analysis for Industrial Equipment, Dalian University of Technology, Dalian, 116024, China

[a] dlutpaper@163.com

Abstract: Using acetylacetone copper as precursor, H_2 and O_2 are used as the explosive source, and Cu @ C core / shell nanoparticles with the grain size below 10nm are synthesized by the method of gaseous detonation. Under the condition of satisfying the negative oxygen balance, the influence of hydrogen, oxygen ratio toward the generated carbon-coated Cu nanoparticles can be explored by varying the amount of explosive gas. XRD, Raman spectroscopy and TEM are adopted to test the generated products, and found that the best result can be achieved when the hydrogen oxygen ratio is close to 2: 1. This conclusion has provided reference for the selection of explosive gas ratio of carbon-coated Cu nanoparticles that synthesized by gaseous detonation method.

Keywords: gaseous detonation, Cu @ C core / shell structure, nanoparticles

ID021: Study on Test Method of Frictionfactor for Energetic Materials and on Factors Influencing Explosive Sensitivity

Hua Cheng[1,2] , Huang Heng-jian[1,2]

1. Institute of Chemical Materials, CAEP, Mianyang 621900, China

2. Robust Munitions Center, CAEP, Mianyang 621900, China

Email**:** huac1988@126.com

Abstract: A new machine and method for testing a series of friction factors between Energetic Materials with rubbers and some material was reported in this paper. The relations between friction factor and H50 was also explored , the principle and results of the test of friction factor among plastic, rubber and explosive were reported.

Using the instrument, assigned mainly to test the frictionfact between plastic, rubber and explosive and to test the frictional temperature, test the friction factors. The instrument consisted of a normal pressure sensor and a moment of torsion sensor, mechanical system and a velocity adjustable system. The measure extend of the pressure sensor was 0～300kgf and 0～2N.m for the moment sensor. The relative precision of them is 5‰.

In the test, usually madeΦ10×4mm sample frictionize with rubber or other materials that was rounding, except in few testing of friction factor, other size of the sample may be used. Meanwhile the results of friction factors were measured by the instrument. the friction factors between the two materials was calculated, according to the principle of moment equation, namely the moment of torsion equated to the frictional moment. There are varies hypothesis in the load distribution on the working surface of frictional sample. Usually, two hypothesis, namely cosine distribution load and even load distribution was used.

Let Q_m, μ, h and S express melt latent, friction factors, hardness respectively, and spreading coefficient. Melt latent heat and hardness of additives as well as friction factors between additives and RDX, spreading coefficient for additives on RDX affect the sensitivity of explosives. So these data was obtained to find this influence. The value of critical height H_{50} was measured by carster Drop Hammer (the weight of Drop Hammer is 5kg, the weight of sample is 50mg)

Then the relations of them can be assumed according to contributions of these

parameters to H_{50}.in the last, we gave a function between them. The following function can be assumed according to contributions of these parameters to H_{50}.

$$H_{50} = f(Q_m, \mu, h, S) = k\frac{Q_m^a S^b}{\mu^d h^e} + c$$

Here, k and c are constants , k=0.27, c=6.58; a, b, d, and e are 0.37, 1.86, 0.10, 0.30

Keywords: energetic material, frictionfactor, calculating method

ID022: "β-to-α" Phase Transformation and Dynamic Mechanical Properties of Ti-10V-2Fe-3Al with Different Heat Treatments

Huaxiang Dai[1, a], Lin Wang[1, b], Ding Wang[1], Anjin Liu[1]

[1]National Key Laboratory of Science and Technology on Materials in Impact Environment, School of Material Science and Engineering, Beijing Institute of Technology, Beijing 100081, China

[a]daihuaxiang9199@163.com,

[b] Linwang@bit.edu.cn

Abstract: Titanium alloys mostly deform by twinning, deformation-induced martensite, dislocation glide on slip planes or even their combination [1]. Ti-10V-2Fe-3Al is a typical metastable beta titanium alloy, in which the retained meta stable β phase may transform to stress induced orthorhombic martensite, α″, when subjected to an external stress [2]. Dynamic mechanical properties and "β-to-α"" phase transformation of Ti-10V-2Fe-3Al with different heat treatments were studied in this paper, in which Split Hopkinson Pressure Bar (SHPB) technique was employed. The β transus temperature was measured to be 785±5℃, and the heat treatments were shown in table 1.

Table 1 Heat treatments list

Piece number	Heat treatments procedure
ST1	830℃/1h/AC
ST2	830℃/1h/OQ
ST3	830℃/1h/WQ

Optical microstructures of Ti-10V-2Fe-3Al alloy after different heat treatments are shown in Fig.1. The only difference among heat treatments is cooling mode, the optical microstructures, however, are significantly different as we can see from the pictures. There is a mass of fine α phase appeared inside β matrix when the specimen was air cooled, as indicated by arrows in Fig.1 (a). But when the cooling mode turned into oil quenching, the morphology of α completely disappeared and the only thing we can see are equiaxed β coarse grains (Fig.1 (b)). As the cooling velocity further increased, namely employing water quenching, there are some quenching martensite (α or α″ laths) generated inside β matrix (Fig.1 (c)). In a word, the cooling mode, also corresponding cooling velocity, has a great influence on microstructures of Ti-10V-2Fe-3Al alloy.

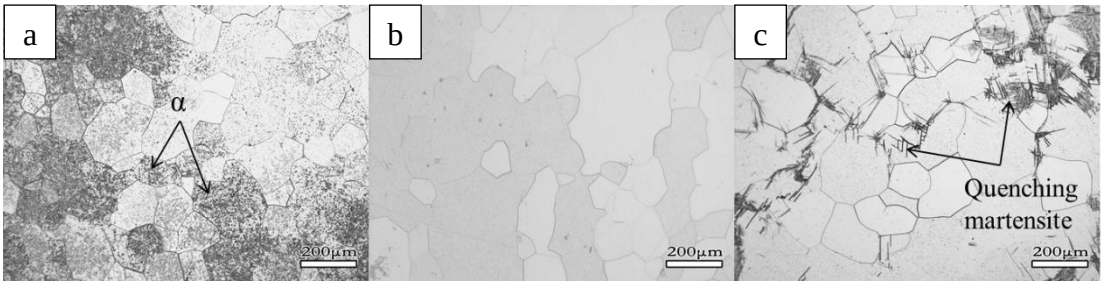

Fig.1 Optical microstructure of the Ti-10V-2Fe-3Al samples with different heat treatments: (a)ST1; (b)ST2; (c) ST3

Fig.2 shows optical images of Ti-10V-2Fe-3Al after being loaded by SHPB, and the strain rate is all about 2000s^{-1}. There are many α″ laths appeared inside β matrix in all three kinds of specimens. In addition, the amount of α″ laths generated in air cooled specimens is apparently less than the ones cooled by oil quenching and water quenching.

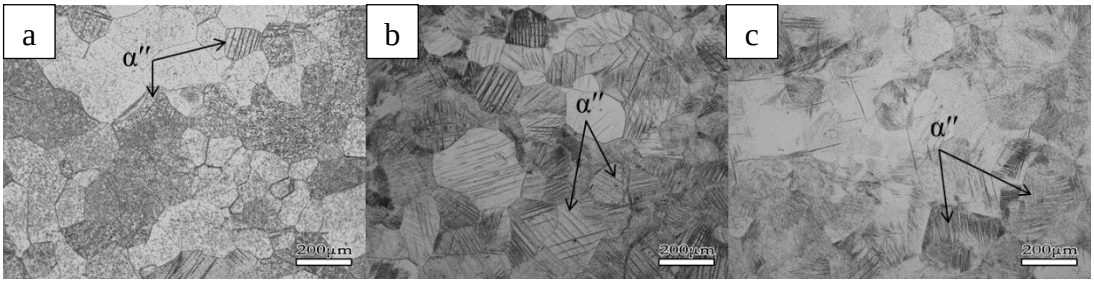

Fig.2 Optical microstructure of the Ti-10V-2Fe-3Al samples loaded by SHPB: (a)ST1 2000s^{-1}; (b)ST2 2000s^{-1}; (c) ST3 2000s^{-1}

The dynamic compression true stress-strain curves of Ti-10V-2Fe-3Al alloy are shown in Fig.3, and the strain rates are all about 2000s^{-1}.The yield strength of ST1 is 1501MPa, as indicated in the curves, which is much higher than the ones of ST2 and ST3, 850MPa and 895MPa respectively. That is mainly because a great quantity of fine α phase appeared inside β matrix in ST1 after heat treatment, and thus the second phase strengthening effect improved the mechanical properties of Ti-10V-2Fe-3Al.

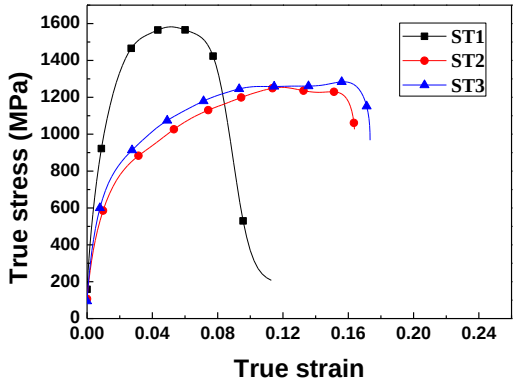

Fig.3 True stress-strain curves of the Ti-10V-2Fe-3Al alloy.

References

[1] Grosdidier T, Combres Y, Gautier E, et al. Effect of microstructure variations on the formation of deformation-induced martensite and associated tensile properties in a β metastable Ti alloy[J]. Metallurgical & Materials Transactions A, 2000, 31(4):1095-1106.

[2] Duerig T W, Albrecht J, Richter D, et al. Formation and reversion of stress induced martensite in Ti-10V-2Fe-3Al[J]. Acta Metallurgica, 1982, 30(12):2161-2172.

ID023: Study of the Dynamics of Size of Particles During Trinitrotoluene Detonation by VEPP-4M Synchrotron Radiation

Rubtsov I.A.[1,4, a] , Ten K.A.[1,4 b] , Pruuel E.R.[1,4], Kashkarov A.O.[1,4], Titov V.M.[1,4], Tolochko B.P.[2,4], Zhulanov V.V.[3,4], Shekhtman L.I.[3,4]

[1]Lavrentyev Institute of Hydrodynamics SB RAS, Novosibirsk 630090, Russia

[2]Institute of Solid State Chemistry and Mechanochemistry SB RAS, Novosibirsk 630090, Russia

[3]Budker Institute of Nuclear Physics SB RAS, Novosibirsk 630090, Russia

[4]Novosibirsk State University, Novosibirsk 630090, Russia

[a]rubtsov@hydro.nsc.ru,

[b]ten@hydro.nsc.ru

Abstract: In this work, we carried out small angle x-ray scattering (SAXS) measurements during detonation of cast trinitrotoluene (TNT) charges of different diameter (30 and 40 mm). Registration of SAXS signal during detonation of high explosives (HEs) allows one to measure the distributions of density. In the case of oxygen-deficient HEs, it is related with the carbon condensation process.

Our experiments with use of synchrotron radiation (SR) were carried out at the SYRAFEEMA (Synchrotron Radiation Facility for Exploring Energetic Materials) station at the accelerating complex VEPP-4M (Budker Institute of Nuclear Physics, Russia, Novosibirsk). This new station (built in 2015) allows one to increase the mass of the explosive charges by 10 times (up to 200 grams) in comparison with the similar station “Extreme states of matter” at the previous accelerating complex VEPP-3 [1].

We also carried out computer simulations of SAXS using real x-ray spectrum. We took into account the spectrum of viggler radiation, TNT absorption and absorption of the DIMEX-3 detector. Comparison of simulated and measured SAXS distributions allowed us to recover the dynamics of average size of nanoparticles behind the detonation front using the “pink” SR beam.

Similar experiments have been conducted at Advanced Photon Source (Argonne National Laboratory, USA). These studies have shown hexanitrostilbene detonation produces carbon particles with radius of gyration of 2.7 nm, which corresponds to the 7 nm diameter of spherical particles, which was registered in 400 ns after detonation front

and remained constant for following several microseconds. It should be noted that small charges of 6 mm in diameter were used in their study [2]. Dynamics of carbon condensation in large charge is more actual problem.

Earlier, the dynamics of carbon nanoparticles growth at detonation of different oxygen-deficient HEs was obtained in [1]. For all HEs there is identical dependence: initial size ≈ 2 nm, then it increased and further remained to constant. The size of particles increased up to ≈ 5 nm within ≈ 1.5 μs for press charge of TNT of 20 mm in diameter.

We observe that the time of nanoparticles growth behind the chemical reaction zone depends on size of initial charge. It increase with increase in diameter of charge.

This work was supported by Russian Foundation for Basic Research (project No. 16-29-01050).

References

[1] K.A. Ten, V.M. Titov, E.R. Pruuel, A.O. Kashkarov, B.P. Tolochko, Yu.A. Aminov, B.G. Loboyko, A.K. Muzyrya and E.B. Smirnov: *Proceedings Fifteenth International Detonation Symposium*, pp. 369-374

[2] M. Bagge-Hansen, L. Lauderbach, R. Hodgin, S. Bastea, L. Fried, A. Jones, T. van Buuren, D. Hansen, J. Benterou, C. May, T. Gra-ber, B. J. Jensen, J. Ilavsky and T. M. Willey: *Journal of Applied Physics.* V. 117. Issue 24. 245902 (2015)

ID024: Effect of Solidification Rate on Microstructure and Strain Rate-related Mechanical Properties of AlCoCrFeNi High-entropy Alloy Prepared by Bridgman Solidification

Jinlian Zhou [a], Yunfei Xue [a, b, *], Fangqiang Yuan [a],Lili Ma [a, c],Tangqing Cao [a], Lu Wang [a,b]

[a] School of Materials Science and Engineering, Beijing Institute of Technology, Beijing, 100081, China.

[b]National Key Laboratory of Science and Technology on Materials under Shock and Impact, Beijing 100081, China.

[c] School of Chemical Engineering, Qinghai University, Xining, 810016, China.

Corresponding author at: School of Materials Science and Engineering, Beijing Institute of Technology, Beijing 100081, China. Tel.: +86 10 68912709 ext.107.

E-mail address: xueyunfei@bit.edu.cn; (Y.F. Xue)

Abstract: The AlCoCrFeNi high-entropy alloys (HEAs) were prepared by Bridgman solidification with different solidification rates. The microstructure and mechanical properties of the alloys were investigated over a wide strain rate range between $10^{-3}s^{-1}$ and $10^{3}s^{-1}$ at ambient temperature. With the solidification rate increase, the microstructure evolved from columnar crystals to equiaxed grains accompanied by a decreasing grain size. Under low strain rate, the alloys exhibited both increased yield strength and fracture plasticity with the solidification rate increase, while under high strain rate, the alloys exhibited increased yield strength but abnormal fracture plasticity, a dramatic fracture plasticity was observed in the alloy with low solidification rate. All of those alloys exhibited positive strain rate sensitivity. Moreover, the fracture mode under low strain rate changed from axial splitting to a mixture of axial splitting and shearing fracture with the increase of solidification rate.

Keywords: High-entropy alloys,Solidification rate,Microstructure, Mechanical properties, Strain rate

ID025: Comparison on Reaction Energy, Impact Sensitivity and Dynamic Response at Various Temperatures in W-PTFE-Mg, W-PTFE-Ti and W-PTFE-Zr Composites

Jinxu Liu [a,b,*], Liu Wang [a], Shukui Li [a,b,c], Xinbo Zhang [a], Song Zhang [a]

[a] School of Material Science and Engineering, Beijing Institute of Technology, No.5 yard, Zhong Guan Cun South Street, Beijing 100081, PR China

[b] National Key Laboratory of Science and Technology on Materials under Shock and Impact, Beijing Institute of Technology, No.5 yard, Zhong Guan Cun South Street, Beijing 100081, China

[c] State Key Laboratory of Explosion Science and Technology, Beijing Institute of Technology, No.5 yard, Zhong Guan Cun South Street, Beijing 100081, PR China

* liujinxu@bit.edu.cn

Abstract: The reaction energy, impact sensitivity and mechanical behavior of W-PTFE-Mg, W-PTFE-Ti and W-PTFE-Zr composites with the same W and PTFE mass ratio are compared. The effect of active metal species on the reaction energy of W-PTFE-active metal mixtures at both oxygen and argon atmosphere are investigated. The role of W in the reaction of composites in oxygen is revealed. Besides, the effect of active metal species on the impact sensitivity is studied. The reaction time, reaction degree, completeness and absorbed critical energy before reaction of all the three kinds of W-PTFE-active metal composites are determined. Moreover, quasi-static compression behavior of W-PTFE-Mg, W-PTFE-Ti and W-PTFE-Zr composites is compared and the corresponding failure mechanism which is responsible for different mechanical behaviors is revealed. Furthermore, dynamic compression behaviors at a temperature range from 288 K to 573 K with 100K intervals are investigated. The effect of active metal species on the dynamic response of W-PTFE-active metal composites at elevated temperatures is compared and the corresponding failure mechanisms are revealed.

ID026: Numerical Simulation on Sympathetic Detonation of Fuse Explosive Train

Junming Yuan[1,a]，Shuo Li[1]，Yucun Liu[1]，Wenzhi Tan[2]，Zongren Xing[2]，Xin Tang[1]
[1]School of Chemical Engineering and Environment, North University of China, Taiyuan 030051, China
[2]Institute of Chemical Materials, CAEP, Mianyang 621900, China
[a]junmingyuan@163.com

Abstract: The safety and reliability of fuse are the decisive factors, which guarantee whether the targets are destroyed accurately or the rate of accidental explosion is reduced during storage, transportation, and handling. The structure model of fuse explosive train was determined and reasonably simplified on the basis of typical medium and large caliber munitions. To observe the reaction state, a related finite element model about fuse explosive train in actual charge condition was established with Lagrange elements by AUTODYN. For modeling of air and donor charge (TNT), the Euler elements were utilized. The JWL parameters were used for TNT and the identical ignition and growth reaction rate parameters were set for JH-14C booster with 1.65 g/cm^3. The fluid-solid coupling method was applied to fuse explosive train on the condition of sympathetic detonation. Through adjusting the distances between TNT and fuse, the pressure histories was analyzed in the reaction of the JH-14C explosive train in fuse, and the two critical distances of sympathetic detonation and safety were gained for the fuse explosive train. The results show that the critical sympathetic detonation distance is 23mm and the corresponding incident pressure is 5.4GPa; the safety distance is 760mm and the corresponding incident pressure is 2.5e-4GPa. The results of this study provide useful information to ensure the reliability and safety of fuse as well as avoid unnecessary explosive accidents in the modern weapon system.

Keywords: Explosion mechanics, Fuse, Sympathetic detonation, Ignition and growth model, Critical distances; Numerical simulation

References

[1] Weijun Tao, Shi Huan. Study on state of the two-dimensional shock initiation of RDX-8701[C].8th mechanics of explosion academic meeting.2007:58-63.
[2] He Zhang, Haojie Li. The Fuze Mechanism[M].Beijing: Beijing Institute of Press.2014:1-9.
[3] Manlin Wu, Yucun Liu. Numerical Modeling of Shock Sensitivity Experiments(SSGT)[J].Initiators&Pyrotechnics.2004,(2):16-19.

ID027: Production of Wire Mesh Reinforced Aluminum Composites Through Explosive Compaction

K.Raghukandan[1] S.Saravanan[2]

[1]Department of Manufacturing Engineering, Annamalai University, Tamilnadu, India
Email: raghukandan@gmail.com Phone: +919443488265

[2]Department of Mechanical Engineering, Annamalai University, Tamilnadu, India
Email: ssvcdm@gmail.com Phone: +919443676936

Abstract: Aluminum based fiber and/or wire reinforced composites are extensively employed in aerospace, space, automobile and other structural applications. This study pertains to the microstructural and mechanical properties of explosive compacted aluminum composite produced by alternatively placing aluminum foils and stainless steel wire meshes. Stacks containing three to four layers of aluminum foils (0.3 mm) and wire mesh are explosively compacted subjected to varied loading ratios. Microstructural characterization of clads reveals the significance of kinetic energy spent at the interface. Mechanical Testing viz., Vickers hardness, Ram tensile tests are conducted on the aluminum wire mesh reinforced composites and the results are presented.

Corresponding author: K.Raghukandan
Department of Manufacturing Engineering,
Annamalai University, Tamilnadu, India
Email: raghukandan@gmail.com

ID028: A Study on Expansion Behavior of the SPHE Cylinder Induced by Explosion

Keishi Matsumoto [1,a] , Kazuhito Fujiwara [1,b]

[1]2-39-1 Kumamoto,Chuo-ku,Kumamoto 860-8555, Japan

[a]158d8559@ st.kumamoto-u.ac.jp

[b]fujiwara@kumamoto-u.ac.jp

Abstract: Some risk has been increased in industrial products due to the high energy concentration in products that brings us high performance and high efficiency. And flammable refrigerant used for prevention of global warming also has a risk to cause the huge accident at compressed condition. High pressure vessels are normally designed by using data from static compressing examinations, but impact stress and high strain rate deformation induced by explosions require the special design manner.

In this study, SPHE cylinder (Steel plate hot-drawn extra) that was a carbon steel and had large ductility was used for our study target, because it was used to be a compressor shell. PETN explosive and smokeless gunpowder were adopted as impact loads realizing high pressure rise-up rate and relatively slow pressure rise rate respectively. Through the results of experiments and numerical simulations, the expansion behavior of SPHE was investigated and the designing manner was discussed including the estimation of strength of the cylinder and crashing timing. The test conditions and schematics are shown in Table 1 and Fig.1. The deformation behavior of the expanding cylinder was observed by a high-speed camera.

Table 1 Test conditions

Test no.	Load method	
1-1	PETN explosive	ϕ 9.0 mm
1-2		ϕ 7.0 mm
2-1	IMR4227 gunpowder	ϕ 34 mm
2-2	IMR3031 gunpowder	

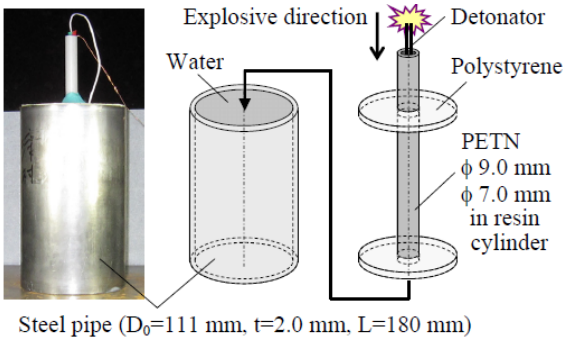

Fig.1 Schematic and photograph of explosion test

Histories of circumferential mean strain showed that the high dynamic effect in the load of PETN explosive accelerated the cylinder wall abruptly and the cylinder was cracked at 7-13% strain value under the 10^3/s order strain rate, while in the gunpowder, the accelerate began more than 2ms after and the fracture appeared at 10-13% strain value

under the the 10^4/s order strain rate. It can be considered that those facts were caused by the difference of the fracture developing mechanism between each load feature and deforming behavior. In initially accelerated cylinder the cumulation of damage depends on the expanding time. On the other hand, slow pressurizing cause the rapid deformation after exceeding some critical pressure such as the static critical pressure.

These results lead new aspects of our industrial design for products related to impact load phenomena.

ID029: Study of Interaction Between Unsteady Supersonic Jet and Vortex Rings Discharged From Elliptical Cell

Kazumasa Kitazono[1, a], Hiroshi Fukuoka[2, b], Nao Kuniyoshi[3], Minoru Yaga[4],Eri Ueno[5], Naoaki Fukuda[6], Toshio Takiya[5]

[1]Advanced Mechanical Engineering Course, Faculty of Advanced Engineering, National Institute of Technology, Nara College, 22 Yata, Yamatokoriyama, Nara, 639-1080, Japan.

[2]Department of Mechanical Engineering, National Institute of Technology, Nara College, 22 Yata, Yamatokoriyama, Nara, 639-1080, Japan.

[3]Department of Marine Electronics and Mechanical Engineering, Tokyo University of Marine Science and Technology, 2-1-6, Etchujima, Koto-ku, Tokyo, 135-8533.

[4]Faculty of Engineering, University of the Ryukyus, 1 Senbaru, Nishihara-cho, Nakagami-gun, Okinawa, 903-0213, Japan.

[5]Technology Research Institute, Hitachi Zosen Corporation, 2-chome, Funamachi, Taisho-ku, Osaka, 551-0022, Japan.

[6]Office of Society-Academia Collaboration for Innovation, Kyoto University, 1-chome, Goryo-Ohara, Nishikyo-ku, Kyoto, 615-8245, Japan.

[a]kitazono.k@class.mech.nara-k.ac.jp,

[b]fukuoka@mech.nara-k.ac.jp

Abstract: In the flow field generated by the shock tube with the elliptical cell, there is the interaction between the vortex ring and the supersonic jet [1]. However, there has been little effort to investigate the interaction between the vortex ring and the jet. The purpose of the present study is to investigate the effect of the vortex ring on the supersonic jet.

The experiment and numerical calculation were carried out by schlieren method and by solving the axisymmetric two-dimensional compressible Navier-Stokes equations, respectively. The experimental flow was visualized by the schlieren method using the still camera and the high-speed camera as a continuous light source with a metal halide lamp. The parameter was the pressure ratio of the shock tube.

Figures 1(a)~(c) show the calculated vorticity contours and computer schlieren images for P_h/P_b=22.6. The time shown in each figure denotes the elapsed time from the moment of the jet injection. Figure 1(a) shows the vortex rings and the jet discharged from the cell exit. We refer to first generated vortex ring and second generated vortex ring

as "VR_1" and "VR_2", respectively. The distance between VR_1 and VR_2 have decreased in Figs.1(a) and (b). Figure 1(c) shows the deformation of the jet and the moment when the deformed jet and the vortex rings are at the same position. It is found that the deformation of the jet is due to the interaction between the vortex ring and the jet.

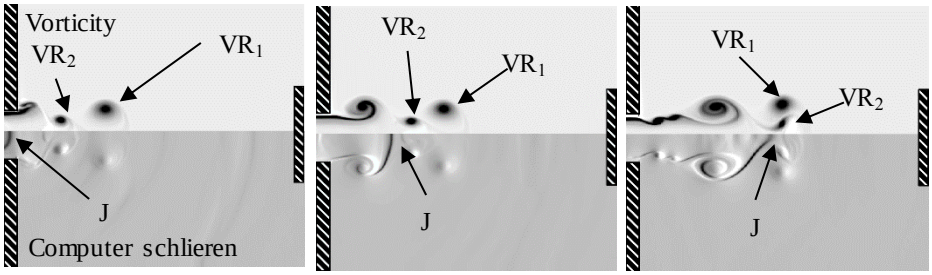

(a) t=567μs (b) t=625μs (c) t=690μs

Fig.1 Vorticity and computer schlieren variations for P_h/P_b=22.6. (VR_1: First generated vortex ring; VR_2: Second generated vortex ring; J: Jet head)

References

[1] Motoki Sakamoto, Masazumi Matsui, Hiroshi Fukuoka, Minoru Yaga and Toshio Takiya,"Study of Unsteady Supersonic Jet using Shock Tube with Small High-Pressure Chamber with Elliptical Cell", International Symposium on Explosion, Shock wave and High-energy reaction Phenomena 2013, March 27-29, 2013, Okinawa National College of Technology, Japan, p.27.

ID030: Some New Approaches of Explosive Welding

Kazuyuki Hokamoto[1, a]

[1]Institute of Pulsed Power Science, Kumamoto University, 2-39-1, Kurokami, Chuo-ku, Kumamoto City, Kumamoto 860-8555, Japan

[a]hokamoto@mech.kumamoto-u.ac.jp

Abstract: This presentation aims to introduce new approaches being made by Explosion Processing Group in the Institute of Pulsed Power Science, Kumamoto University, trying to find out new applications of the explosive welding technique. Two major approaches are demonstrated.

One important method developed by the group is “underwater explosive welding technique” which renders it possible to weld various difficult-to-weld materials [1-6] under controlled energetic condition. Encouraging positive results have been confirmed for various hard materials such as ceramics, tool steel, rapidly solidified foil, tungsten sheet and others. Besides, the method is also good to weld magnesium alloy and other materials, which may cause melting or reactions easily. By using the method, the final surface facade of the welded surface is kept clean and the method is considered beneficial for the welding of thin plate - which is generally considered difficult to weld by conventional explosive welding technique.

The other recent approach is the making of unidirectional pored structure (UniPore) through explosive welding using well known cylindrical geometry. The process is simple and executed by using many small pipes inserted solid paraffin. The small pipes are filled in an outer pipe, and the pipe was compressed by the detonation of an explosive placed outside of the outer pipe. The recovered samples showed quite uniform pored structure, and each channel was isolated by the wall of the small pipes welded tightly to each other even by using a thin pipe whose thickness was only 0.2 mm [7-8]. The mechanism of the welding is considered to be achieved by the activation of thin metal surface (atomic order) by the metal jet between the small pipes, because jet trapped region was confirmed at the triple point of the small pipes. In the presentation, an alternative method making similar UniPore structure is demonstrated using rolled thin metal plate with spacers as well [9]. These materials are expected to be applied for energy absorption material having un-isotropic mechanical property and for heat-exchanger or other related purposes.

References

[1] K. Hokamoto, M. Fujita, H. Shimokawa, H. Okugawa: *Journal of Materials Processing Technology* Vol.85 (1999), pp 175-179

[2] W. Sun, X. Li, H. Yan, K. Hokamoto: *Journal of Materials Engineering and Performance* Vol.23 (2014), pp 421-428

[3] K. Hokamoto, K. Nakata, A. Mori, S. Tsuda, T. Tsumura, A. Inoue: *Journal of Alloys and Compounds* Vol.472 (2009), pp 507-511

[4] K. Hokamoto, K. Nakata, A. Mori, S. Ii, R. Tomoshige, S. Tsuda, T. Tsumura, A. Inoue: *Journal of Alloys and Compounds* Vol.485 (2009), pp 817-821

[5] P. Manikandan, J.O. Lee, K. Mizumachi, A. Mori, K. Raghukandan, K. Hokamoto: *Journal of Nuclear Materials* Vol.418 (2011), pp 281-285

[6] M.A. Habib, H. Keno, R. Uchida, A. Mori, K. Hokamoto: *Journal of Materials Processing Technology* Vol.217 (2015), pp 310-316

[7] K. Hokamoto, M. Vesenjak, Z. Ren: *Materials Letters* 137 (2014), pp323-327

[8] M. Vesenjak, H. Hokamoto, M. Sakamoto, T. Nishi, L. Krstulović-Opara, Z. Ren: *Materials and Design* 90 (2016), pp867-880

[9] M. Vesenjak, H. Hokamoto, S. Matsumoto, Y. Marumo, Z. Ren: *Materials Letters* 170 (2016), pp39-43

ID031: A New Electrometric Method for the Continuous Measurement of Underwater Explosion Parameters

Kebin Li[1], Xiaojie Li[1,2,a], Honghao Yan[1], Xiaohong Wang[1]

[1]Department of Engineering Mechanics, Dalian University of Technology, Dalian, Liaoning 116024, China

[2]State Key Laboratory of Structural Analysis for Industrial Equipment, Dalian, Liaoning 116024, China

[a]boomlee@qq.com

Abstract: A method using a self-designed continuous resistance wire sensor has been developed for measuring the detonation wave and the near-field parameters in a single underwater explosion. The new sensor improved from the conventional permits measurement in underwater explosion test, wave discontinuities like gap and jump being relieved with the interference suppression from electromagnetic wave, advanced air shock wave and metal jet. Underwater explosion parametric test systems in near field for Cylindrical and spherical charge have been carried out. The time-history curve of oblique shock wave generated by the cylindrical is analyzed, from which the parameters of the JWL EOS can be determined via a fitting and calculating process. By compared with the simulated result from coefficient-revised AUTODYN program, the present method may provide a feasible and reliable means for underwater explosion measurement.

ID032:Influence of Axial Length on Axially Compressed Aluminum Polygonal Tube

Keisuke Yokoya[1], Makoto Miyazaki[1, a], Yusuke Tojo[2]

[1]National Institute of Technology, Nagano College, 716 Tokuma, Nagano-city, Nagano 381-8550, Japan

[2]Denso Aircool Corporation, 2027-9 Kita-Hodaka, Hodaka, Azumino-city, Nagano 399-8386, Japan

[a]miyazaki@nagano-nct.ac.jp

Abstract: Aluminum tubes are efficient energy absorbing components and are widely used in the automobile industry. Many studies on the deformation of a circular tube have been done, but there are a few research reports on a square or polygonal tube deformation, such as the experiment of axial dynamic deformation and bending stiffness [1,2]. In the previous report, the authors experimented on axial impact squeezing test of square tubes that had the reinforcing ribs in the cross-sectional [3]. The influence of cross-sectional shape on axially compressed aluminum tube (square, pentagonal, hexagonal, heptagonal and octagonal) was investigated by compressive tests and numerical analysis [4]. However, there are only a few reports on length of aluminum tube [4,5].

This paper deals with the influence of axial length and reinforcing rib on dynamic axial compressed aluminum polygonal tube in order to obtain the basic data of buckling and impact resistance. A numerical analysis of the dynamic deformation process of the polygonal tube was made with a finite element method. The specimen used in this analysis is an aluminum polygonal tube (JIS A6063-T5, 40 mm wide, 1 mm thickness, 300-500 mm length). The cross-sectional shapes are square, hexagonal and octagonal, and the reinforcing rib is used to bind in the center from each corner. In the analysis, the deformed tube is assumed to be composed of bilinear four-node shell elements, and the weight is assumed to be a rigid body of three-dimensional with eight-node, isoparametric element. An example of analytical model is shown in Fig. 1.

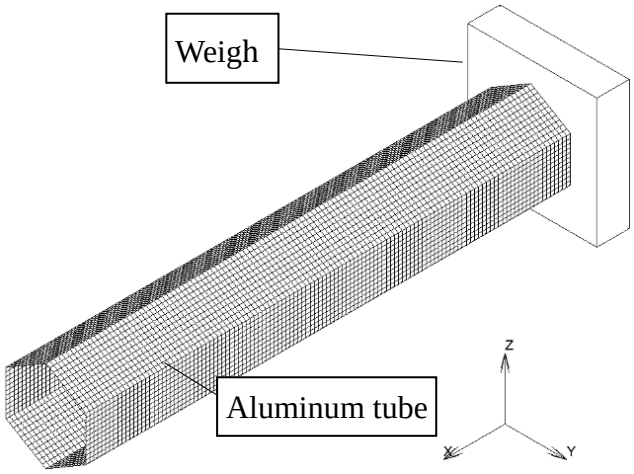

Fig. 1 Analytical model of hexagonal tube (l=300mm).

The results were summarized as follows; even if the axial length was changed, there was no difference in the trend of the load-displacement curve in each cross-sectional shape. However, the maximum load part on load-displacement curve was changed. Also the trend of the load-displacement curve was affected by the reinforcing ribs. The buckling was generated partially and the deformation was larger at the corners in each axial length and cross-sectional shape. In the case of square tube, the deformation shape has concave-convex in adjoining surfaces, and crushed in a bellows-like.

References

[1] W. Abramowicz and N. Jones: *International Journal Impact Engineering* 2-2 (1984), pp. 179-208.

[2] D-K. Kim, S. Lee and M. Rhee: *Materials & Design* 19-4 (1998), pp. 179-185.

[3] M. Miyazaki and H. Negishi: *Proceedings of the 53rd Japanese Conference for the Technology of Plasticity* (2002), pp. 83-84.

[4] M. Miyazaki and M Yamaguchi: *Procedia Engineering* 81 (2014), pp. 1067-1072.

[5] M. Miyazaki and H. Negishi: *Materials Transactions* 44-8 (2003), pp. 1566-1570.

ID033: Experimental Study for the Optimal Conditions for the Softening of Pork Using Underwater Shock Wave

Ken Shimojima[1,a], Osamu Higa[1, b], Yoshikazu Higa[1,c], Hirofumi Iyama[2], Atsushi Yasuda[3] and Shigeru Itoh[4]

1 Dept. Mechanical Systems Engineering, National Institute of Technology, Okinawa College, 905 Henoko, Nago, Okinawa 905-2192, Japan

2 Dept. Mechanical & Intelligent System Engineering, National Institute of Technology, Kumamoto College, Kumamoto 866-8501, Japan

3 Osaka Sanitary Co., 1 -7-46 Torikaihonmachi, Settsu-shi, Ōsaka-fu 566-0052, Japan

4 Professor Emeritus, Kumamoto University & National Institute of Technology, Okinawa College

[a]k_shimo@okinawa-ct.ac.jp

[b]osamu@kumamoto-nct.ac.jp

[c]y.higa@kumamoto-nct.ac.jp

Abstract: The National Institute of Technology, Okinawa College has developed the food processing machine using the underwater shock wave by wire discharge.Those effect were sterilization, milling flour, softening, extraction, and so on[1-4] .In this report, we examined the conditions for the food of softening experimentally. The pork was been selected for target of experiment. Figure 1 shows an overview of the experimental apparatus for the grinding of pork.

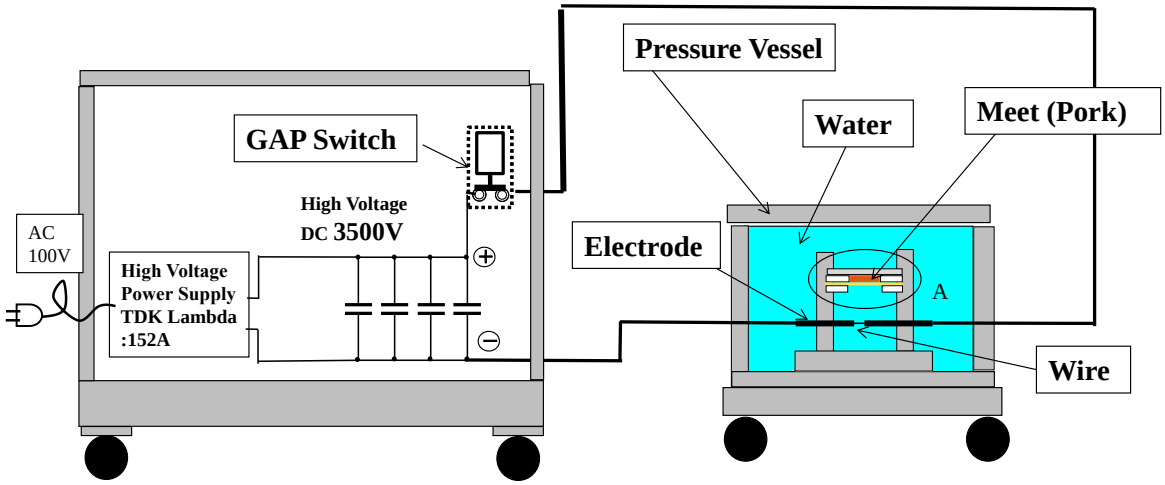

Fig.1 Experimental equipment using underwater shock wave

The pork was been selected for target of experiment. The relationship between the

results of soften and the distance of shock wave generation point, and a number of shockwave is revealed.

References

[1] S. Itoh, K. Hokamoto, Explosion, Shock Wave and Hypervelocity Phenomena in Materials II, Materials Science Forum (Volume 566), November 2007,pp. 361-372

[2] K. Shimojima, A. Takemoto, M. Vesenjak, Y. Higa, Z. Ren, S. Itoh,The effect of improving the oil extraction of Slovenia production seed by underwater shock wave,MULTIPHYSICS 2015,10-11 Dec 2015, London, United Kingdom,P.9

[3] Ken shimojima，Osamu Higa，Katsuya Higa，Yoshikazu Higa，Ayumi Takemoto，Atsushi Yasuda，Michiya Yamato，Minoru Nakazawa，Hirofumi Iyama，Toshiaki Watanabe，Shigeru Itoh,Development of Milling Flour Machine of Rice Powder Using Instantaneous High Pressure,1st Report, Development of Continuous Driving Device and Componential Analysis of Rice Powder, Japan society for food engineering, Vol.16,No.4(2015)

[4] K. Izena, A. Takemoto, M. Yamato H. Mizukami, O. Higa, K. Shimojima, K. Higa, K. Hokamoto, S. Itoh On the powder sterilization by instantaneous high pressure loading 23rd Annual Meeting of The Materials Research Society of Japan, 9-11December 2013 Yokohama, Japan

ID034: Computational Simulation for Milling Flour of Rice Powder Using Under Water Shock Wave

Ken Shimojima[1,a], Osamu Higa[1, b], Yoshikazu Higa[1,c], Hirofumi Iyama[2], Atsushi Yasuda[3] and Shigeru Itoh[4]

1 Dept. Mechanical Systems Engineering, National Institute of Technology, Okinawa College, 905 Henoko, Nago, Okinawa 905-2192, Japan

2 Dept. Mechanical & Intelligent System Engineering, National Institute of Technology, Kumamoto College, Kumamoto 866-8501, Japan

3 Osaka Sanitary Co., 1-7-46 Torikaihonmachi, Settsu-shi, Ōsaka-fu 566-0052, Japan

4 Professor Emeritus, Kumamoto University & National Institute of Technology, Okinawa College

[a]k_shimo@okinawa-ct.ac.jp [b]osamu@kumamoto-nct.ac.jp,[c]y.higa@kumamoto-nct.ac.jp

Abstract: The National Institute of Technology, Okinawa College has developed a milling flour machine of rice using the underwater shock wave. The rice flour by this method was high quality compared to the general milling method[1].The rice flour production machine is composed by the pressure vessels for milling, and the high voltage generator, the circulation and filtration device of the water. In this report, in order to realize a highly efficient milling, the propagation of the shock wave in the pressure vessel was analyzed by computer simulation. The experiment and the results of the particle velocity of rice for analysis is shown. The results of numerical analysis based on the particle velocity is shown.

References

[1] Ken shimojima, Osamu Higa, Katsuya Higa, Yoshikazu Higa, Ayumi Takemoto, Atsushi Yasuda, Michiya Yamato, Minoru Nakazawa, Hirofumi Iyama, Toshiaki Watanabe, Shigeru Itoh,Development of Milling Flour Machine of Rice Powder Using Instantaneous High Pressure,1st Report, Development of Continuous Driving Device and Componential Analysis of Rice Powder, Japan society for food engineering, Vol.16,No.4(2015)

[2] K. Shimojima, Y. Higa, O. Higa, K. Higa, A. Takemoto, S. Itoh, Production and Evaluation of Pressure Vessel for highly effective Rice Powder Manufacturing using Underwater Shock Wave 2013 ASME Pressure Vessels & Piping Conference Paris Marriott Rive Gauche Hotel & Conference CenterJuly 14-18, 2013, Paris, PVP 2013-97829, P.31

ID035: Detection of the Emission of the Particles From a Free Surface of Metals Loaded by Strong Shock Wave Using the Synchrotron Radiation Methods.

Konstantin A. Ten[1, 5] , Edward R. Pruuel[1, 5] , Alexey O. Kashkarov[1, 5], Ivan A. Rubtsov[1, 5] , Lev I. Shechtman[2, 5] , Vladimir V. Zhulanov[2, 5], Boris P. Tolochko[3], Gennadiy N. Rykovanov[4], Alexandr K. Muzyrya[4], Evgeniy B. Smirnov[4], Mikhail Yu. Stolbikov[4], Kirill M. Prosvirnin[4]

[1] Lavrentyev Institute of Hydrodynamic SB RAS, Novosibirsk 630090, Russia

[2] Budker Institute of Nuclear Physics SB RAS, Novosibirsk 630090, Russia

[3]Institute of solid state chemistry and mechanochemistry SB RAS, Novosibirsk, 630128, Russia

[4]Russian federal nuclear center - Zababakhin All-Russia Research Institute of Technical Physics, Snezhinsk, 456770, Russia

[5]Novosibirsk State University, Novosibirsk, 630090, Russia.

ten@hydro.nsc.ru

Abstract: When a strong shock wave leavesa metal, flows of particles of different sizes are ejected from the wave's free surface (shock-wave "dusting", ejecta) [1,2]. Unlike a cumulative jet, such aflow consists of separate particleshaving a size of a few microns to hundreds of microns. It was assumed that there are also finer particles in such aflow, but the existing techniques are not able to resolve them.

This report presents the results of experiments using SR from the colliders VEPP-3 and VEPP-4 at BINP. Precision measurement of transmitted SR (of an energyof 2 GeV on VEPP-3) was applied to exploration ofmicroparticle flows from a free surface of various materials (copper, tin, and tantalum). Mass distributions along microjetsoriginating from micron-sized slits were obtained. Dynamic detection of small-angle X-ray scattering (SAXS) of synchrotron radiation (SR) from the collider VEPP-4M (energy of 4 GeV) was implemented on the facility SYRAFEEMA (Synchrotron Radiation Facility for ExploringEnergetic Materials). A technique of SAXS measurement on this facility enables detection of nanoparticles ranging in size from 4 to 200 nm. Flows of nanoparticles of about 100 nm in size from a surface of smooth foil (tin and tantalum) affected by compressed HMX were detected for the first time.

References

[1] K. Hokamoto, S. Tanaka, M. Fujita, S, Itoh, M.A. Meyers, and H.C. Chen: *Physica B* 239(1997) pp1-5

[1]. V. A. Ogorodnikov, A. G. Ivanov, A. L. Mikhailov,, N.I. Kryukov, A.P. Tolochko, and V.A. Golubev. Combustion, Explosion and Shock Waves. vol.34 (1998), pp 696-700.

[2]. Thibaut De Resseguier, Didier Loison, EmilienLescoute, Loic Signor, Andre Dragon. Journal of the Theoretical and Applied Mechanics, vol. 48 (2010), pp. 957-972.

ID036: Wire Mesh/Ceramic Particle Reinforced Aluminum Based Composite Using Explosive Cladding

Lalu Gladson Robin[1, a], Raghukandan Krishnamurthy[1, b], Saravanan Somasundaram[2]

[1]Department of Manufacturing Engineering, Faculty of Engineering and Technology, Annamalai University, Annamalai Nagar, India – 608 002.

[2]Department of Mechanical Engineering, Faculty of Engineering and Technology, Annamalai University, Annamalai Nager, India – 608 002.

[a]lalugrobin@gmail.com, [b]raghukandan@gmail.com

Abstract: Explosive cladding, a solid state metal joining technique suited for bonding metals having varied physical and metallurgical properties. In explosive cladding, the controlled energy stored in a chemical explosive is used to create a metallurgical bond between two similar or dissimilar metals. Explosive cladding has been applied to fabricate the clad materials and some composites such as multilayered and wire-reinforced materials. The process has been fully developed with large-scale production in the Manufacturing sector for various kinds of applications. In particular, aerospace industries relay on the specific applications related to wire mesh/ceramic reinforced aluminum based composites.

In this study, dissimilar aluminum plates were explosively cladded by placing wire mesh/ceramic particle between them. The stainless steel 316 meshes were placed at 3 different orientations (30^0, 45^0 and 90^0 respectively) with SiCp (0%, 5% and 10% respectively). The wire mesh and the ceramic particles were used to improve the Mechanical properties of the explosively cladded aluminum composites. Toughness, tensile strength, hardness and microstructure of the explosively cladded composite materials were evaluated. Significant improvement in the mechanical properties of the wire mesh/ceramic particle reinforced explosively cladded dissimilar aluminum composites is established.

References

[1] Gülenç, B., Kaya, Y., Durgutlu, A., Gülenç, İ.T., Yıldırım, M.S. and Kahraman, N., 2016. Production of wire reinforced composite materials through explosive welding. *Archives of Civil and Mechanical Engineering*, *16*(1), pp.1-8.

[2] Raghukandan, K., Hokamoto, K., Lee, J.S., Chiba, A. and Pai, B.C., 2003. An investigation on underwater shock consolidated carbon fiber reinforced Al composites. *Journal of materials processing technology*, *134*(3), pp.329-337.

[3] Bhalla, A.K. and Williams, J.D., 1977. Production of stainless steel wire-reinforced aluminium composite sheet by explosive compaction. *Journal of Materials Science*, *12*(3), pp.522-530.

[4] Nishida, M., Minakuchi, K., Ando, K., Araki, T. and Hyodo, K., 1995. Fabrication of high-strength steel fibre reinforced metal matrix composites by explosive bonding and their tensile properties. *Welding international*, *9*(3), pp.179-184.

Corresponding author: Lalu Gladson Robin
Department of Manufacturing Engineering,
Annamalai University, Tamilnadu, India
Email: lalugrobin@gmail.com

ID037: Dynamic Behavior of Ti-6Al-4V Micro-Lattice Structure

Lijun Xiao[1, a], Weidong Song[1, b], Huiping Tang[2], Nan Liu[2]

[1]State Key Laboratory of Explosion Science and Technology, Beijing Institute of Technology, Beijing 100081, China

[2]State Key Laboratory of Porous Metal Materials, Northwest Institute for Non-ferrous Metal Research, Xi'an 710016, China

[a]1512005@ bit.edu.cn,

[b]swdgh@bit.edu.cn

Abstract: Cellular materials have attracted much attention in the applications in energy absorption, heat exchange and light weight load-bearing, due to their excellent properties combining light weight, outstanding mechanical behavior and low thermal conductivity [1,2]. With the rapid development of additive manufacturing technology, periodic micro-lattice structures have attracted much attention due to their better properties than stochastic foams. Titanium and its alloys, which have higher specific strengths, modulus and melting temperatures than aluminum and steel, exhibit a promising prospect in applying as the matrix of cellular materials [3].

In this paper, Electron beam melting(EBM) method is adopted to fabricate the Ti-6Al-4V micro-lattice structure (Fig.1). Dynamic experiments are performed to investigate the mechanical properties of the specimens by SHPB apparatus. In order to reveal the effect of surface imperfection on the dynamic properties, finite element model considering the surface quality of struts (Fig.2) is built and numerical simulation is conducted to exhibit the stress distribution and deformation evolution of the lattice structures under different impact speeds.

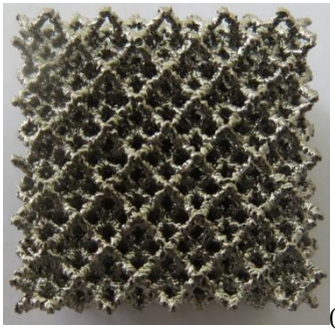
(a)
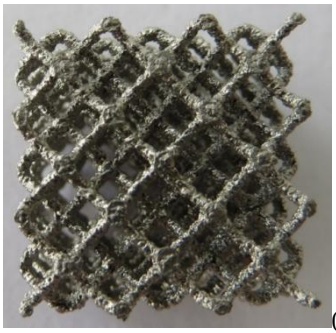
(b)

Fig.1 Micro-lattice specimens fabricated by EBM: (a) unit cell size of 3mm; (b) unit cell size of 3mm

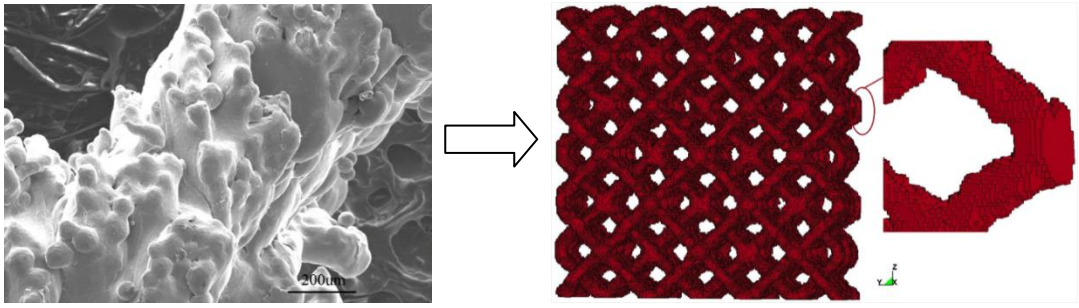

Fig.2 3D FE model of Ti-6Al-4V lattice structure

References

[1] L. J. Gibson, and M. F. Ashby. *Cambridge University Press* (1988).

[2]V. S. Deshpande, N.A. Fleck. *International Journal of Impact Engineering* Vol.24 (2000), pp277-298.

[3]Z. Ozdemir Z, E. Hernandez-Nava, A. Tyas, et al. *International Journal of Impact Engineering* Vol.89 (2015), pp49-61.

ID038: Analysis on Effect of Individual SEFAE Rocket by Environment

Lili Wu[a], Yukui Ding, Jianwei Zhen

Department of Ammunition Engineering, Ordnance Engineering College, He Bei Shijiazhuang 050003, China

[a]15614101135@163.com

Abstract: It introduce the constitution and the action principle of individual SEFAE rocket, the parts of individual SEFAE rocket lose effectiveness easily under the influence of environment and it would result the whole ammunition become invalid, by way of analyze the parts of the individual SEFAE rocket ,such as shell case, Fuel Air Explosive, detonator,primer, propellant.

References

[1] Yunping Ai, Qiong Liu, Zhonglin Feng, Pengfei Ma: Logistics Engineering and Management Vol.35(2013) pp146-147

[2] Weifang Xuan, Shiying Chen, Yi Yuan: Equipment Environmental Engineering Vol.4 (2007), pp1-4

[3] Sen Xu, Dabin Liu, Junming Hui, Liping Chen: Chinese Journal of Explosives ＆.Propellants Vol.31 (2008), pp46-49

[4] Lingchun Li, Hongwei Wang, Zhiqiang Tan: Packaging Engineering Vol.23 (2002), pp68-70

[5] Zhen Wang, Haiguang Li, Xudong Ben: Equipment Environmental Engineering Vol.9 (2012), pp82-86

ID039: Collision Behavior in Magnetic Pressure Seam Welding of Aluminum Sheets

Makoto Miyazaki[1, a], Yohei Kajiro[1], Yasuaki Miyamoto[2]

[1]National Institute of Technology, Nagano College, 716 Tokuma, Nagano-city,Nagano 381-8550, Japan

[2]Ebara Corporation, 11-1 Haneda-asahi, Ota-ku, Tokyo 144-8510, Japan

[a]miyazaki@nagano-nct.ac.jp

Abstract: The Aluminum has higher electric conductivity and thermal conductivity than iron. Welding of aluminum sheet is difficult because of low heating efficiency. Therefore, various joining methods are studied. One of the joining methods of the aluminum sheet includes friction stir welding or explosive welding. Magnetic pressure seam welding attracts attention as a new welding method [1]-[4]. Magnetic pressure seam welding is a collision welding process, similar to explosive welding, utilizing electromagnetic force as the acceleration mechanism. Magnetic pressure seam welding uses electromagnetic force to accelerate one metal sheet (flyer plate) onto another stationary metal sheet (parent plate). Welding principle is shown in Fig. 1.

This paper deals with dynamic deformation process on magnetic pressure seam welding of aluminum sheets. Numerical analysis of the dynamic deformation process of the aluminum sheets is made by a finite element method. In this analysis, the aluminum sheets (100 mm width, 1 mm thickness) were assumed to be composed of 20000 plane-strain quadrilateral elements. Discharge energy was each in 0.8kJ, 1.0kJ and 1.2kJ. Gap length between flyer plate and parent plate was 1.0 mm.

The result shows that when a collision angle becomes bigger than a constant value, the collision frictional stress increases. In addition, the increase in collision frictional stress is proportional to a collision angle. The maximum of the collision frictional stress is proportional to discharge energy.

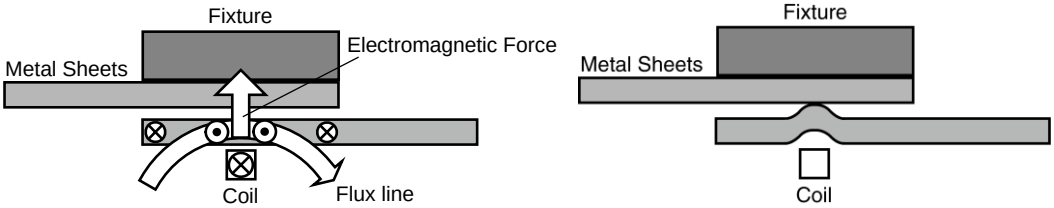

(a) Before (b) After

Fig.1 Metal sheets with coil and magnetic flux lines (cross sectional view)

References

[1] T. Aizawa, K. Okagawa, M. Yoshizawa and N. Henmi: *Proceedings of 4th International Symposium on Impact Engineering*, (2001), pp. 827-832.

[2] M. Miyazaki, K. Okagawa, T. Aizawa and M. Kumagai: *Journal of Japan Institute of Light Metals*, **57**-2 (2007), pp. 47-51.

[3] M. Miyazaki, K. Sasaki and M. Okada: *Proceedings of the 12th International Conference on Aluminium Alloys*, (2010), pp. 1752-1756.

[4] S. Kakizaki1, M. Watanabe and S. Kumai: *Materials Transactions*, **52**-5 (2011) pp. 1003-1008

ID040: Numerical Modelling of Cellular Materials and Their Dynamic Behavior

Matej Vesenjak[a], Matej Borovinšek[b], Miran Ulbin[c],Aljaž Kovačič[d], Nejc Novak[e], Zoran Ren[f]

Faculty of Mechanical Engineering, University of Maribor, 2000 Maribor, Slovenia
[a]matej.vesenjak@um.si, [b]matej.borovinsek@um.si, [c]miran.ulbin@um.si,
[d]aljaz.kovacic@um.si, [e]nejc.novak5@um.si, [f]zoran.ren@um.si

Abstract: Cellular materials have been increasingly used in modern engineering applications over the past decade due to their unique mechanical and thermal properties which depend on their cellular structure [1]. The presentation focuses on geometrical and mechanical characterization and modelling of three very different cellular materials (Fig. 1): Advanced Pore Morphology (APM) foam [2, 3], open-cell aluminum foam [4, 5] and Metallic Hollow Sphere Structure (MHSS) [6].

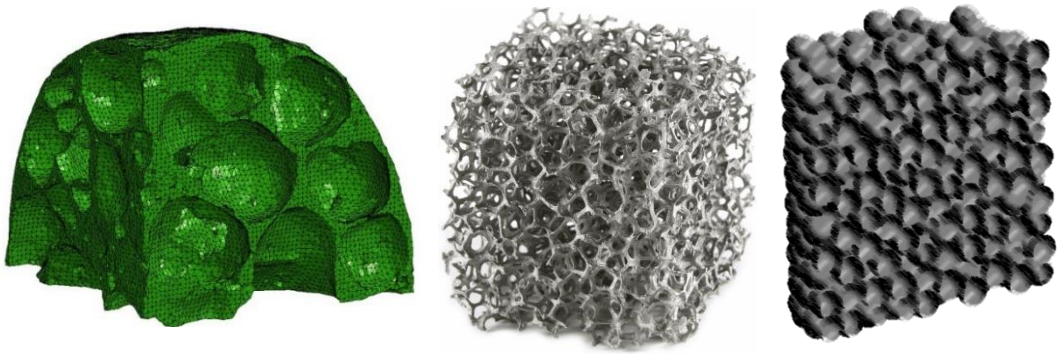

Fig.1 APM foam element, open-cell foam and MHSS.

The geometrical characterization is based on proper recognition of their internal cellular structure reconstructed from micro-computed tomography scans, taking into account the statistical distribution of geometrical parameters (topology and morphology). The conducted geometrical analysis provided means for methodology development for representative 2D and 3D geometrical modelling of irregular cellular structures and consequent formation of parametric numerical models. These were then used to study the dynamic response of analyzed cellular structures by means of advanced nonlinear computational simulations using the ABAQUS and LS-DYNA code. Computational results were compared and validated by experimental testing program.

References

[1] M.F. Ashby, A. Evans, N.A. Fleck, et al., Wadley, Metal foams: a design guide, Elsevier Sci., Burlington, Massachusetts, 2000.

[2] M.A. Sulong, M. Vesenjak, I.V. Belova, et al., Mater. Sci. Eng. A, 607 (2014) 498-504.

[3] M. Ulbin, M. Borovinšek, Y. Higa, et al., Mater. Lett., 136 (2014) 416-419.

[4] S. Tanaka, K. Hokamoto, S. Irie, et al., Measurement, 44 (2011) 2185-2189.

[5] M. Vesenjak, C. Veyhl, T. Fiedler, Mater. Sci. Eng. A, 541 (2012) 105-109.

[6] O. Andersen, U. Waag, L. Schneider, et al., Adv. Eng. Mater., 2 (2000) 192-195.

ID041: Different Energy Absorption Properties of Sandwich Structures with Different Boundary Conditions

Mingle PAN[1], Xinming QIU[1,a]

[1] Department of Engineering Mechanics, Tsinghua University, Beijing 100084, China

[a]qxm@mail.tsinghua.edu.cn

Abstract: Composed of two strong face-sheets and a soft core, sandwich structures are popularly used in energy absorptions, especially under dynamic loading. In this study, the energy absorption properties of sandwich plates with metallic foam core under dynamic loading are numerically analyzed, considering the difference of boundary conditions and shapes of plates. that is, part of the flat plate, cylindrical plate or spherical plate. The deformation profile and the energy absorption efficiency are discussed.

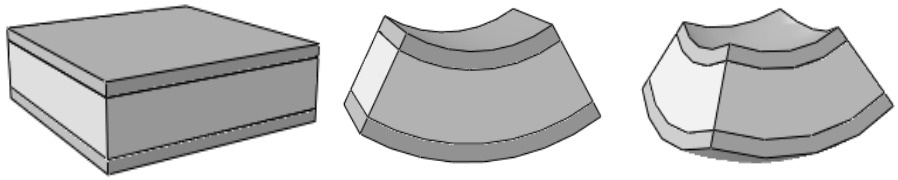

Fig. 1 The sandwich plates with different shapes: (a) planar; (b) cylindrical; (c) spherical

Acknowledgements

The authors gratefully acknowledge the financial support from NSFC No.11372163.

References

[1] Gibson L J, Ashby M F. Cellular solids : structure and properties[M]. Cambridge University Press, 1999.

[2] Shen J, Lu G, Wang Z, et al. Experiments on curved sandwich panels under blast loading[J]. International Journal of Impact Engineering, 2010, 37(9):960-970.

[3] Li W, Huang G, Bai Y, et al. Dynamic response of spherical sandwich shells with metallic foam core under external air blast loading – Numerical simulation[J]. Composite Structures, 2014, 116(9):612-625.

ID042: High Velocity Impact Resistance of Carbon Fiber and Carbon Fiber-reinforced Aluminum Laminates

Guangyan Huang[1*], Mingming Xu[1] , Zhiwei Guo[1], Shunshan Feng[1]

[1]State Key Laboratory of Explosion Science and Technology, Beijing Institute of Technology, Beijing 100081, China

[*]huanggy@bit.edu.cn

Abstract: Carbon fiber-reinforced metal laminate (FMLs) is currently the growing trend in lightweight protective structure design in the military and aerospace fields[1]. A new type of carbon-fiber-reinforced aluminum alloy laminates (CRALL) was designed in this study for high speed impact protection of intercontinental missiles and spacecrafts.

In this study, the mechanical properties in 0 ° and 90 ° direction of the unidirectional carbon fiber (CFRP) were obtained through the material test. The tensile energy to break of the CFRP, Al2024-T3 aluminum alloy and CRALL were compared in Fig. 1(a). Results showed that, CRALL is a strain rate sensitive material and exhibits significant ductility[2,3], especially under high strain rate tensile impact. The deformation energy of CRALL 3/2 before rupture is less than CFRP and Al 2024-T3 at quasi state rate, but much larger than both when reached strain rate 600 s^{-1}.

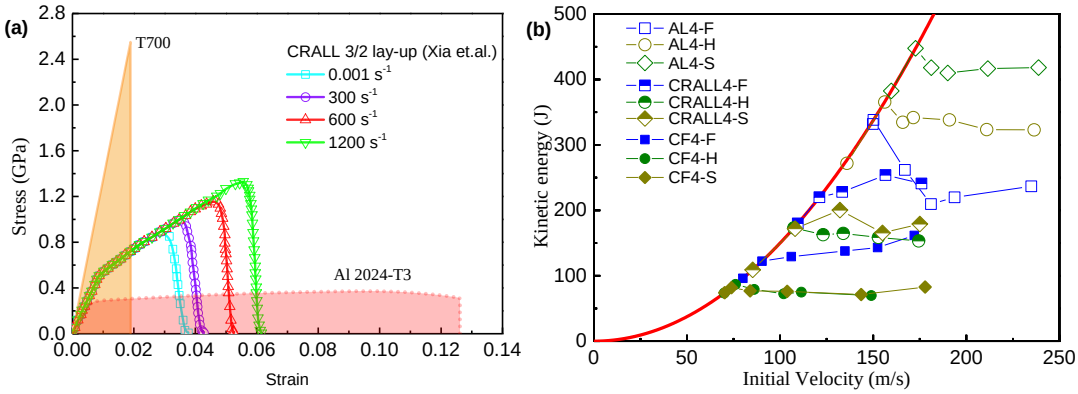

Fig.1(a) Tensile stress–strain curves of CFRP, CRALL3/2 and Al2024-T3 ; (b) Kinetic energy loss of projectiles after impact

Then in the high-velocity impact test, the plate deformation, failure modes and ballistic protective properties of CFRP, Al2024-T3 and CRALL targets were investigated under flat nose, hemispherical nose and sharp nose projectiles impacting. Results of this study show that, CRALL targets have significant advantages in mechanical performance, layers damage, ballistic limit and the impact energy absorption capability than carbon fiber composite materials (CFRP)[4]. CRALL targets the strongest impact resistance for flat

nose projectile impact than hemispherical nose and sharp nose projectiles. At similar thickness, the ballistic protection performance and energy absorption capability of CRALL targets achieved same level with aluminum alloy Al2024-T3.

This study provides the theoretical basis and reference value for the optimal design of lightweight protective structure under high-speed impact, has the important value in engineering application.

Keywords: Carbon fiber reinforced metal; ballistic test; failure mode; impact resistance

References

[1] Hoo-Fatt MS, Lin C, Revilock DM, Hopkins DA. Ballistic impact of GLARE™ fiber–metal laminates. *Composite Structures*. 2003;61:73-88.

[2] Xia Y, Wang Y, Zhou Y, Jeelani S. Effect of strain rate on tensile behavior of carbon fiber reinforced aluminum laminates. *Materials Letters*. 2007;61:213-5.

[3]Zhou Y, Wang Y, Jeelani S, Xia Y. Experimental Study on Tensile Behavior of Carbon Fiber and Carbon Fiber Reinforced Aluminum at Different Strain Rate. *Applied Composite Materials.* 2007;14:17-31.

[4] Wang S, Wu L, Ma L. Low-velocity impact and residual tensile strength analysis to carbon fiber composite laminates. *Materials & Design*. 2010;31:118-25.

ID043: Plastic Anisotropy of Nanofoam Aluminum Subjected to High Rate Uniaxial Compression

Minjie Diwu[1], Xiaomian Hu[2,a]

[1]Beijing Institute of Applied Physics and Computational Mathematics, Beijing 100088, China

[2]National Lab of Computational Physics, Beijing Institute of Applied Physics and Computational Mathematics, Beijing 100088, China

[a]hu_xiaomian@iapcm.ac.cn

Abstract: The mechanical behavior of nanofoam aluminum with low porosity (~3.3%) subjected to high rate (~$2\times10^{9}s^{-1}$) uniaxial compression was investigated using molecular dynamics (MD) simulations. The deformation was applied along the [100], [110] and [111] crystallographic orientations. At the onset of plastic deformation, pores acted as the source of dislocation nucleation, the leading Shockley partial dislocations nucleated at the same strain (3.8%) independent of applied loading directions. Due to the emission of trail partials, the accumulation of dislocation density can be divided in slow multiplication stage and fast multiplication stage by the dislocation density multiplication rate $d\rho_d/d\varepsilon$. There is a post-yield softening corresponding to the onset of rapid dislocation density multiplication at higher dislocation densities. When the loading direction was in [100] or [111], the dislocations were mainly consist of mobile dislocations, while when subjected to [110] compression, the mobile dislocation density was about one magnitude lower than the total dislocation density. Prismatic dislocation loops were formed gliding along loading direction when the loading was in [110], probably because of sufficient space for prismatic loops formation. These results reveal the significant influence of loading orientations on the patterns of dislocation movements.

ID044: Bending Collapse Behavior of Tubular Structure Under Impact

Minoru Yamashita[1, a], Naoki Kunieda[2] and Makoto Nikawa[1]

[1]Dept. of Mechanical Engineering, Gifu University, Gifu 501-1193, Japan

[2]Graduate student, Ditto.

[a]minoruy@gifu-u.ac.jp

Corresponding author: Minoru YAMASHITA, Prof. Gifu Univ., minoruy@gifu-u.ac.jp

Abstract: Three point bending test of aluminum tubular structure with hat cross-section was carried out under impact condition. The central portion of the structure was impacted at 10 m/s by the upper anvil attached to the drop-weight. The tubular material was an aluminum alloy A5052-H34 sheet with 1 mm thickness. The structure consists of a hat-shaped part fabricated with V-bending operation and a flat sheet. They are adhesively bonded at the flange with a thermosetting epoxide resin. In addition to the aluminum structure (standard structure), the structure with carbon fiber reinforced thermos-plastic (CFRTP) sheet was also tested. The sheet was also adhesively bonded. The objective of the present study is to exhibit the effect of such attachment on the deforming behavior in the bending.

Figure 1 demonstrates the collapse patterns for the standard structure and those with the CFRTP attachment at hat-top or hat-side. Different collapse modes are observed such that two buckling lobes caused by compressive force develop at hat-top in the standard structure, on the other hand, a large lobe is observed at the center in the CFRTP attached structures. The frictional coefficient affecting the deformation constraint at the interface between the upper anvil and the structural surface possibly dominates the mode, because it was measured to be about 0.5 or 0.2 for aluminum to aluminum or aluminum to CFRTP contact. The CFRTP sheet peels off and partially fractures in the case of hat-side attachment. Such behaviors also absorb the impact energy in addition to the plastic deformation of the aluminum material.

The anvil force during bending is exhibited in Fig.2. Peak force followed by the sharp decrease is observed for the case of the standard structure, which is a typical manner in bending collapse. The structural strength is increased in the early deformation stage by attaching CFRTP sheet compared with that of the standard structure. It is more prominent in the structure with hat-side attachment. Judging from that the sharp force

drop is not observed in the sheet attached structure, such attachment contributes to prevent catastrophic behavior, though the absorbed energy in 0 - 80 mm anvil stroke is almost equivalent for that of the standard structure and the effect of the attachment thickness is not clear.

(a) Standard (b) CFRTP at hat-top (c) CFRTP at hat-sides

Fig.1 Examples of collapsed structures in impact 3-point bending

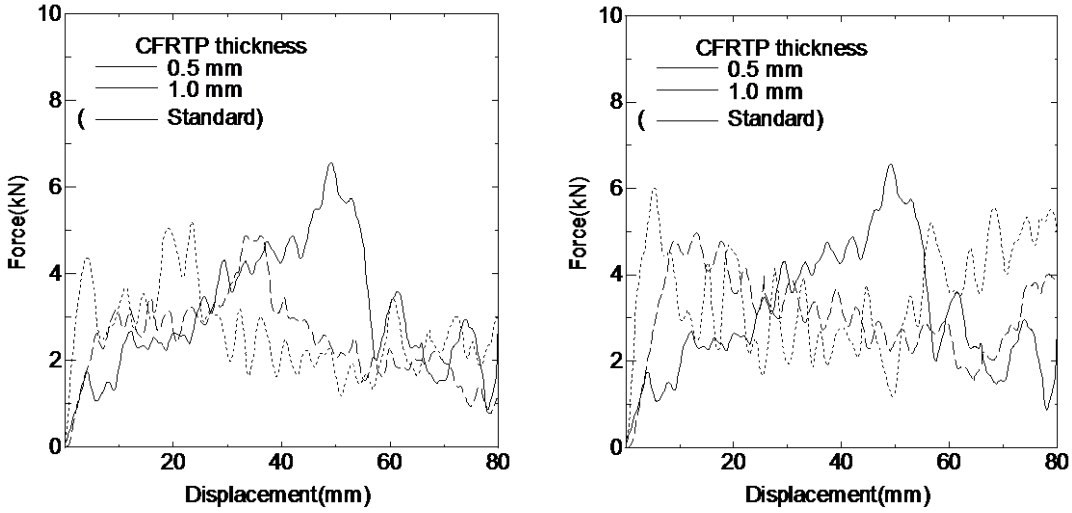

(a) CFRTP at hat-top (b) CFRTP at hat-side

Fig.2 Anvil force variation in impact 3-point bending

ID045: Impact Joining of Similar and Dissimilar Metal Plates at Their Edges

Minoru Yamashita[1, a], Yuki Tokushige[2] and Makoto Nikawa[1]

[1]Dept. of Mechanical Engineering, Gifu University, Gifu 501-1193, Japan

[2]Graduate student, Ditto.

[a]minoruy@gifu-u.ac.jp

Corresponding author: Minoru YAMASHITA, Prof. Gifu Univ., minoruy@gifu-u.ac.jp

Abstract: A novel plate joining method was proposed by one of the authors. It makes use of the thermally activated cut faces obtained by high-speed shear. The joining process is illustrated in Fig.1 [1]. A pair of metal plates to be joined is simultaneously sheared along the dotted line under high-speed condition. The material temperature elevates remarkably and it softens in the adiabatic shear band. The lower plate is stationary. The upper plate continues the downward motion, thus the cut face of the upper plate immediately contacts the lower cut face with slight overlap. The joining process is completed when the upper plate reaches the prescribed position. The present joining method is a kind of diffusion bonding which is known as solid-state welding technique.

In the present study, the test materials were a mild steel plate SPC with 3.2 mm thickness and a pure titanium plate TP340C with 3.0 mm thickness. Their tensile strengths were 303 and 401 MPa, respectively. The shearing punch was driven by the drop-hammer with 10 m/s impact velocity. The order of the strain-rate was roughly estimated 10^4 /s in high-speed shear. The combinations of SPC + SPC and TP340C + SPC plates were tested, where the overlap length was varied. Examples of joining boundaries are exhibited in Fig.2. Joining is achieved at the central portion in both cases, though the gap opening is observed near plate surfaces.

Applying the tensile force normal to the joining boundary plane, the joining efficiency α was evaluated by the following equation.

α = [Fracture stress in tension] / [Ultimate tensile strength] $\times$ 100 (%)

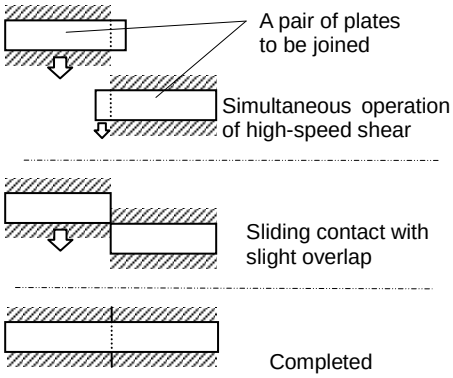

Fig.1 Impact joining process

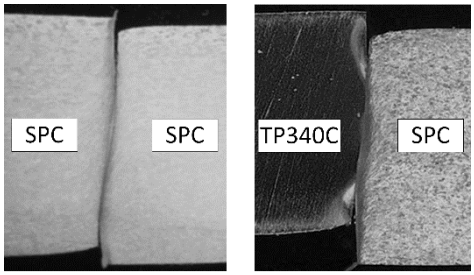

Fig.2 Joining boundary

The average joining efficiency is higher in the case of SPC + SPC joining than that of TP340C + SPC, as shown in Fig.3. The appearance of cut face obtained by high-speed shear was smoother in the SPC material. On the other hand, it was rather rough in TP340C. Hence, this may cause large scattering in TP340C + SPC joining.

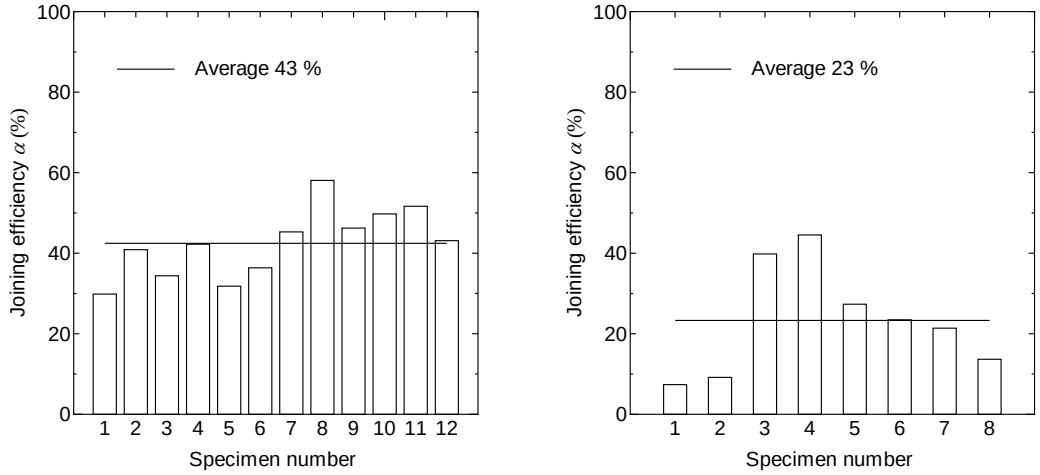

(a) SPC + SPC (b) TP340C + SPC

Fig.3 Joining efficiency (0.2 mm overlap length)

References

[1] M. Yamashita, T. Tezuka and T. Hattori: *Applied Mechanics and Materials* 566 (2014), pp379-384

ID046: Analysis Method of City Gas Pipeline Explosion Simulation and Consequences

MU Jie, Zhang Jinfeng, Huan wu, Xia yifeng, Wang shenghua
Scientific Research Institute of Work Safety of Zhejiang Province,Hangzhou,310012
E-mail: mujie108@163.com

Abstract: The pipeline explosion produces the damage effect, and the air shock wave will cause damage to the surrounding buildings. In some cases, the limited space of gas explosion is equivalent to the rationality of the TNT equivalent, and the corresponding numerical simulation model was established based on AUTODYN. It provides a new train of thought to buried pipeline explosion simulation. It Uses the established model to analysis the pipeline failure process under explosion load, damage rule and the attenuation law of explosion wave in the air of different buried depth and different wall thickness to establish a comprehensive index system of urban underground pipeline risk assessment and determine the safety standard to provide the reference. Get the following conclusion: TNT equivalent weight method used for buried pipeline explosion numerical simulation is a feasible method. Basing on the analysis results can effectively simulate the buried pipeline blast damage consequences; With the increase of buried depth, formation damage in the air damage range smaller, every 0.1m increase of buried depth, its air ultra reduce 4.5% - 5.1%; Every increase of pipe wall thickness 5mm, its air ultra reduce 8.3% - 12.1%.

Keywords: Buried pipeline explosion,numerical simulation,AUTODYN,security distance

ID048: The Diagnostics of the Reaction Zone of Condensed High Explosives at the Detonation

Nataliya P. Satonkina

Lavrentyev Institute of Hydrodynamics SB RAS, Novosibirsk 630090, Russia

Novosibirsk State University, Novosibirsk 630090, Russia

snp@hydro.nsc.ru

According to the Zeldovich – von Neumann – Doring (ZND) theory, detonation wave consists of the thin (several intermolecular distances) shock wave region, the chemical reaction zone, the Chapman – Jouguet plane (CJ point, CJP, in one-dimensional case), and the Taylor rarefaction wave. It is commonly accepted that the CJ point which divids the regions of subsonic and supersonic flows corresponds to the ending of the chemical reaction zone. However, a strict validation of the link between the ending of the chemical peak and the CJ point is absent. Since the chemical peak in the ZND model is defined as a region of high pressure, it is investigated solely using the time dependencies of the pressure obtained by different methods. Many authors note the difficulty to set the CJ point which is explained, for example, by an incomplete chemical reaction.

Data on the duration of the chemical peak show large scatter (for a review see [1]) as well as the different dependence on the charge configuration, density, length and diameter. This could be due to the absence of the universal way to find the singularity (the kink point) at the pressure profile, and also it indicates the methodical difficulties with the notions used.

Neither density nor pressure give the direct information on the chemical composition of the matter. Zeldovich and Kompaneets noted in their book on the detonation theory [2] that the detonation velocity, the mass velocity of the explosion products, and the pressure do not depend on the speed of the chemical reaction if the reaction mechanism ensures the tangent condition of the Michelson line and the Hugoniot adiabata.

An alternative method of diagnostic of detonation is connected with electrical conductivity.

In 1965, Hayes [3] proposed the correlation between the maximum value of the conductivity at the detonation and the free carbon content in the detonation products. The density of condensed carbon was obtained numerically taking into account the

compression of the medium in the detonation wave. The density was taken in the CJP, and the maximum value of the conductivity was used. In the works of Gilev [4,5], the relation between the maximum conductivity and the total carbon content was mentioned. There, based on the percolation model, the carbon content was claimed to be insufficient for the explanation of high conductivity in TNT (250 $Om^{-1}cm^{-1}$). The necessary existence of long highly conductive structures already in the chemical peak was pointed out.

In the work [6], the maximum value of conductivity for five HE is connected with the total carbon content, and the conductivity in the CJP is connected with the free condensed carbon. The correlation obtained from the experimental data allows us to claim that the conductivity in the whole detonation wave is provided by the carbon nets in conductive phase except the cases with low volume fraction of carbon (less than 0.07). Thus, the dynamics of conductivity tracks the evolution of carbon nanostructures.

In this work, a new method was proposed for the diagnostics of the state of the matter in the chemical peak region. The method is based on the link between the magnitude of electric conductivity and the amount of carbon condensed to nanostructures. The spatial distribution of conductivity provides the real time information by the tracing the carbon transition from a nonconductive state to a conductive one.

References

[1]. B. G. Loboiko, S. N. Lubyatinsky: *Combustion, Explosives, and Shock Waves:* Vol.36 (2000), N 6, p. 716.

[2]. *Theory of Detonation* by Ya. B. Zeldovich, A. S. Kompaneets: N.-Y.: Academic Press, 1960. 330 p.

[3]. B. Hayes, *in Proceedings of the 4th (International) Symposium on Detonation*, White Oak, Maryland, ACR-126 (1965), pp. 595-605.

[4]. S.D. Gilev and A. M. Trubachev, *in Proceedings of the 12th international Detonation Symposium*, San Diego, CA (2002), Paper No. ONR333-05-2, p. 240.

[5]. S.D. Gilev, *Doctoral dissertation*, Institute of Hydrodynemics, Novosibirsk, Russia, 2009.

[6]. N.P. Satonkina: *Journal of Applied Physics*, Vol. 118 (2015), pp. 245901-1 – 245901-4.

ID049: On Existence of Free Electrons at the Detonation of Condensed High Explosives

Nataliya P. Satonkina[1,2,a], Dmitry A. Medvedev[1,2,b]

[1]Lavrentyev Institute of Hydrodynamics SB RAS, Novosibirsk 630090, Russia

[2]Novosibirsk State University, Novosibirsk 630090, Russia

[a]snp@hydro.nsc.ru,

[b]dmedv@hydro.nsc.ru

Presence of free electrons can be detected investigating the electric properties of the medium.The question of high electric conductivity at the detonation of condensed high explosives occupies brains of researchers for more than 60 years. A model explaining all the experimental data is still missing.

There is a significant progress in understanding the electric properties at the detonation of gas mixtures. In the work [1], the electric conductivity due to the thermal ionization is considered. The model from [2] is used improved with the quantum mechanics. A comparison with experimental data is performed, and a good agreement is achieved. The model used is based on the presence of free electrons in detonation products. The formula used was derived in the approximation of rare collisions. This is valid for the detonation of gases but not applicable for condensed high explosives which have density three orders of magnitude higher than the density of gases. Despite the superficial similarity of the detonation process in gases and condensed explosives, the nature of electric properties is different, and the values electric conductivity differ by three orders of magnitude.

Hypotheses on the nature of electric conductivity in the chemical peak (von Neumann peak) and behind the Chapman-Jouguet point consider following conductivity mechanisms: thermal ionization, thermal emission, thermal ionization in a dense medium, chemoionization, ionic mechanism, contact mechanism, ionic mechanism due to ionization of water. Except the contact one, all these mechanisms are related to the presence of free electrons.

The analysis of data on the electric properties of four individual condensed high explosives (cyclotrimethylene-trinitramine, or hexogen (RDX), cyclotetramethylene tetranitramine, or octogen (HMX), pentaerythritol tetranitrate (PETN), trinitrotoluene

(TNT))bases on the experimental results of works [3-8] and the calculations of Tanaka [9] demonstrated the absence of free electrons at the detonation both in the region of the chemical peak and in the Taylor wave.

References

[1] X. Wang, D. Ye, and F. Gu: *Combustion, Explosives, and Shock Waves*. Vol. 44, (2008), N 1, pp. 101-109.

[2] D. H. Edwards and T. R. Lawrences: *Proc. Roy. Soc. London, Ser. A: Math. Phys. Sci.*, V. 286, 1965, P.415-439.

[3] A.P. Ershov, N.P. Satonkina, O.A. Dibirov, S.V. Tsykin, Yu.V. Yanilkin: *Combustion, Explosives, and Shock Waves*. Vol. 36 (2000), N 5, pp.639-649.

[4] A.P. Ershov, N.P. Satonkina, I.V. Ivanov: *Technical Physics Letters*. Vol. 30 (2004), N 12, pp. 1048-1050.

[5] A.P. Ershov, N.P. Satonkina, G. M. Ivanov: *Rus. J. Phys. Chem.* B. Vol.1 (2007), pp. 588 – 599. DOI: 10.1134/S1990793107060139

[6] A.P. Ershov, N.P. Satonkina: *Combustion and Flame*. Vol. 157 (2010), pp. 1022-1026.

[7] A.P. Ershov, N.P. Satonkina: *Combustion, Explosives, and Shock Waves:* Vol.45 (2009), N 2, pp. 205-210.

[8] N.P. Satonkina, A.A. Safonov: *J. Eng. Thermophys.* Vol. 18 (2009), N 2, pp.177-181.

[9] K. Tanaka, Detonation Properties of Condensed Explosives Computed Using the Kihara-Hikita-Tanaka Equation of State. National Chemical Laboratory for Industry, Tsukuba Research Center (1983).

ID050: Optimal Design of Polyurea Coated Aluminum Plates Under Hydrodynamic Loading. Does Side Matter?

O.Rijensky and D.Rittel

Mechanical Engineering Faculty, Technion- Israel Institute of Technology, Haifa, Israel

Abstract: We report on the dynamic behavior of a polyurea-coated 6061 aluminum plate under hydro dynamic loading condition. The plate's deflection was measured using ultra-fast stereoscopic photography, and analyzed using 3D-DIC (digital image correlation) technique. The residual deformation of the plate after several shocks was measured using conventional cameras and the DIC technique. The experimental results show the benefits of the polyurea coating, and clearly show that polyurea will better mitigate the shock if positioned on the side in contact with water. Preliminary numerical results are shown to shed some light on the experimental results.

1. Introduction

Wave slamming endangers the structural integrity of planning boats [1]. The eventuality of hull breaching increases significantly with the speed of the boat, and therefore becomes a prime concern for the design of fast vessels. To reduce the risk of hull breach, lightweight and flexible polyurea coating of the aluminum hull plates can be considered as a means to keep the vessel impervious for some time**.**

This experimental study examines the performance of polyurea coated aluminum plates in comparison with uncoated aluminum plates. The study shows the potential of the polyurea as an active load-carrying member in case of hydrodynamic loads. It is also observed that the nature of the fluid-structure interaction, between the water and the tested plate, affects the overall momentum history absorbed by the plate due to shocks in the water. This interaction emphasizes the importance of the *selection of the coated side of plate*. We will characterize the resultant structural behavior when hydrodynamic loads encounter a layer of (initially) soft polyurea, or the tougher aluminum side. We will show that, just by changing the coated side, one can significantly improve the performance of the hull plates. The study consists of experiments aimed at simulating violent hydrodynamic loads that mimic wave slamming at high cruising speeds.

2. Experimental and results

A compressed air gun was used to accelerate a steel projectile onto an incident bar (Hopkinson bar setup). The impact induces an elastic stress wave which propagates along the incident bar. The latter is positioned in contact with the back side of a piston confined by a pressure cylinder. As the stress wave reaches the piston, it compresses the water inside the cylinder to create a hydrodynamic shock wave. The shock wave propagates through the water, and the pressure history is measured via a fast response pressure sensor. It then hits almost immediately the target plate. The hydrodynamic shock was inflicted onto three aluminum alloy plates. The deforming plate was photographed with video cameras at a rate of 2 fps. Those "static" images, showing the plate between consecutive shocks, were taken with aims to measure the accumulated deflection of the plate as a result of repeated shocks. To record the dynamic behavior of the plate, A Kirana ultra-fast camera, equipped with Loreo split lens was used. the Kirana camera was triggered to record 180 consecutive photos of the deforming plate. The Loreo split allows capturing a stereographic image with the use of a single camera (similar to the technique described in [2]). The images obtained from both sets of cameras were analyzed using Match-ID 3D-DIC [3]software to measure the three dimensional full field strain and plate deflections.

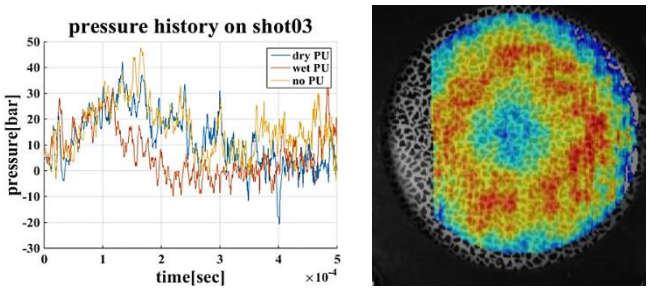

Figure 1. (a)pressure history recorded during shot 03 with all three specimens
(b) deflection of the plate as obtaind form the DIC analysis

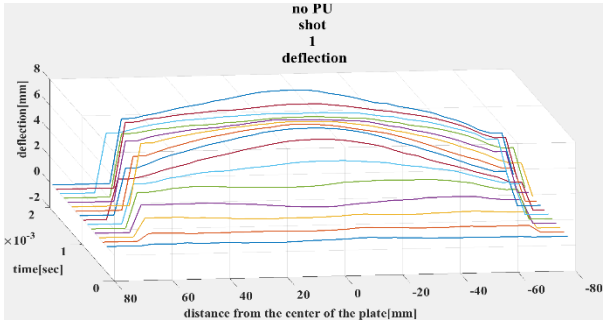

Figure 2. Deflection of a cross section of the plate as it changes during the shock

3. Conclusions

Full field recordings of deflections and strains of the deforming plates were obtained with the use of a single camera 3D-DIC technique. Results show both different behaviors of the coated and uncoated plates, as well as the change in overall performance after 11 consecutive shots. A significant improvement in performance can be achieved just by selection of the polyurea coated side of the plate.

Acknowledgements

The authors would like to acknowledge the financial support of the MAYMAD program under grant 2020391.

References

[1] O. M. Faltinsen, M. Landrini, and M. Greco, “Slamming in marine applications,” *J. Eng. Math.*, vol. 48, no. 3/4, pp. 187–217, Apr. 2004.

[2] K. Genovese, L. Casaletto, J. A. Rayas, V. Flores, and A. Martinez, “Stereo-Digital Image Correlation (DIC) measurements with a single camera using a biprism,” *Opt. Lasers Eng.*, vol. 51, no. 3, pp. 278–285, Mar. 2013.

[3] P. Lava and D. Debruyne, “MatchID*2010* ”,.

ID051: Development of High Voltage Pulsed Power Device Using Compact Marx Generator for Food Processing

Osamu Higa[1,2,a], Kazuki Tokeshi[1,b], Shoichi Tanifuji[1,c], Kazuyuki Hokamoto[2,d] and Shigeru Itoh[1,2,e]

1 National Institute of Technology, Okinawa College, 905 Henoko, Nago ,Okinawa, 905-2192, Japan

2 Kumamoto University, 2-39-1 Kurokami, chuuou-ku, Kumamoto, 860-8555, Japan

[a]osamu@okinawa-ct.ac.jp, [b]ic121226@edu.okinawa-ct.ac.jp,

[c]tanifuji@okinawa-ct.ac.jp, [d]hokamoto@mech.kumamoto-u.ac.jp,

[e]itoh_lab@okinawa-ct.ac.jp

Abstract: We have been researching generating technology of underwater shock wave using high voltage discharge in water [1]. Additionally, we aim to apply the underwater shock wave to a food processing [2]. However, our device have disadvantage such as a slow generation cycle, excessive discharge energy. Therefore, purpose of this reserch is to develop the shock wave generating device such as lower charging energy and faster operating cycle. We developed the device based on Cockcroft-Walton circuit and Marx generator. The device have capacity of charging energy of 0.3kJ, operating cycle is 30 shot/minutes. In experiment, the voltage current characteristics was measured, and the underwater shock wave visualized (Figure 1) by schlieren method using a high speed camera for the purpose of to estimate the peak power and the shock wave. As a results, the peak power of 3.2MW was rapidly applied to the underwater electrode, the shock wave was observed such as that the propagation velocity of 1490m/s and the shock pressure of several MPa. It was shown that the device is benefit to the food processing.

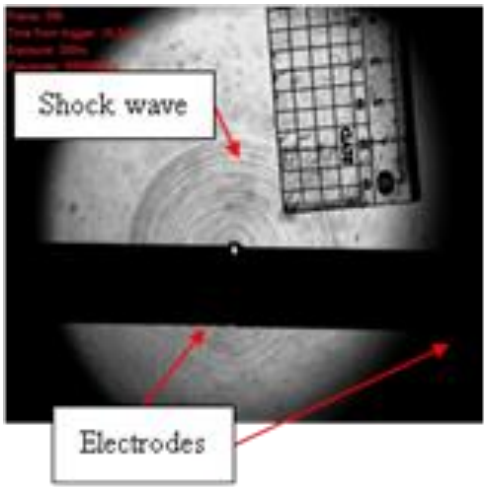

Fig. 1 Photograph of under water shock wave caused by spark discharge

References

[1] O. Higa, K. Higa, H. Maehara, S. Tanaka, K. Shimojima, A. Takemoto, K. Hokamoto, S. Itoh: The International Journal of Multiphysics, Vol.8, No.2 (2014), pp.245-252

[2] K. Shimojima, O. Higa, K. Higa, Y. Higa, A. Takemoto, A. Yasuda, M. Yamato, M. Nakazawa, H. Iyama, T. Watanabe, S. Itoh: Japan journal of food engineering, Vol.16 No. 4 (2015), pp.297-302

ID052: The Influence Analysis of Flat Steel on Loading of Explosive Inside Closed Cabin

Pan Chen[1, a]

[1]China Ship Development and Design Center, National Key Laboratory on Ship Vibiration &Noise, Hubei Wuhan 430064, China

[a]panda3267@126.com

Abstract: Explosive loading was one of the loadings of warship structural under anti-ship missile. The computing method of explosive loading inside closed cabin was the key of accurate calculating the response of stiffened plates. Warship cabins were made up by stiffened plates and stiffeners on one side of siffened plate, so buikheads were palte or stiffened plate. Numerical method was used in studying the influence of flat steel on loading of ecplosion inside closed cabin. Flat steel has obvious influence on explosion loading inside cabin, converging shock waves were formed on the side towards blasting source. The diffraction effect of explosion shock wave on another side of flat steel was analyzed, and reflceted shock waves of bulkheads were propagating between buikheads until the pressure of cabin become equivalent .

Keywords：Explosive inside cabin, stiffened plate, converged shock wave, reflected shock wave

Introduction

The environment of warship cabins was closed, the research of shock wave loading of explosion inside cabin was the key of calculating the response of warship cabin structures. A series of experiments and simulations of explosion of TNT inside cabin were researched [1], shock waves and reflected waves were analyzed. Experiments of explosion of different equivalent TNT with different shapes in closed cabin were done [2], the experiment results showed that peak pressure of axial shock wave was larger than peak pressure of radial shock wave. Experiments of explosion on the ground were studied [3,4], and explosive loading that act on structures on the ground was obtained. Experiments and numerical methods were used in studying the explosion loading of explosion inside cabin with vent [5], and a simplified calculation method of pressure of explosion inside cabin was present. A experiment of explosion in scale model of typical

ship cabin was researched [6], converging shock wave and intensity of shock wave in cabin corner were analyzed. A seriesof experiments of explosion of different equivalent TNT in closed cabin were done [7,8], characteristic of explosion loading inside cabin and three different transition corners effect on converging shock wave in cabin corner were researched. The above processes were explain by accurately numerical calculation. Based on the reliability of numerical method, the influence of bulkhead with or without flat steel on explosion loading inside cabin were analyzed in this paper.

1. The verification of numerical calculation

In order to research the peak overpressure of shock wave, impulse and arrival time of shock wave of explosion inside cabin, series of experiments of explosion inside closed or unclosed cabin were carried out [9], see Fig.1, fully-closed, 3/4 closed, 1/2 closed and 1/4 closed conditions were considered in this equipment, the influence of close extent on pressure of measure points were explored.

Fig. 1 Experiment equipment

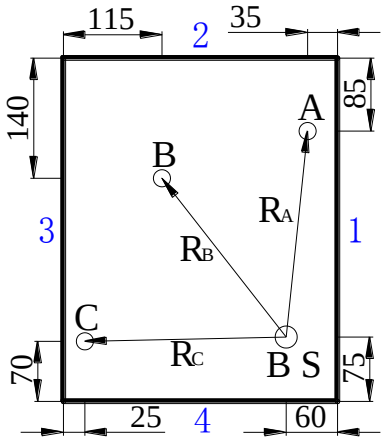

Fig. 2 Arrangement of points

The arrangement of measuring points in experiment could be seen Fig.2, the position of the larger circle(B S) was blasting source, measure point A, B and C were set on the deck. The respective distance between measure point and blast source was R_A=241mm, R_B=251mm, R_C=235mm. TNT mass in blasting source was 0.106g. The dimension of equipment was 400×320×250mm, walls of equipment was rigidity fibreboard in 16mm. Numerical method was used to simulate experiment conditions, simultaneously, pressure of points were compared and analyzed.

The state equation of ideal gas of air inside cabin in numerical calculation was:

$$p=(\gamma-1)\rho e \tag{1}$$

γ, ρ and e, respectively, was specific heat ratio, density and internal energy of air. Correspondingly, the value was $\gamma = 1.4$, $\rho = 1.225\times10^{-3} g/cm^3$, $e = 2.068\times10^5 \mu J$ in numerical calculation.

JWL state equation of TNT in paper was:

$$p = C_1\left(1-\frac{\omega}{r_1 v}\right)\mathrm{e}^{-r_1 v} + C_2\left(1-\frac{\omega}{r_2 v}\right)\mathrm{e}^{-r_2 v} + \frac{\omega \mathrm{e}}{v} \tag{2}$$

C_1, C_2, r_1 and r_2 were constant and concrete parameters can be seen in Tab.1.

Tab.1 Parameters of state equation of TNT

C_1 ($10^{11}Pa$)	C_2 ($10^{11}Pa$)	r_1	r_2	ω	Density ρ(kg/m^3)	Detonation velocity D(m/s)	CJ Pressure ($10^{11}Pa$)
3.738	0.03747	4.15	0.9	0.35	1630	6930	0.21

Euler-FCT method was used in numerical calculation. The shape of explosive TNT was spherically cylindrical. Firstly, explosion process was calculated in two-dimensional space, the calculation was stopped before shock wave arrived at the cabin wall. The result in two-dimensional space was mapped to three-dimensional space and the computation continued. Take computing power and computational accuracy into account, selected 4000 as grid density in two-dimensional space after multiple computations. Selected 65×80×50 as grid density in three-dimensional space, and the total amount of Euler element in three-dimension space was 260000. Flow-out boundary was set in simulation model with open boundary.

Pressure curves of measure points were given. Under several typical conditions, pressure curves of measure point A were seen in Fig.3-Fig.6. The contrasting results between simulation and experiment can be seen in follow figures.

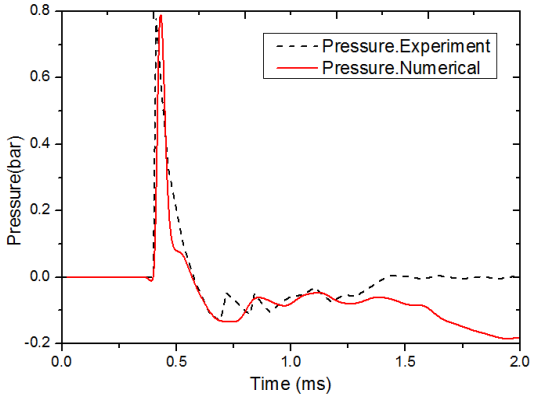

Fig. 3 Pressure of point A(Wall 1)

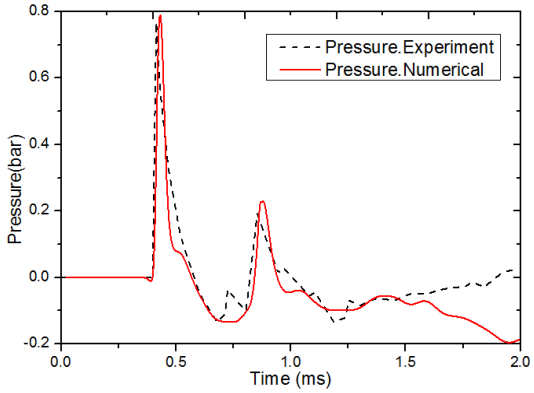

Fig. 4 Pressure of point A(Wall 1, 2)

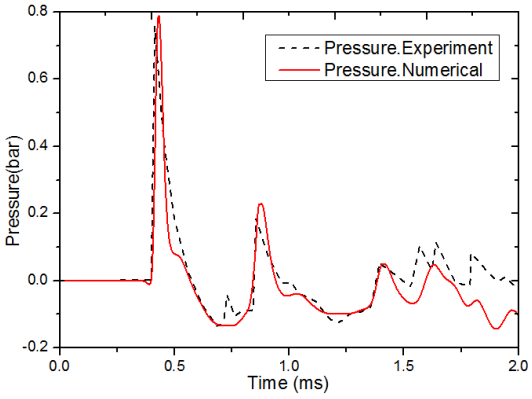

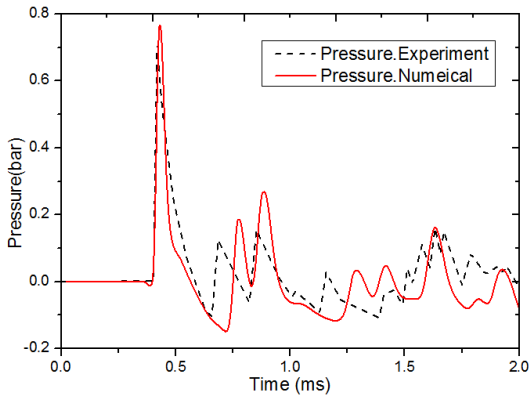

Fig. 5 Pressure of point A(Wall 1,2,3) Fig. 6 Pressure of point A(Wall 1, 2,3,4)

Pressure curves comparison between simulation and experiment of measure point A can be seen in Fig.3(condition: Wall 1), arrive time and peak pressure of initial shock wave were simulated in simulation method. Peak pressure between experiment and simulation only was separated by 0.3 percentage points. Pressure curves comparison between simulation and experiment of measure point A can be seen in Fig.4(condition: Wall 1 and2). Except for simulating arrive time and peak pressure of initial shock wave well in simulation method, also arrive time and peak pressure of reflected shock wave on wall 2 well was. Smaller reflected peak pressure for the long propagating travel was captured by measure point A. Pressure curves comparison between simulation and experiment of measure point A can be seen in Fig. 5(condition: Wall 1, 2 and 3). Arrive time and peak pressure of initial shock wave and reflected waves of other walls well were simulated in simulation method. Pressure curves comparison between simulation and experiment of measure point A can be seen in Fig. 6(condition: Wall 1, 2, 3 and 4), simulate arrive time and peak pressure of initial shock wave and reflected waves of other walls well in simulation method. Except for very small difference in arrive time of shock wave, pressure temporal curves of simulation and experiment overlap well. Simulation results were less than experiment results after 1.25ms in Fig.3 and Fig.4, and simulation results were less than experiment results after 1.5ms in Fig.5. This phenomenon could be explained as follow, flow-out boundary was the model boundary, while air can't flow in the model, so low pressure aroused after initial shock wave. Simulation and experiment had almost some peak pressure, because this case was in enclosed cabin air can't flow out or flow in, in other words, simulation and experiment have some boundary.

From the comparison between simulation results and experiment results, the

numerical method of simulating impulse, arrive time and peak pressure of shock wave in explosion inside cabin well was verified. This method was better in simulation of reflected shock wave of various walls.

2. Analytical model

The stiffened plate specifications could be seen in reference [6], in this paper, three dimensional spatial domain model was selected, which was 600mm×600mm×600mm. Supposing explosives were placed in the middle of the cabin, considering XYZ symmetric, take 1/8 space of the computational domain. Calculation stiffened plate was showed in Fig. 7. Consider only unidirectional reinforcement stiffened plate, there are two single reinforcement in space of 200mm. To study the shock wave propagation characteristic on the cabin, the reinforced rib is flat steel and the size was 60mm×3mm.

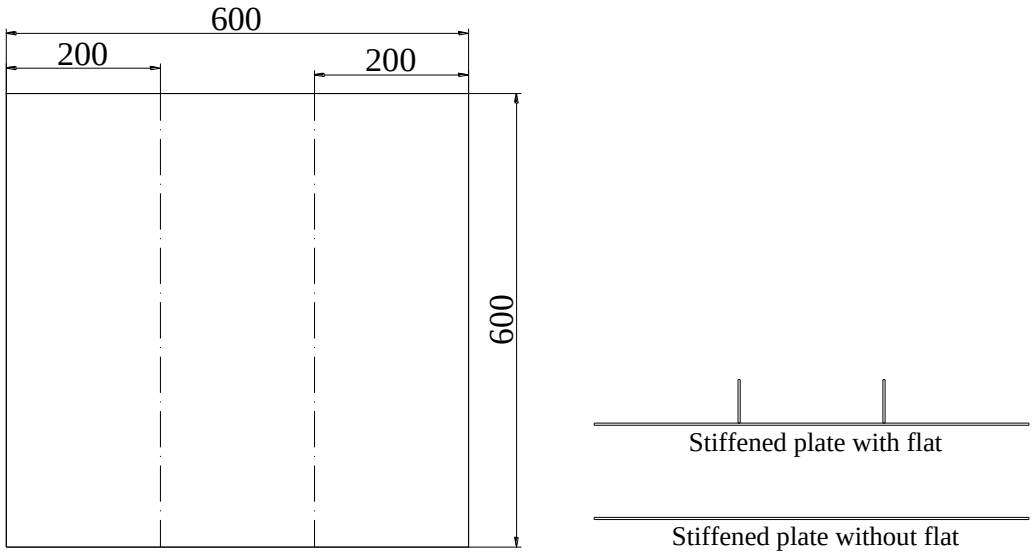

Fig.7 Two different stiffened plates

Explosion shock wave in closed cabin was calculated by using Euler-FCT solver in Autodyn code. Explosive was spherical and the equivalent mass was 2.24 kg, the spherical radius was 68.98mm. The mapping techniques was applied to calculate shock waves. Firstly, the spherical explosive in one dimensional space was simulated. The calculation was carried on until the blasting shock wave was close to the ground or the reinforced. One-dimensional result was transformed to three-dimensional space by mapping method and the calculation continued.

The distance between explosive source and stiffened plate was 300mm. The shock

waves propagated in near field of space, follow-up pressure accuracy depended on this result. Firstly, the calculations of different mesh density in one-dimensional was compared, on this case, one-dimensional wedge radius was 300mm and explosive was placed in the center. Pressure measuring point was arranged in axial direction, see Fig. 8. The surface explosive load was particular concerned, the measuring point nearest wall was selected to assess the pressure. Therefore, measuring point 9 and 10 were selected to compare the measuring pressure, the corresponding numerical results were shown in Table 2.

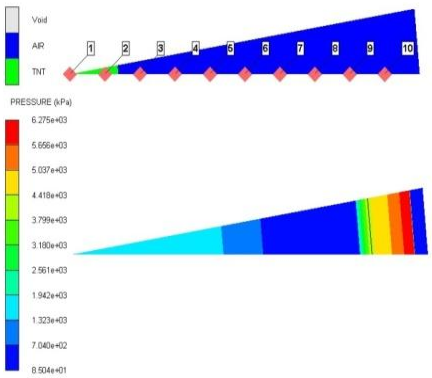

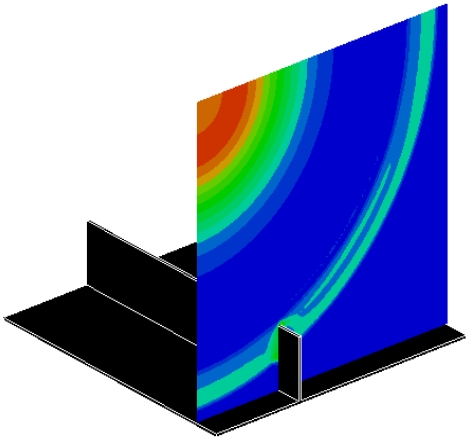

Fig.8 Shock wave in one-dimensional space Fig.9 Simulation model of shock wave

Table 2 Pressure peak under different mesh sizes

Condition	Charge mass（*kg*）	Mesh density	Point 9 （*kPa*）	error	Point 10 （*kPa*）	error
1	2.24	2000	7098.7	-	6350.9	-
2	2.24	5000	8167.1	15.05%	6419.6	1.08%
3	2.24	10000	8243.8	0.94%	6493.2	1.15%
4	2.24	25000	8255.5	0.14%	6537.1	0.68%
5	2.24	50000	8324.2	0.83%	6601.6	0.99%

With the increase of the mesh density, the computation accuracy was increased. However, with the mesh density increased, the computing consuming-time increased significantly. So peak pressure of different measuring points in different mesh density were compared. According to result comparisons and analysis, the calculation result of mesh density in 25000 was selected as the mapping load. Compared result of 10000 mesh density to 25000 mesh density, the error percent was smaller. The calculation results in one-dimensional space was mapped to three-dimensional space, The size of calculation spatial cabin was 300mm×300mm× 300mm, and 100 × 100 × 100 mesh density was selected as three-dimensional grid and the number of total Euler-element was one million. In order to better simulate the coupling between shock wave and stiffened plate, stiffened

plate was modeled by solid element. Relationship between Euler of air and Lagrange of stiffened plate was fully coupled, numerical model was shown in Fig. 9.

3. Analysis of shock wave propagation in cabin

Shock wave propagation screenshots were extracted on working conditions with or without flat steel. Fig. 10 showed shock wave propagation at 0.055ms, at this time the shock wave had not yet reached the bulkhead, but the shock wave had reached the upper end of the flat steel.

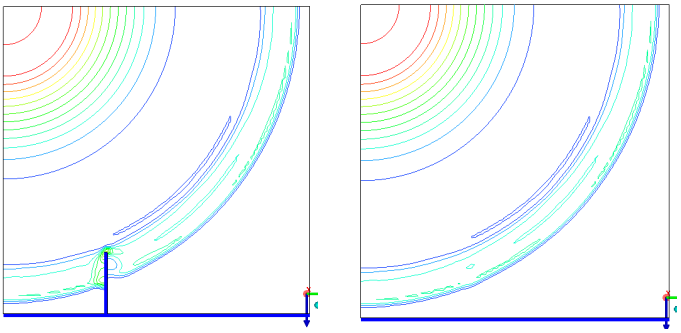

Fig.10 Shock wave at 0.055ms in closed cabin

Since the steel flat blocked the propagation of shock wave, explosive shock wave reflected on the side direction to source, while the another side was facing the diffraction shock wave, the pressure values between two sides were different largely. The condition without flat steel, shock wave was distributed evenly at the same place. Fig. 11 showed the propagation state of shock wave at 0.065ms, at this time, shock wave had reached the bulkhead and shock wave reflection had happened. The existence of flat steel resulted in the gathered shock wave, which was at the place of root of the flat side toward the explosion source. Since the flat steel blocked the propagation of shock waves, wave pressure on the other side of flat steel could be negligible.

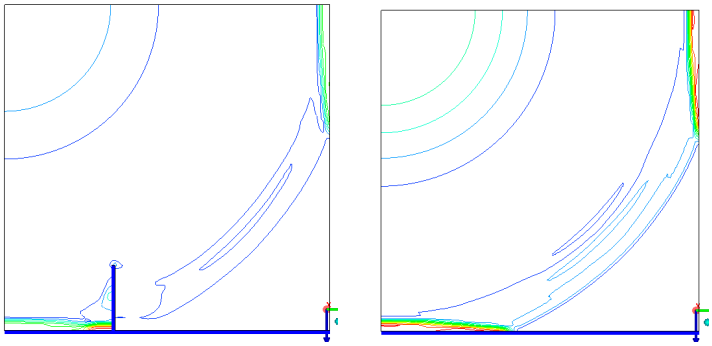

Fig.11 Shock wave at 0.065ms in closed cabin

Fig.12 showed the propagation state of shock wave at 0.085ms, shock wave between flat steels propagated back and forth. Shock wave gathered gradually along the direction of height of flat steel. At this time, shock wave arrived at the plate that between flat steel and bulkhead, and shock wave gathered at the connection of the bulkhead and plate. Fig. 13 showed the propagation of shock wave at 1.405ms, the shock wave gathered at the intersecting of flat steel and plate corner, another stronger shock wave was formed again.

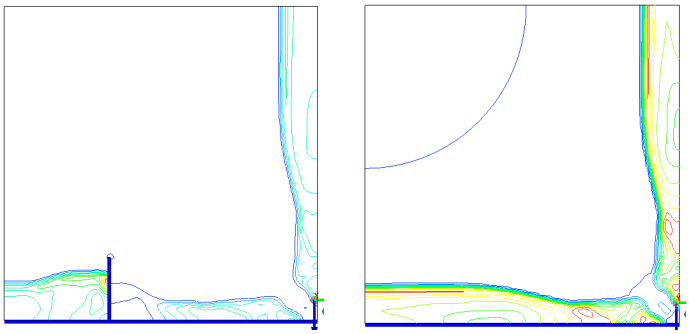

Fig.12 Shock wave at 0.095ms in closed cabin

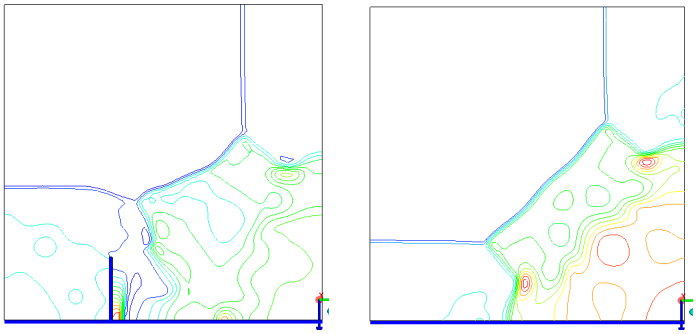

Fig. 13 Shock wave at 1.405ms in closed cabin

Initial shock wave propagated from the explosion source outwardly in spherical shape, when shock waves arrived the bulkhead wall, the shock waves continued spreading along the wall. For stiffened plate, when the shock waves encountered flat steel, the converged shock wave was formed in corner between plate and flat steel. Since the shock wave propagation was blocked by flat steel, shock wave diffract along the stiffeners , which resulted in lower shock wave peak pressure behind the flat steel.

4. Analysis of shock wave at typical region

In order to analyze the influence of the stiffener on shock wave loading of explosion in closed cabin, 7 measuring points were selected on explosion source plane. The distribution of measuring points were shown in Fig. 14, the measuring points A and B were below the explosive source, meeasuring points C and D were on the side of flat steel

that toward to blast source, measuring point C was located at the top of flat steel and measuring point D was located at the corner of flat steel and plate. Measuring points E and F located at another side of flat, measuring point E located at the top of flat, measuring point F located at the corner of flat steel and plate. Measuring point G located on the plate.

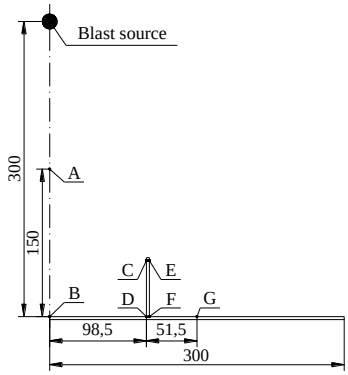

Fig. 14 Arrangement of points

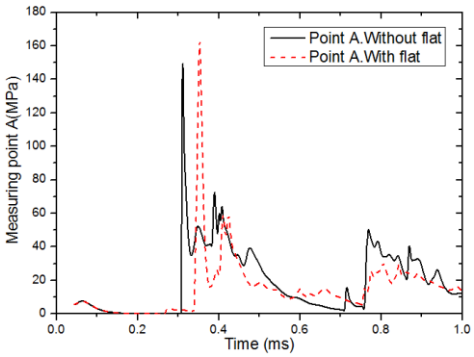

Fig. 15 Pressure curves of point A

Fig. 15 showed time-history pressure curve of point A, mapped region took 200mm over the measuring point A, so the initial shock wave can't be captured. The reflected shock wave was captured at 0.065ms, for the reason of shock wave meet no structural barriers, the arrival time, peak and attenuation trend were the same between two conditions. The maximum shock values were captured both on two conditions at nearby 0.3ms, because of the shock wave back and forth propagation in the cabin, this peak pressure was formed. Which phenomenon would continue until cabin pressure become evenly. Therefore the peak pressure captured by point A at 0.75ms was oscillation shock wave, this pressure peak had been reduced substantially comparing to peak pressure at 0.3ms.

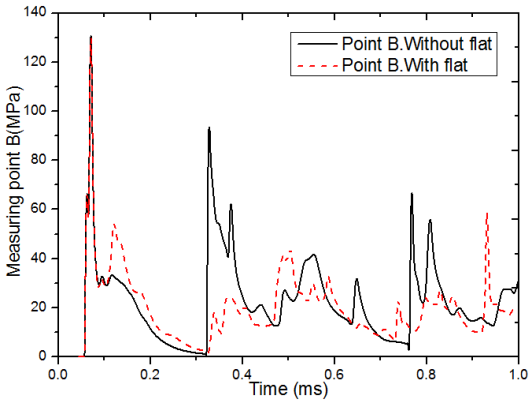

Fig. 16 Pressure curves of point B

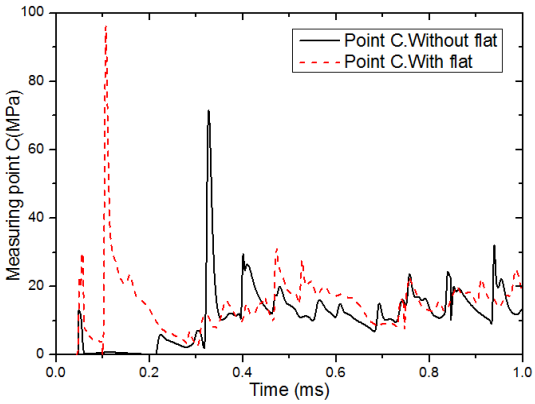

Fig. 17 Pressure curves of point C

Fig. 16 showed time-history pressure curves of point B, measuring point was located at the center of stiffened plate. Pressure curves were consistent in 0.08ms on conditions with or without flat, at this period time, the reflected wave on the plate wall were measured. Because the shock wave was subject to no blockage, two pressure history curves were fully consistent. After the initial peak pressure, pressure captured by measuring point B was decreased exponentially. Pressure peak was captured again near 0.1ms, this peak pressure was reflected on sidewall, then the reflected wave was weakening in the condition without flat. Pressure peak was captured by measuring point B once again on the condition with flat, the peak pressure was reflected on flat web, the propagation distance from flat web was relatively shorter than reflection shock wave on sidewall. Therefore, reflection shock wave on flat web had a larger peak pressure. Two pressure curves were different after 0.08ms, especially at nearby 0.3ms, from upper segment that point A know that this peak pressure was reflected pressure of bulkhead, point B catch the reflected shock wave from bulkhead on the condition without flat steel. On the condition with flat steel, point B didn't catch reflected pressure because reflected pressure from bulkhead was blocked by flat steel. On the condition with flat, the captured peak pressure was smaller than with flat. The pressure at nearby 0.76ms could be explain by the same reason.

Fig. 17 showed time-history pressure curves of point C on two conditions. Shock wave arrived measuring point C at 0.065ms. On the condition without flat, measuring point was located in air field, the captured pressure was the initial shock wave. On condition with flat, measuring point was located at the place toward to blast source end of flat steel. The pressure captured by measuring point was reflected on flat. On two conditions, although the shock wave arrived simultaneously, the types of captured shock wave varied. So the peak of pressure curves were completely different, the peak of reflected wave from flat was bigger. At about 0.107ms, the peak pressure was captured once again by measuring point. On the condition without flat, reflected shock wave was captured, due to propagation distance increased, its peak pressure was lower than initial shock wave peak pressure. On the condition with flat, the captured peak pressure was greater than the initial shock wave peak pressure, for shock wave collect between flat steels, shock wave captured by measuring point was converged shock wave.

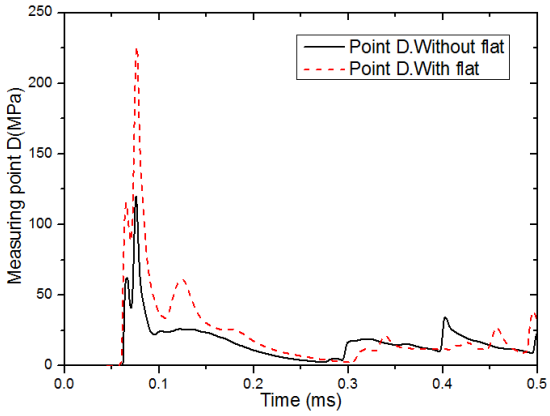

Fig. 18 Pressure curves of point D

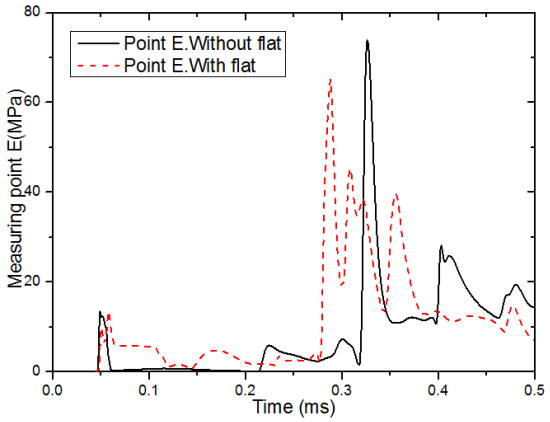

Fig. 19 Pressure curves of point E

Fig. 18 showed time-history pressure curves of point D, reflection shock wave from wall was captured at 0.075ms on the condition without flat. Converging shock wave form at the corner between plate and flat steel. The measuring point was located at the corner, converging shock wave was caught by point, and this peak pressure was larger than the condition without flat.

Fig. 19 showed time-history pressure curves of point E, shock wave arrived at measuring point E at 0.046ms. The condition without flat had no blockage, the incident wave was caught by measuring point. The condition with flat, shock wave cannot directly reach the measuring point, so the diffraction pressure was measured, which was lower than the pressure of condition without flat. However, due to the presence of flat steel, the converging shock wave was formed at the corner between plate and flat. Therefore, converging shock wave was captured at about 0.06ms after the initial shock wave.

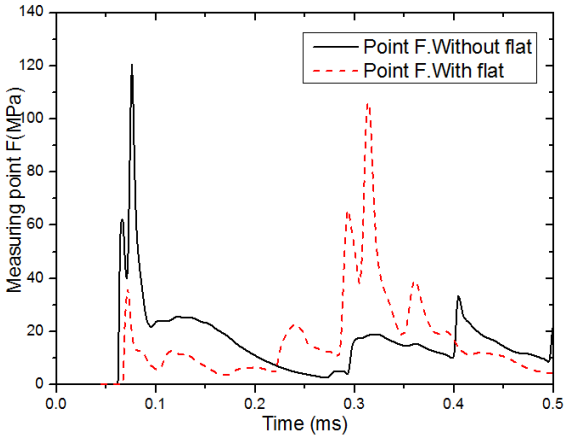

Fig. 20 Pressure curves of point F

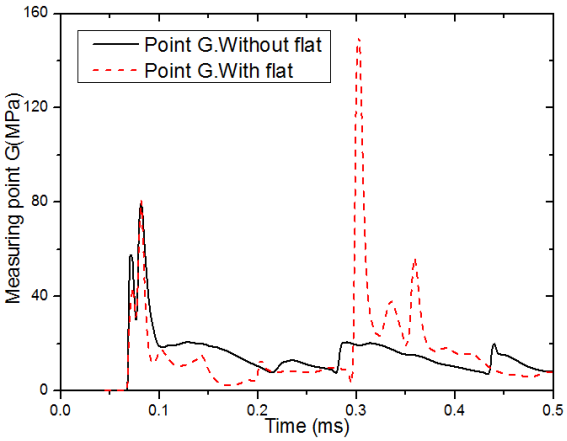

Fig. 21 Pressure curves of point G

Fig. 20 showed time-history pressure curves of point F. On the condition without flat,

reflected shock wave was captured at 0.062ms. However, on the condition with flat, shock wave was captured at 0.067ms. The reason for the longer time was the existence of flat which had influence on the propagating of shock wave. The diffraction shock wave was measured on the condition with flat, so peak pressure of condition with flat was smaller than peak on condition without flat. Shock wave peak pressure was captured once again about 0.3ms, the shock wave was propagating back and forth. Because measuring point F was located at the intersection of flat and bulkhead, shock wave was propagating back and forth between flat and bulkhead, so shock wave of back and forth was captured.

Fig. 21 showed time-history pressure curves of point G. Flat had no influence on the initial shock wave of measuring point G, so the initial shock peak and arrival time were the same on two conditions. However, due to the presence of flat, the shock wave between the flat and bulkhead was converging and propagating back and forth. Finally, a larger converging shock wave was captured at 0.3ms.

5. Conclusions

Firstly, an experiment was carried out to verify the reliability of numerical method that computed the shock wave inside cabin. The influence of flat steel on the propagation of shock wave was analyzed. The time-history pressure curves of measuring point in typical area were compared and analyzed. The conclusions were as below:

1. The presence of flat has a significant effect on shock wave propagation in closed cabin, which could block shock wave propagation along the bulkhead and shock wave converged at the connection of flat and bulkhead.

2. After shock wave arrived at the bulkhead, shock wave oscillated back and forth between flats or between flat and bulkhead, finally converged at the corner to form a strong shock wave until pressure evenly in cabin.

3. The flat steel in cabin had a certain influence on oscillation time and pressure peak of follow-up shock wave in cabin, especially the pressure distribution nearby flat steel.

Reference

[1] A. Zyskowski, I. Sochet, G. Mavrot, P. Bailly, and J. Renard: *Journal of Loss Prevention in the Process Industries* 17.4(2004), pp291-299

[2] C. Wu, M. Lukaszewicz, K. Schebella, and L. Antanovskii: *Journal of Loss*

Prevention in the Process Industries 26.26(2013), pp737-750

[3] K. Cheval, O. Loiseau, V. Vala: *Journal of Loss Prevention in the Process Industries* 25.3(2012), pp 436-442

[4] S. Tr dat, I. Sochet, B. Autrusson, O. Loiseau, and K. Cheval: *Shock Waves* 16.4-5(2007), pp349-357

[5] V.R. Feldgun, Y.S. Karinski, D.Z. Yankelevsky: *International Journal of Impact Engineering* 38.12(2011), pp964-975

[6] H.L. Hou, X. Zhu, W. Li, and Z.Y. Mei: *Journal of Ship Mechanics* 14.8(2010), pp901-907

[7] X.S. Kong, W.G. Wu, J. Li, P. Chen, F. Liu: *International Journal of Impact Engineering* 65.2(2014), pp146–162

[8] X.S. Kong, W.G. Wu, X.B. Li, S.X. Xu, and T. Huang: *Chinese Journal of Ship Research* 4.4(2009), pp7-11

[9] P.E. Sauvan, I. Sochet, S. Tr dat: *Shock Waves* 22.3(2012), pp253-264

ID053: Simulating Texture Development of Polycrystalline Aluminum Under Shock Loading Conditions

Hao Pan[a] , Xiaomian Hu, Zihui Wu

Key Laboratory of Computational Physics, Institute of Applied Physics and Computational Mathematics, Beijing, 100088, China

[a] panhao1979@sina.com

Abstract: Dynamic response of polycrystalline metals is very complex which includes many mechanisms and effects. Polycrystalline texture development under dynamic loading attracted much attention because of interesting phenomena and great challenges to experiment and simulation. The objective of the present work was to gain insight into the inelastic deformation mechanisms that govern the response of shocked single and polycrystalline aluminum. We improve the elasticity, dislocation dynamic and work hardening formulation in the crystal plasticity model to suffice for the microstructures development at high pressure and strain rates. Strength data of polycrystalline under high pressure are used to calibrate model's parameters. Taylor hypothesis and crystal plasticity finite element method (CPFEM) are used to model the texture development of polycrystalline aluminum under shock wave loading separately. The calculated results indicate grains have an obvious rotation especially at high pressure. The velocity profile of polycrystalline Al/LiF calculated by the thermoelastic-viscoplastic crystal plastic model shows a phenomena of quasi-elastic releasing which is close to the experiment.

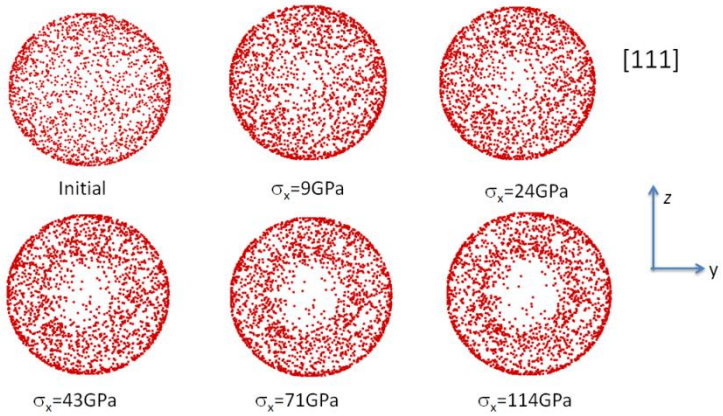

Fig.1 Texture evolution of polycrystalline Al at high pressure and strain rates

ID054: The Effect of In-situ Stress on Rock Cracking Process During Pre-split Blasting

Qi He[1,2,a], Peng Yan[1,2,b], Wenbo Lu[1,2], Ming Chen[1,2], Gaohui Wang[1,2]

[1]State Key Laboratory of Water Resources and Hydropower Engineering Science，Wuhan University，Wuhan，Hubei430072，China

[2]Key Laboratory of Rock Mechanics in Hydraulic Structural Engineering Ministry of Education, Wuhan University, Wuhan, Hubei430072, China

[a]13026185409@163.com,

[b]pyanwhu@whu.edu.cn

Abstract: Except for rock mass quality, blasting load and in-situ stress are the two main factors for rock cracking and blasting damage zone developing. To reveal the rock cracking process during pre-split blasting, the numerical simulation model of damage zone around a single-hole and double-holes are analyzed through ANSYS/LS-DYNA. Various kinds of cases with different in-situ stress levels and states are discussed. A simplified empirical equation (1) is established to describe the correlation between peak particle vibration (PPV) and damage extent index, and the linear charging density under different in-situ stress levels is also evaluated. The result indicates that the damage zone decreases with increasing of the in-situ stress level. The damage zone mainly develops along with the direction of major principal stress, which has been verified during the excavation of abutment slot in the Baihetan Hydropower Station in China. Thus, to increase the effects of presplit blasting, linear charging density should be reasonable and the connection line of presplit blasting holes should be parallel to the major principal stress.

Equation: The relationship between PPV and damage extent index:

$$D = 1 - \left(\frac{V_0 - V}{V_0} \right)^2 \tag{1}$$

Where D is the damage extent index, V is the peak particle vibration (PPV), V_0 is the PPV on the blast-hole wall.

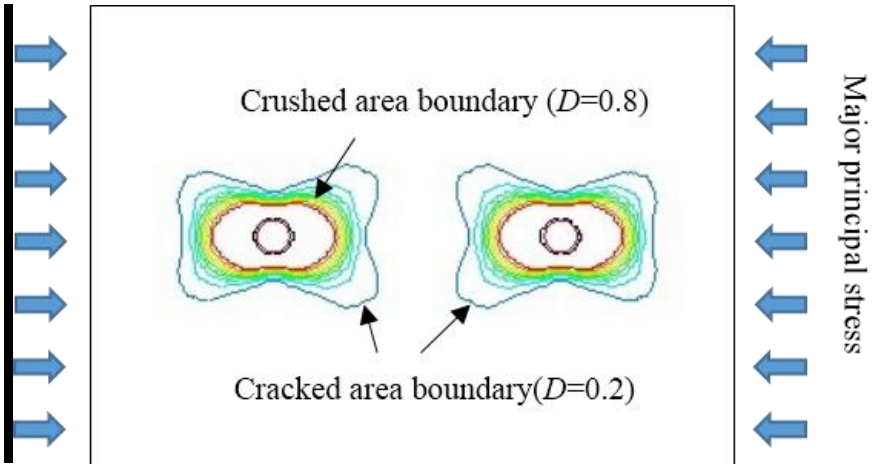

Fig. 1 Damage zone area when the lateral pressure coefficientsλ=2.5

ID055: Damage Characteristics of Concrete Gravity Dams Subjected to Underwater Contact Explosion

Qi Li[1, a], Gaohui Wang[*1, b], Wenbo Lu[1], Peng Yan[1], Xinqiang Niu[1,2]

[1]State Key Laboratory of Water Resources and Hydropower Engineering Science, Wuhan University, Wuhan 430072, China

[2]Changjiang Institute of Survey, Planning, Design and Research, Changjiang Water Resources Commission, Wuhan 430010, China

[a]qliwhu@whu.edu.cn, [b] wanggaohui@whu.edu.cn

The study of damage characteristics of concrete gravity dams subjected to underwater contact explosion is a critical issue to assess the dam's protective performance. The process of underwater contact explosion always accompanies with strong nonlinearity, such as the discontinuity and jump of fluid dynamics, the large-deformation and fracture of dams. In this paper, a fully coupled numerical approach with combined Lagrangian and Eulerian methods, incorporating the explosion process, is performed. To verify the feasibility of the numerical simulation and calculation method, the performance of reinforced concrete (RC) subjected to contact explosion in free air is simulated and discussed as a comparison with the published experimental results [1]. In order to evaluate the dynamic response and damage characteristics of concrete gravity dams subjected to underwater contact explosion, three different blast points are considered in this study, i.e., upper blast point, middle blast point and lower blast point. Shock wave propagation characteristics of underwater contact explosion are investigated. The dynamic response and damage characteristics of concrete gravity dams subjected to underwater contact explosions with different blast positions are compared. In addition, the damage characteristics of the dam subjected to underwater contact explosion and non-contact explosion (with 10m detonation depth and 10m standoff distance) are also compared and analyzed. The results show that the blast position has a significant influence on the damage characteristics and dynamic response of concrete gravity dams. Compared with underwater non-contact explosion, underwater contact explosion causes significantly more damage to the dam head while nearly equivalent damage to the dam heel and even less damage to the change in upstream slope.

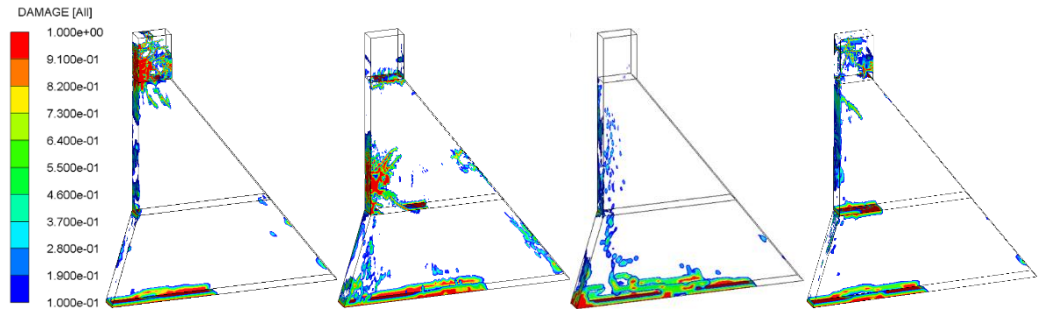

(a) Blast in the upper zone (b) Blast in the middle zone (c) Blast in the lower zone (d) Non-contact explosion

Fig.1 Damage characteristics of dams subjected to underwater contact and non-contact explosions.

References

[1] J Li, C Wu, H Hao, Z Wang, Y Su: *International Journal of Impact Engineering* 93 (2016), pp 62-75.

ID056: Determination of Dynamic Fracture Initiation, Propagation, and Arrest Toughness of Rock Using SCDC Specimen

Caigui Zhang[1], Fu Cao[2], Lian Li[1], Yan Zhou[1], Runqiu Huang[3], Qizhi Wang[1,2,3,a]

[1]Department of Civil Engineering and Applied Mechanics, Sichuan University, Chengdu 610065, China

[2]State Key Laboratory of Hydraulics and Mountain River Engineering, Chengdu 610065, China

[3]State Key Laboratory of Geohazard Prevention and Geoenvironmental Protection, Chengdu 610059, China

[a]qzwang2004@163.com

Inevitable man-made or natural disasters such as explosion, impact, earthquake, etc often cause the failure of a large number of civil engineering facilities, hence rock breakage behavior under dynamic loading has become the focus of special attention. Dynamic fracture toughness of rock is the material parameter for characterizing its resistance to dynamic crack initiation, propagation and arrest. Developing the method for testing rock dynamic fracture toughness constitutes high demand for research on the related theoretical basis and experimental technique. Rock dynamic fracture toughness is classified into three kinds: dynamic initiation, dynamic propagation, and dynamic arrest. Although there were some achievements for studying dynamic initiation and propagation, the study on rock dynamic arrest, being a puzzling problem, has been so far almost ignored. In the present research, the single cleavage drilled compression (SCDC, Fig. 1) specimen [1,2] of rock was impacted by split Hopkinson pressure bar in the model-I dynamic fracture test, where a crack propagation gauge (CPG) was glued on the SCDC specimen, the CPG was used to monitor the whole fracture process, including dynamic initiation, propagation, and arrest. An experimental-numerical-analytical approach was adopted to determine the dynamic initiation, propagation, and arrest toughness of rock material. Especially worth pointing out is that the dynamic arrest toughness of rock is measured for the first time. The CPG signal indicated that after the arrest of the crack in the SCDC, the stopped crack initiated again for the second time, and propagated out of the CPG monitoring range. This dynamic arrest process is analyzed from an energy perspective, and some required attentions in determining the rock dynamic arrest

toughness are pointed out. The results show that the rock dynamic initiation toughness

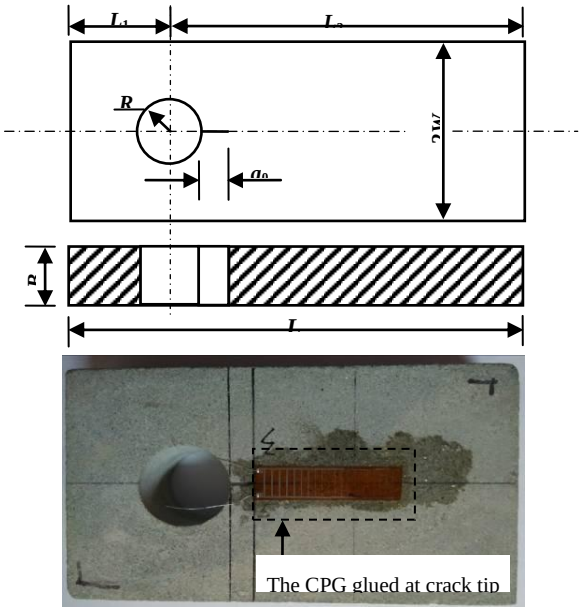

Fig.1 Sketch and photo of SCDC specimen

and propagation toughness increase with the increasing dynamic loading rate and crack propagation velocity, respectively, and the dynamic initiation toughness is larger than the dynamic arrest toughness.

References

[1] M Ni, XP Gou, QZ Wang. Stress intensity factor formulas for DCDC and SCDC specimens. *Chinese Journal of Theoretical and Applied Mechanics*, 2013, 45(1): 94-102.

[2] M NI, XP Gou, QZ Wang. Test method for rock dynamic fracture toughness using single cleavage drilled compression specimen impacted by split Hopkinson pressure bar. *Engineering Mechanics*, 2013, 30(1): 365-372.

ID058: Observation of Supersonic Jet Using Small Volume High-Pressure Shock Tube

Ryohei Takemura[1,a], Hiroshi Fukuoka[2,b], Shinichi Enoki[2], Shigeto Nakamura[3] and Kazuki Hiro[2]

[1] Advanced Mechanical Engineering Course, Faculty of Advanced Engineering, National Institute of Technology, Nara College, 22 Yata, Yamatokoriyama, Nara, 639-1080, Japan.

[2] Department of Mechanical Engineering, National Institute of Technology, Nara College, 22 Yata, Yamatokoriyama, Nara, 639-1080, Japan.

[3] Department of Control Engineering, National Institute of Technology, Nara College, 22 Yata, Yamatokoriyama, Nara, 639-1080, Japan.

[a] takemura.r@class.mech.nara-k.ac.jp,

[b] fukuoka@mech.nara-k.ac.jp

The unsteady supersonic jet and the shock wave were formed by the shock tube with small high-pressure section. We examined the effect of the length of high-pressure chamber and gas pressure on the behavior of the jet and the shock wave. The visualization was carried out by background-oriented schlieren (BOS) method.

Figure 1 shows a schematic diagram of the experimental apparatus. The high and low pressure chambers were separated by the lumirror film. The high pressure air was discharged into the atmosphere by the bursting of the diaphragm. The flow was visualized by BOS method using high-speed camera as a continuous light source with a metal halide lamp. The simple open-ended shock tube had a diameter, D, of 10mm. The dimension of the high-pressure chamber was 10 and 100mm in length. That of the low-pressure chamber was 12mm in length. A sheet of Lumirror (polyethylene tereph-thalate) was used as a diaphragm. In order to change the pressure ratio, the pressure ratio of shock tube was defined by the ratio of the pressure in the high pressure section P_h to the low pressure P_l, P_h/P_l, which corresponds to the film thickness, T_f.

Figures 2(a)-(h) show the typical flow fields for L_h=10mm, P_h/P_l =50.2. Figure 2(a) shows the moment when the diaphragm bursts at t=0μs. The stripe pattern is the background for BOS method. Figures 2(b) and (c) show that the jet reach x=20.7 and 37.6mm respectively. The underexpanded jet is observed in Fig.2(c). Figures 2(d) and (e)

show that the jet reach x=52.0 and 62.9mm respectively. In other words, the distance between open end and head of the jet is short with the lapse of time. This is because propulsion force is shorter than a general shock tube by the small high-pressure section. For this reason, the jet is decreasing in an early stage. We found that the injection period of the jet is short by the shock tube with small high-pressure section. We visualized the shock wave and jet.

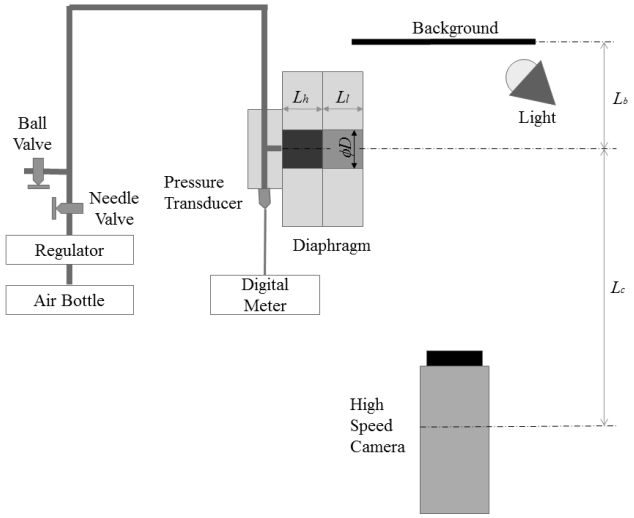

Fig.1 experimental apparatus

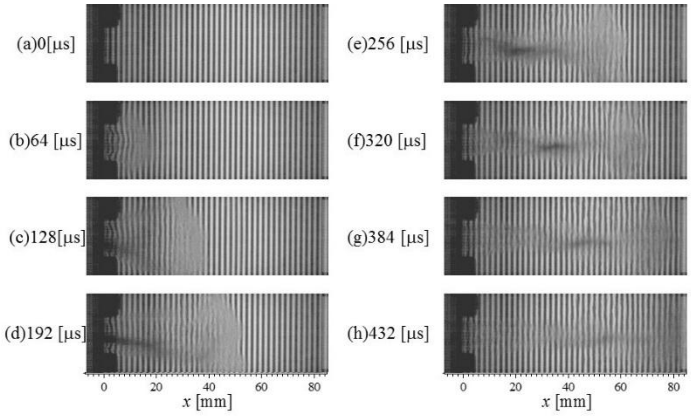

Fig.2 Sequence photographs for L_h=10,L_l=12, T_f =100μm(P_h/P_b=50.2)

ID059: Explosive Welding of Thin Stainless Plate on Copper Plate Using Modified Pressure Transmitting Medium

S. Otsuka[1, a], D. Inao[2], S. Tanaka[3], K. Hokamoto[3]

[1]Graduate School of Science and Technology, Kumamoto University, 2-39-1 Kurokami, Chuo-ku, Kumamoto 860-8555, Japan

[2] Faculty of Engineering, Kumamoto University, Kumamoto, Japan

[3] Institute of Pulsed Power Science, Kumamoto University, Kumamoto, Japan

[a]153d8511@st.kumamoto-u.ac.jp

Explosive welding is one of the methods to bond different kinds of materials. This method uses an intense dynamic energy driven from an explosive to create a tight bonding between metals surfaces. In general, explosive welding is performed parallel assembly using flyer and base plates in air atmosphere. However, the bonding of thin or brittle materials is difficult by such a regular method. In such a case, explosive welding using underwater shock wave is very effective for good bonding with clean surface [1]. The underwater explosive welding is possible to accelerate a thin plate uniformly within a very short distance to achieve a high velocity enough to satisfy the condition of bonding, but the method is slightly difficult to industrialize due to the use of water as a pressure transmitting medium. Therefore, authors tried to obtain similar joints by using gelatin plate instead of water. It is known that the gelatin has similar shock wave response with water [2], so, the designing the experimental conditions seem not quite difficult. In this research, 200 μm-thick stainless steel flyer plate was welded on 2 mm-thick copper base plate, where 10mm-thick gelatin plate put above the flyer plate using PAVEX explosive (detonation velocity 2-2.5km/s). As a result of experiments, the bonding of stainless steel and copper was successfully accomplished with waves and the recovered surface was kept clean.

References

[1] P. Manikandan, J.O. Lee, K. Mizumachi, A. Mori, K. Raghukandan, K. Hokamoto: *Journal of Nuclear Materials* 418 (2011), pp281-285

[2] C.J. Shepherd, G.J. Appleby-Thomas, P.J. Hazell, D.F. Allsop: *AIP Conference Proceedings* 1195 (2009), pp1399-1402

ID060: Metallurgical and Mechanical Properties of Wire Mesh Reinforced Dissimilar Explosive Cladding

S.Saravanan[1] K.Raghukandan[2]

[1]Department of Mechanical Engineering, Annamalai University, Tamilnadu, India
Email: ssvcdm@gmail.com Phone: +919443676936

[2]Department of Manufacturing Engineering, Annamalai University, Tamilnadu, India
Email: raghukandan@gmail.com Phone: +919443488265

Abstract: Explosive cladding employs a controlled chemical explosive detonation to craft a metallurgical bond between similar and dissimilar metals. In this study, aluminum 5052-copper and pure aluminum-aluminum 5052 plates were explosively cladded by placing a steel wire mesh having 90^0 orientation between them by varying the process parameters viz., loading ratio (mass of explosive/mass of flyer plate), preset angle and standoff distance. Microstructural, corrosion and mechanical strength of the clads Viz., Vickers Hardness, tensile and shear strength were evaluated as per relevant standards and the results are presented. The introduction of wire mesh interlayer enhances the mechanical strength of the dissimilar explosive clads.

Corresponding author: S.Saravanan
Department of Mechanical Engineering,
Annamalai University, Tamilnadu, India
Email: ssvcdm@gmail.com

ID061: Experimental Studies on Steel Box Girder Scale Model Under Near Explosive Effect

Shao-bo Geng[1,2,a], Ya-ling Liu[1], Jian-ying Xue[1]

[1]Ministry of Civil Engineering, North University of China, Taiyuan, 030051, China

[2]Bridge structure safety technology National Engineering Laboratory, Chang'an University, Xi'an, 710064, China,

[a] gengshaobo@nuc.edu.cn),

Supported by: National Natural Science Foundation of China (51408558);
Bridge structure safety technology national engineering laboratory open fund (2014G1502002) experimental

Abstract: Steel box girder bridge structure, which can reduce dead weight and improve construction speed, is widely used in city bridges. Both the transportation of dangerous goods and terrorist attacks are major risk factors to the steel box girder bridge structure operation. As a special and different effect, explosive can generate strong air shock wave in a short time and destroy the key components of bridge structure [1~3]. Seriously this effect can cause continuous collapse of bridge structure, highway transportation interruption and secondary disasters. The current domestic bridge design specifications don't contain guideline about explosive effect in China. The foreign bridge specifications also lack the detailed provisions. One of the most important reasons is that the lack of experimental studies. Because of experimental expensive and explosives scarcity, bridge engineering researchers focus on the numerical simulation by FEM. Sometimes the experimental studies is still required for objective recognition and model verification. The research group designed a flexible and removable explosive experiment platform for bridge structure. The scale model of single box with three rooms is made of Q235A steel from Taiyuan Steel Group. Model dimensions with width of 0.48m, height of 0.15m, length of 1.8m and plate thickness of 3mm are employed. The mechanical properties of Composition B explosive and Q235A steel should be calibrated respectively. With the different locations and the same explosive equivalent, the local failure characteristics and global deformation are examined under the nearby blast wave. The failure type of the top plate, the bottom plate and the internal structure are measured through the blast wave propagation process. This experimental design, including steel box girder, experimental

process and platform, can provide verification model for other researchers who are interested in explosive load effects on structures.

Keywords:steel box girder,explosive effect,blast load,scale model,failure characteristics, Composition B explosive; bridge engineering.

Fig.1 Failure characteristics of top plate of steel box girder

References

[1] Li Zhong-xian,Lu Jian-hui,Shi Yan-chao,Ding Yang. Reliability analysis of steel girder under uncertain blast load [J]. *Journal of engineering mechanics,* 42(2014), pp112-118

[2] Chen Hai-long,Fan Hua-lin,Jin Feng-nian. Dynamic structural analysis of underground arch under blast load [J]. *Journal of engineering mechanics,* 36(2013),pp169-174.

[3] Fang Qin, Liu Jin-chun,Zhang Ya-dong,Qian Qi-hu. Finite element analysis of reinforced concrete beam failure pattern under blast load [J]. *Journal of engineering mechanics,* 11(2001),pp1-8.

ID062: Surface Coating of Tungsten Carbide Particles on Metal Plate by Dynamic Collision

Shigeru Tanaka[1, a] , Kazuyuki Hokamoto[1, b] , Hayato Oda[2]

[1]Institute of Pulsed Power Science, Kumamoto University, 2-39-1 Kurokami, Chuo-ku, Kumamoto, Kumamoto 8608555, Japan

[2]Graduate School of Science and Technology, Kumamoto University, 2-39-1 Kurokami, Chuo-ku, Kumamoto, Kumamoto 8608555, Japan

[a]tanaka@mech.kumamoto-u.ac.jp,

[b]hokamoto@mech.kumamoto-u.ac.jp

Abstract: Some techniques of explosive materials processing have been industrialized such as explosive forming and welding, shock wave compaction of powder. A new method for surface coating of an aluminum plate by diamond particles is developed by authors [1]. In this study, stainless steel and copper plate surfaces were coated by angular shaped tungsten carbide (WC) powder using above cited reference technique. The metal plates were accelerated by explosive explosion, and then collided to the WC powder. The particles were stuck into the metal surface easily. In a cross-sectional observation, it was confirmed that the particles were strongly held by the metal substrate. Furthermore, crashed particles were surrounded by melting substrate in part.

References

[1] S. Tanaka, K. Hokamoto, S. Torii, M. Touge, S. Itoh: Journal of Materials Processing Technology, Volume 210, Issue 1 (2010) PP 32-36

ID063: Detonation Wave on the System Consisting of Explosives and Various Gaps

Shiro Kubota[1, a] , Tei Saburi [1,] , Kunihito Nagayama[2]

[1]National Institute of Advanced Industrial Science and Technology, Tsukuba, Japan

[2] Kyushu University, Fukuoka, Japan

[a]kubota.46@aist.go.jp

Abstract: The experimental and numerical study for the detonation propagation on the system consisting on the explosive and various gaps was conducted. The experimental system consists of the pellet explosives and the gap materials, PMMA pipe, and two grams Composition C4 booster[1)]. The sample explosive is a composition A5 (RDX 98.8wt%). The thickness of the explosive is 5 or 10 mm, and the radius is 20mm. The gap materials are air, PMMA, and SUS304. The thickness of gap is 5 or 10 mm. Two PVDF gauges (Dynasen PVF2-11) are set to measure arrival time of the detonation wave. Using the arrival times and a distance between two gauges, the average velocity of the detonation wave is estimated. The numerical simulations are carried out and are compared with the experimental results.

References

[1] S. Kubota, T. Saburi, Y. Ogata, Y. Wada, and K. Nagayama: Journal of Physics: Conference Series 500(2014) 052022

ID064: Experiment Study on Stable Bio-Emulsion Fuel by Underwater Explosion

Shuichi Torii[1,a], Keisuke Goto [1], and Shigeru Tanaka[2,b]

1Graduate Schools of Science and Technology, Kumamoto University, 860-8555, Japan

2Faculty of Engineering, Kumamoto University, Kumamoto 860-8555, Japan

atorii@mech.kumamoto-u.ac.jp, b shock-compaction@docomo.ne.jp

Abstract: Experimental study is performed on the production of the bio-diesel emulsion fuel. In this research, a bubble pulse caused by an underwater explosion is used to emulsify samples, i.e., water (in the range of 5–20%) and bio-diesel fuel with two-different specific surfactants. This mechanism of the emulsification is observed by a high speed video camera and calorimeter (SHIMADZU CA-4AJ) and Zetasizer Nano ZS (Malvern Co.) are employed to measure heat value and particle size of the emulsion fuel produced here, respectively. It is found that (i) the process of generating emulsification under the underwater explosion is disclosed, (ii) the stable emulsion fuel and water particle size in it are affected by HLB, i.e., the ratio of two-different specific surfactants and the timewise stability of the emulsion fuel is attributed to the scattering intensity of the measured water particle size (Fig. 1).

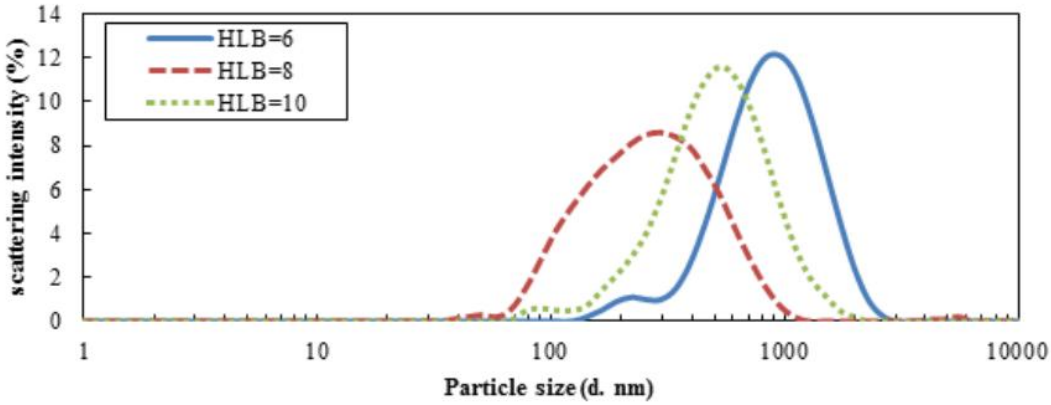

Fig.1 Particle size distribution of emulsion sample

ID065: Preparation and Characterization of Metalized Explosive Containing B and Al Powder

Song Qingguan[1, 2*], Gao Dayuan[1,2], Zheng Baohui[1], Cao Wei[1,2], Cao Luoxia[1,2], Tan Kaiyuan[1,2]

1. Institute of Chemical Materials, CAEP, Mianyang 621900, China;

2. Robust Munitions Center, CAEP, Mianyang 621900, China

Abstract: Metallized explosives achieve both excellent power ability and high blast energy. In this paper, new HMX based explosive formulations containing B and Al powder, AP were developed and (seen in Fig.1), effects of the component content and the B and Al powder size on the properties of metallized explosives were discussed. The morphology of B, Al and B-Al compound powder was observed by SEM and the SEM images at different sizes were obtained (seen in Fig.2).

（a）explosive containing Al powder　（b）explosive containing B powder　（c）metalized explosive containing B and Al powder

Fig.1 Appearance photograph of metalized explosive

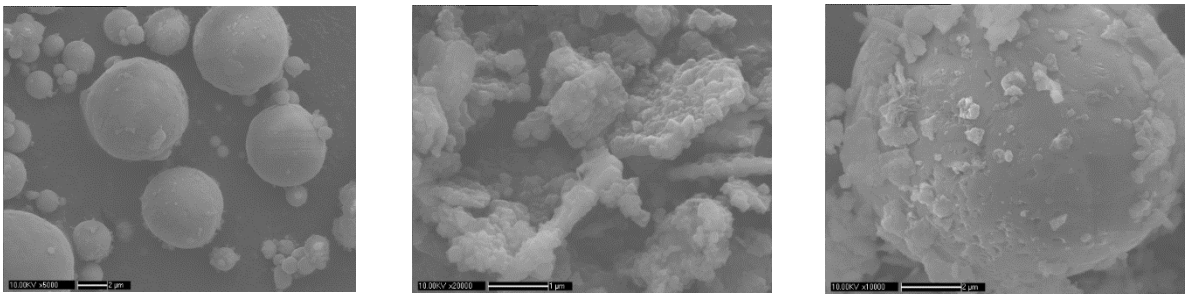

(a) Al powder　（b）amorphous B powder　（c）B and Al compound powder

Fig.2 SEM of metal powder

Effects of HMX and AP on oxidation properties of B and Al powder were

Fundation: Supported by National Natural Science Foundation of China (Grant No.11572359, 11502249) and Science and Technology Fund of CAEP (2015B0101012)

First author: Song Qingguan (1991–), Male, research intern, Master's degree, Study on the detonation properties and safety of energetic materials.

Corresponding author: Gao Dayuan (1962–), Male, associate researcher, Doctor's degree, Study on the thermal analysis, detonation properties and safety of energetic materials.

investigated with thermal analysis method, which lead to a better understanding of the reaction kinetics, ignition and combustion conditions and self-sustaining combustion heat release mechanism. The characteristic spectrum of combustion and detonation products of metalized explosive containing B and Al powder was measured by means of the spectroscopy technique and ICCD system, characteristics of microscopic reaction were studied. The impact sensitivity, friction sensitivity, electrostatic spark sensitivity and cap initiation sensitivity were measured with the drop hammer device, WM-1 friction device, electrostatic spark tester and cap sensitivity test respectively, which did fully acknowledge of the safety of metallized explosives under different external energy stimuli. Based on plate dent test, the ignition and propagation properties of metallized explosives were investigated, and the detonation propagation and power ability of metallized explosives containing B and Al powder were understood (seen in Fig.3 and Fig.4).

Fig.3 Photograph of plate dent test

（a）device of test

（b）witness plate under layer

Fig.4 Photograph of cap sensitivity test

The results show that the Al powder are 1-5μm spherical particles, and partial particles have agglomeration. The structure of B powder is amorphous flake crystallite shape whose sizes are between 1-5μm. For the B-Al compound powder, there are many little amorphous flake B powder on surface of Al powder. In condition of room temperature to 500℃ and N_2 atmosphere, although heat rate and pressure have effects on thermal decomposition peak temperature of HMX and AP, Al powder and amorphous B powder occur to partial oxidation but no combustion. In condition of room temperature to 1100℃, Al powder and amorphous B powder occur to combustion no matter in air, CO_2 or O_2 atmosphere. Furthermore, metalized explosive containing B and Al powder was ignited by nanosecond pulse laser with energy of 0.02J and duration of 9ns, and the

characteristic spectrum of metal powder combustion reaction was obtained. The impact sensitivity, friction sensitivity and electrostatic spark sensitivity of metalized explosive containing B and Al powder are between 60%-80%, 100% and 3.83kV-6.40kV respectively. When insensitive HMX and AP were used, impact sensitivity and electrostatic spark sensitivity are reduced obviously. The metalized explosive containing B and Al powder with density of 0.90g.cm^{-3} to 1.35g.cm^{-3} and diameter of Φ50mm has cap ignition sensitivity, and can propagate stable detonation. The high-temperature and high-pressure detonation products not only blast upper 1 mm thick Q235 steel into debris, but also blast down 8mm thick Q235 steel with a 90mm diameter hole. It is indicated that metalized explosion containing B and Al powder has strong after-effect power ability.

Keywords: explosion mechanics, metalized explosive containing B and Al powder, preparation, safety, laser ignition, power ability

ID067: A Basic Study on Shock Resistant Design for Explosion Pit

Tatsuya.Yamamoto[1,a], Masatoshi Nishi[2], Masahide Katayama[3] andKazuyuki Hokamoto[4]

[1]Graduate School of Science and Technology, Kumamoto University, 2-39-1 Kurokami, Chuo-ku, Kumamoto 860-8555, Japan

[2]National Institute of Technology, Kumamoto College, 2627, Hirayamashinmachi, Yatsushiro City, Kumamoto 866-8501, Japan

[3]ITOCHU Techno-Solutions Corporation, 3-2-5, Kasumigaseki, Chiyoda-ku, Tokyo 100-6080, Japan

[4]Institute of Pulsed Power Science, Kumamoto University, 2-39-1, Kurokami,Chuo-ku, Kumamoto City, Kumamoto 860-8555, Japan

[a]168d8555@st.kumamoto-u.ac.jp

Abstract: In this paper, the mechanism of damage on the structure of an explosion pit A belongs to the Institute of Pulsed Power Science, Kumamoto University is investigated. The authors have been studied on optimizing the design of an explosion pit made by reinforced concrete structure covered with a steel plate based on numerical simulation using Autodyn code against impulsive load like explosion. So far, a simplified model of the pit is analyzed [1], and the simulation revealed that the vibrations of the reinforced concrete wall caused by impulsive pressure result in the damage at the side wall and top of the egg shaped pit. In this study, three-dimensional model with square opening (door) is used to simulate by numerical simulation. The result implies that firstly the cracks were occurred at the corners of the door and were grown larger. The numerical result is in a good agreement with the distribution of the cracks on the pit. The numerically simulated results for a spherical pit are also demonstrated at the time of the presentation.

Reference

[1] M. Nishi, M. Katayama, K. Hokamoto: *Science Technology of Energetic Materials* Vol.76 (2015), pp133-138

ID068: Dynamic Response Analysis of Mortar Block Under Blast Loading Using Digital Image Correlation

Tei Saburi[1, a], Yoshiaki Takahashi[2], Shiro Kubota[1], Yuji Ogata[1]

[1]Research Institute of Science for Safety and Sustainability, National Institute of Advanced Industrial Science and Technology, Onogawa 16-1, Tsukuba, Ibaraki 305-8569, Japan

[2]Department of Earth Resources Engineering, Faculty of Engineering, Kyushu University, 744 Motooka, Nishiku, Fukuoka 819-0395, Japan

[a]t.saburi@aist.go.jp

Abstract: The dynamic strain distribution behavior of a mortar block blasting was experimentally investigated. A development of countermeasure technique against environmental impacts such as ground vibration and flyrock in mining field is become important as well as economical and efficient aspects. The understanding of the fracture mechanism in blasting is essential to optimize the blasting design. However, it is inconvenient to conduct investigation in field experiments because that experimental rock/geological condition is difficult to arrange in actual mining field. In this study, a small-scale blasting experiment using a mortar block with well-defined property is conducted and dynamic strain distribution on the mortal block surface is analyzed by a Digital Image Correlation (DIC) method. The block was blasted by an electric detonator and 3g of Composition C4 explosive, and the behavior of the block surface was observed by two high-speed cameras and a strain profile was measured by a strain-gauge. The set of two high-speed video image sequences were used to analyze the three-dimensional strain distribution using DIC method. A point strain profile extracted from the analyzed strain distribution data was compared with a directly observed strain profile using the strain gauge.

(a) Before the shot (b) After the shot

Fig.1 Example photos of mortar block

ID069: A Fast Method for Preparing $TiO_2/Na_2Ti_6O_{13}$ Powder

Tiejun Zhao[1] , Honghao Yan[1,a] , Xiaojie Li[1], Yang Wang[1]

[1]State Key Laboratory of Structural Analysis for Industrial Equipment, Dalian University of Technology, Dalian, 116024, China

[a]dlutpaper@163.com

Abstract: An easy and fast method was design to prepared $TiO_2/Na_2Ti_6O_{13}$ powders, which by using vacuum detonation method. The mixed explosives were prepared by usage of Ti-Na-contained precursor, ammonium nitrate, hexogen and a certain mass of polystyrene foam ball (EPS) in beaker, and they were detonated in a vacuum detonation reactor to synthesize powders. The prepared frech grey powders were characterized by powder X-ray diffractometer and transmission electron microscopy to ascertain the phase composition and morphology. It found that the powders were consist of TiO_2 and $Na_2Ti_6O_{13}$, and the TiO_2 almost was rutile phase. The intensity of $Na_2Ti_6O_{13}$ peak was enlarged with increase of EPS mass. The $TiO_2/Na_2Ti_6O_{13}$ particles were irregular sphere or long rhombus, and some particles were 10 nm. In generial, the dispersity of the powers was decreased with the mass of EPS increased.

Keywords: $Na_2Ti_6O_{13}$, TiO_2, detonation method, vacuum

ID070: Comparison Between Simple Seam Welding and Adjacent Parallel Seam Welding by Magnetic Pulse Sheet-Welding Method

Tomokatsu Aizawa[1], Kazuo Matsuzawa[2]

[1]Tokyo Metropolitan College of Technology, Sinagawa Tokyo 140-0011 Japan

[2]Tokyo Metropolitan College of Industrial Technology, Sinagawa Tokyo 140-0011 Japan

[1]aizawa@mem.iee.or.jp, [2]maz@metro-cit.ac.jp

Magnetic Pulse Welding (MPW) is an impact welding process analogous to explosive welding. In the MPW process, electromagnetic forces are used to weld metal work-pieces. Its technique is based on discharging a high pulse current through a coil to produce electromagnetic forces. For a long time, MPW has been used for welding tubular work-pieces [1-3]. Recently, this method is applied to flat work-pieces [4-8]. The mechanism and the features of MPW are considerably well known.

In the case of flat work-pieces, the most common configuration consists of a lap joint of similar or dissimilar sheet metals. At the high-speed collision, two metal jets emitted from Al-Al sheets were observed by us [4]. The jets emitted brilliant lights in the air. The length of the observed lights was 1~2mm. The weld interface can be cleaned by the emission of metal jets. Usually, two metal jets occur near to the opposite direction each other. The sheets are welded in two narrow weld zones (seam weld zones) [4-6]. Two metal jets do not collide. We decide to call such a welding “simple seam welding”.

On the other hand, four metal jets can occur when the simple seam welding is carried out in two parallel. If such parallel seam welding accompanied the collision of metal jets, the increase of seam weld zones were observed [7,8]. The increase of the parallel seam-weld zones is not sufficiently understood yet. We decide to call such welding “adjacent parallel seam welding”.

This paper describes the comparison between the simple seam welding and the adjacent parallel seam welding for Al-Al sheets. In the case of the parallel seam welding, the sheets collided at high speed in two parallel along the narrow central part (5 mm wide) of the coil. The central part had two parallel upper parts [8]. The width (5 mm) of the central part was same as that of the simple seam welding. Four metal jets can occur near to each other and two metal jets occurring in the inside can collide if the experimental conditions are suitable. We observed and confirmed the increase (more than double in total) of the

parallel seam-weld zones in comparison with the simple seam-weld zones.

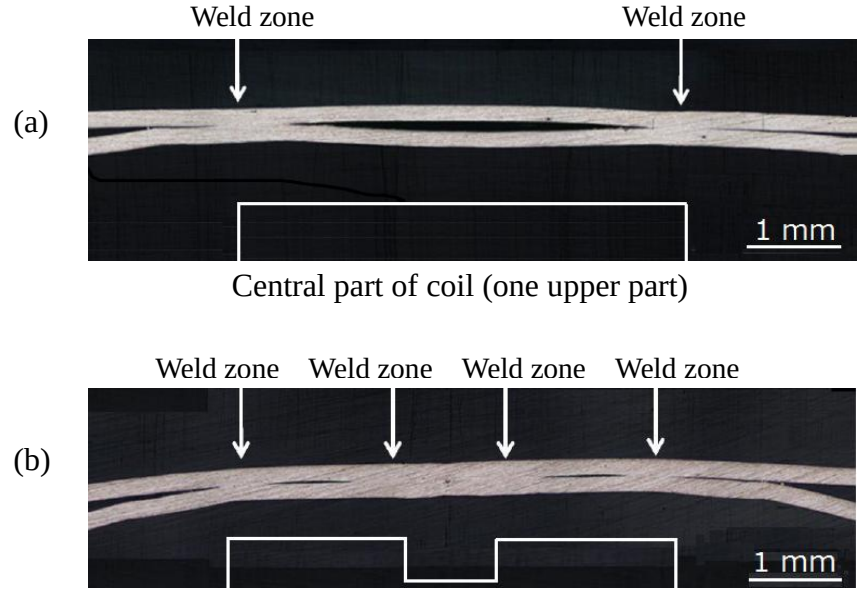

Fig.1 Cross sectional appearances of weld interface of seam welded Al-Al sheets. In the case of (a) simple seam welding, (b) adjacent parallel seam welding.

References

[1] I. Masumoto, K. Tamaki, M. Kojima: *Transactions of the Japan Welding Society*, 16 (1985) 110-116.

[2] H. Hokari, T. Sato, K. Kawauchi, A. Muto: *Welding International*, 12 (1998) 619-626.

[3] V. Shribman, A. Stern, Y. Livshitz, O. Gafri: *Welding Journal*, 81 (2002) 33-37.

[4] M. Watanabe, S. Kumai, K. Okagawa, T. Aizawa: *Aluminium Alloys*, 2 (2008) 1992-1997.

[5] T. Aizawa, M. Kashani, K. Okagawa: *Welding Journal*, 86 (2007) 119s-124s.

[6] S.D.Kore, P.P.Date, S.V.Kulkarni: *International Journal of Impact Engineering*, 34 (2007) 1327-1341.

[7] T. Aizawa, K. Matsuzawa, K. Okagawa, M. Ishibashi: *Materials Science Forum*, 767 (2014) 171-176.

[8] T. Aizawa, K. Matsuzawa: *Quarterly Journal of the Japan Welding Society*, 33 (2015) 130s-134s.

ID071: Blast Wave Mitigation From the Straight Tube by Using Water Part I –Small Scale Experiment–

Tomotaka Homae[1, a], Yuta Sugiyama[2], Kunihiko Wakabayashi[2], Tomoharu Matsumura[2], Yoshio Nakayama[2]

[1]National Institute of Technology, Toyama College, 1-2 Ebie-neriya, Imizu, Toyama 933-0293, Japan

[2]National Institute of Advanced Industrial Science and Technology, Central 5, Higashi 1-1-1, Tsukuba, Ibaraki, Japan

[a]homae@nc-toyama.ac.jp

Abstract: A subsurface magazine has an explosive storage chamber, a horizontal passageway, and a vertical shaft for vent. It was proposed and legislated in Japan. The authors found that small amount of water on the floor of its storage chamber mitigated the blast pressure remarkably [1]. The mechanism of the mitigation has been studied. In this study, the explosion experiments in a transparent, square cross section, and straight tube were carried out to examine mechanism of mitigation. The blast pressure in the tube and around the tube was measured. A high-speed camera was also used to observe inside the tube.

A specially designed electric detonator with 100 mg lead azide was used as a test explosive. The tube was made of PMMA plate, thickness of 10 mm. The length of the tube was 330 mm. The cross section was square, whose length of a side was 30 mm. In case of experiments for examination of water effect, tap water was poured into the tube. The water depth was 5 mm. The water did not contact with the explosive. The detonator was fixed at 10 mm from the base and detonated. The blast pressure on inside surface of the tube was measured at four points, 80 mm, 140 mm, 200 mm, and 260 mm from the detonator. The blast pressure on the extended line of the tube axis was also measured at four points from 4.3 $m \cdot kg^{-1/3}$ to 30.2 $m \cdot kg^{-1/3}$. A high-speed camera was used to record inside the tube to observe the interaction between explosion and water. The frame interval was 16 μs or 32 μs.

The pictures obtained by the high-speed camera showed that water inside the tube do not move apparently during the period of recording. The difference was not clear in cases of the tube without water and the tube with water.

The measurement of the blast pressure inside the tube is summarized in Fig. 1. The water inside the tube mitigated the peak overpressure and reduced the propagation velocity.

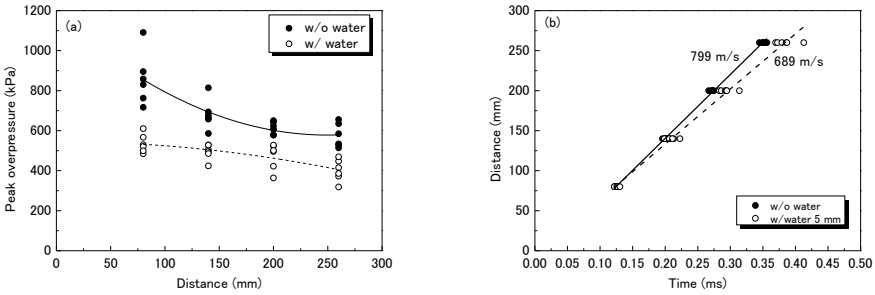

Fig. 1 (a) Relation between peak overpressure and distance from the point of explosion. (b) Relation between time of shockwave arrival and distance. Shock velocities obtained by linear fitting are also shown.

The blast pressure outside the tube is depicted in Fig. 2. In accordance with our previous study [1], the water mitigated the peak overpressure and the scaled impulse.

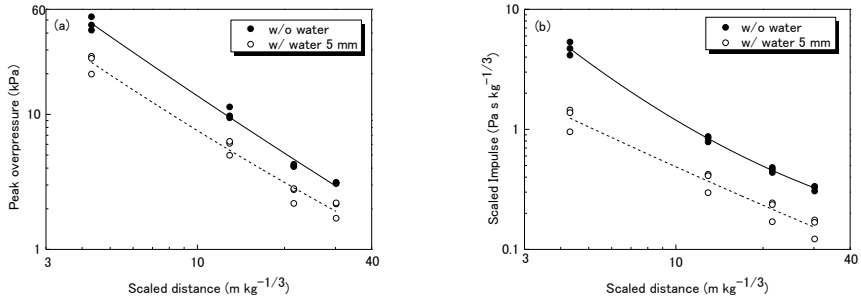

Fig. 2 Relation between (a) peak overpressure and (b) scaled impulse and scaled distance from the exit of the tube.

The results of this study suggest that the mitigation of blast pressure by water is due to the interaction between the explosion and the water near the explosion point.

References

[1] T. Homae, Y. Sugiyama, K. Wakabayashi, T. Matsumura and Y. Nakayama: *Science and Technology of Energetic Materials* 77, (2016) pp18-21.

ID075: Numerical Analysis of Behavior of Opposing Unsteady Supersonic Jets in a Flow Field with Shields

Toshiki Kinoshita[1, a], Hiroshi Fukuoka[2, b], Ikurou Umezu[3]

[1]Advanced Mechanical Engineering Course, Faculty of Advanced Engineering, National Institute of Technology, Nara College, 22 Yata, Yamatokoriyama, Nara, 639-1080, Japan

[2]Department of Mechanical Engineering, National Institute of Technology, Nara College, 22 Yata, Yamatokoriyama, Nara, 639-1080, Japan

[3]Department of physics, Konan University, Kobe 658-8501, Japan

[a]kinoshita.t@class.mech.nara-k.ac.jp

[b] fukuoka@mech.nara-k.ac.jp

Opposing unsteady supersonic jets are suddenly injected into a flow field having shields with shock waves. The jets collide with each other, pass shields and impinge on a substrate. This kind of flow field is complication by the interaction between jet and jet; jet and shock wave; shock wave and shock wave. The purpose of this present study has been to establish the behavior of the jets and the shock waves.

Numerical simulations were carried out by using the ANSYS Fluent 14.0.0 code. In this numerical calculations, we used the axisymmetric two-dimensional compressible Euler equations and solved using the finite volume method. Figure 1 shows the flow field for the computation and boundary condition. The initial injection velocity of Si and Ge jets were given by 18000m/s. Helium gas was introduced as background gas and initial temperature was set at 300K.

The calculation results are shown in Figs. 2(a)-(h) for the substrate-shield length L/D=3.0 and the background gas pressure P_b=1000Pa. The He mass fraction and density contours (black line) correspond to the Si and Ge jets and the shock waves, respectively. The arrows indicate the direction of the shock waves propagation. The shock waves are generated by the sudden injection of the Si and Ge jets. The shock waves radially propagate together with the Si and Ge jets at t=145ns after the jet injection as shown in Fig. 2(a). Figure 2(b) shows that the opposing shock waves collide on the center of the flow field and Si and Ge jets progress toward there. In Fig. 2(c), we can observe that the shock waves reach the substrate. The jets that collided on the center of the flow field

change the direction toward the substrate. In Figures 2(d)-(e) show that the jets are forced back by the passing of the reflected shock waves from the substrate. Subsequently, the shock waves impinge on the outside walls of the shields. Figure 2(f) shows the moment at which the head of the jets arrives at the substrate. Thereafter, Figs. 2(g)-(h) show that the jets impinged on the substrate spread radially along the surface. It was found that the shock waves affect the progress of the jets.

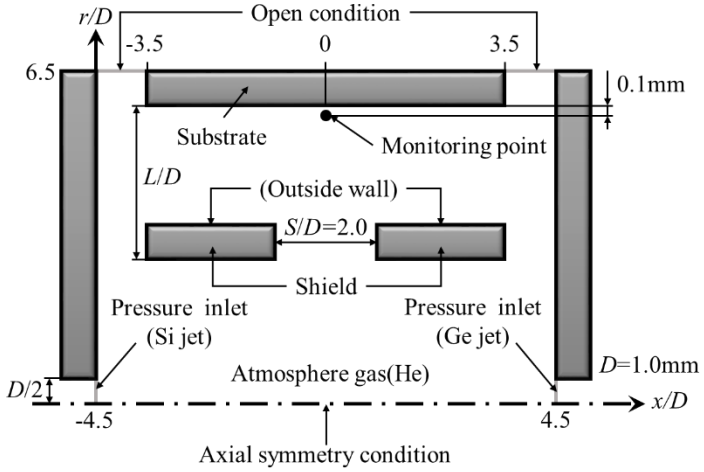

Fig. 1 Flow field for the computation and boundary condition

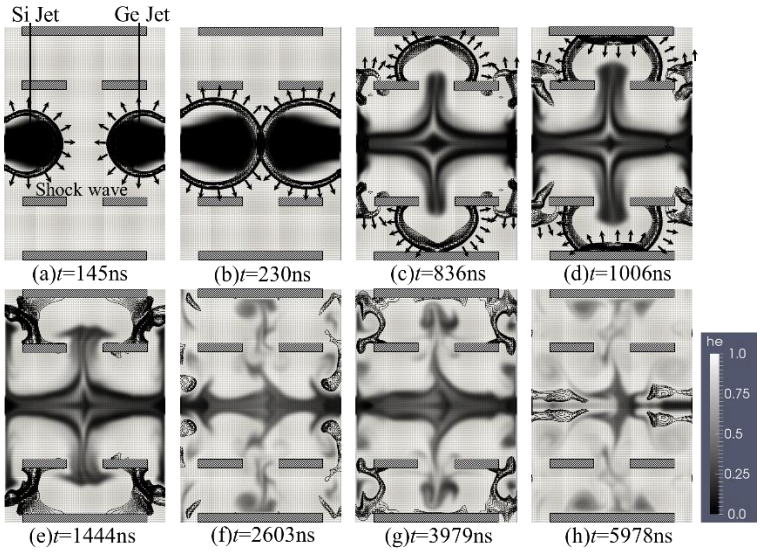

Fig.2 He mass fraction and density contours for L/D=3.0 and S/D=2.0

ID076: Theoretical and Numerical Investigation of the Transmitted Pulse Wave and its Shock Initiation Characteristics Generated by Multi-flyer

Wanjun Wang[1, a], Junjun Lv[1], Mingshui Zhu[1, b], Yao Wang[1], Yuan Gao[1], Qiubo Fu[1]

[1]Institute of Chemical Materials, China Academy of Engineering Physics, Mianyang 621900, China

[a]wangwanjun@caep.cn, [b]zhumsi12@163.com

Abstract: The accurate control of transmitted pulse wave plays an important role in the area of shock initiation, which involves in a series of physical process like the deviation of Hugoniot curve after shock compression, shock wave interaction and the propagation of rarefaction wave. In this paper, we respectively obtained the analytical solution of the transmitted pulse wave in PBX-9404 explosive generated by aluminum flyer, polyimide flyer and aluminum-polyimide multi-flyer with different thickness ratios. Numerical simulation of shock initiation was carried out systematically. By comparing the simulation result impacted by different flyer (monolayer or multi-layer), the influence of maximum pressure, impulse duration and the secondary compression wave to chemical reaction rate and growing distance to detonation was studied in detail.

Fig.1 Aluminum flyer

Fig.2 Polyimide flyer

（a）1:1　　（b）2:1　　（c）1:2

Fig.3 Aluminum-polyimide multi-flyer of different thickness ratio

Structures of different flyers are shown in Figure 1~3. Grüneisen EOS based on experiment Hugoniot[1] curve is adopted for aluminum, polyimide and unreacted PBX-9404, Grüneisen coefficient and a first order volume correction factor are introduced to describe the dynamic characteristics of the material.

It is convenient to establish a Grüneisen form of equation of state based on the shock Hugoniot:

$$P - P_H(v) = \frac{\gamma}{v}(e - e_H(v))$$

The first order volume correction factor is as follows:

$$\gamma = \gamma_0 - a(1-1/\eta)$$

Where, $\eta \equiv \rho/\rho_0$, and material parameters is shown in Table 1.

Table.1 Material parameters of aluminum, polyimide and unreacted PBX-9404(*kg, m, ms*)

Material	ρ_0	C_0	λ	γ_0	a
Aluminum[2]	2703	5.38	1.339	1.97	0.48
Polyimide[3]	1360	2.62	1.25	2.1	0.0
PBX-9404	1867	2.71	1.61	0.675	0.0

Hugoniot curve will deviate from the original one after going through a compression process. Formula 3 shows the P-v Hugoniot relation of a subsequent compression process on the basis of the previous shock Hugoniot curve, the analytical solution of the transmission wave generated by multi-layer was obtained by combining conservation equations and interface continuity conditions.

$$P = \frac{2P_H - \gamma(P_H - P_1)(v_0 - v)/v}{2 - \gamma(v_1 - v)/v}$$

Table 2 shows the analytical pressure, specific volume, specific internal energy and particle velocity of polyimide material during multiple compression process when the impact velocity is set to be 2000m/s, table 3 shows the analytical pressure, specific volume, specific internal energy and particle velocity of PBX-9404 during multiple compression process.

Table.2 Variables of polyimide material during multiple compression process(Kg, m, ms, MPa)

	pressure	specific volume	specific internal energy	particle velocity
The first compression	6399.6	0.000526	0.6695	0.8428
The second compression	10440.0	0.000420	1.5659	1.3780
The third compression	11960.0	0.000415	1.6140	1.2980

Table.3 Variables of PBX-9404 during multiple compression process(Kg, m, ms, MPa)

	pressure	specific volume	specific internal energy	particle velocity
The first compression	6399.6	0.000425	0.3552	0.8428
The second compression	11960.0	0.000387	0.6967	1.2980

References

[1] Shouzhong Zhang. Explosion and impact dynamics. The Publishing House of Ordnance Industry, 1993

[2] Steinberg D J, Cochran S G, Guinan M W. Constitutive model for metals applicable at high strain rate. J App Phys, 1980, 51(3): 1498~1503

[3] Hua Chen, Yuanji He. Experimental study of Hugoniot curve for polyimide material. Demonstration and Research, 2015, 31(2): 60~62

ID077: In-situ Observation of Dynamic Fracture Processes in Geomaterials Using High-speed X-ray Imaging

Niranjan Parab[1, a], Zherui Guo[1], Matthew Hudspeth[1], Benjamin Claus[1], Boon Him Lim[1], Tao Sun[2], Xianghui Xiao[2], Kamel Fezzaa[2], Weinong Chen[1, 3, b]

1School of Aeronautics and Astronautics, Purdue University, West Lafayette IN 47907, USA

2Advanced Photon Source, Argonne National Laboratory, Lemont, IL 60439, USA

3School of Materials Engineering, Purdue University, West Lafayette IN 47907, USA

anparab@purdue.edu, bwchen@purdue.edu

Abstract: *In-situ* dynamic cracking inside opaque geomaterials is desired to be understood but cannot be visualized using traditional optical imaging methods. In this study, the *in-situ* internal dynamic failure mechanisms in a concrete and Indiana limestone under dynamic loading was studied using high speed synchrotron X-ray phase contrast imaging. Dynamic compressive loading was applied using a modified Kolsky bar and fracture images were recorded using a synchronized high speed synchrotron X-ray imaging setup. 3-D synchrotron X-ray tomography was also performed to record the microstructure of the specimens before dynamic loading. In the concrete, both straight cracking and angular cracking with respect to the direction of loading were observed. In limestone, cracks followed the grain boundaries and voids before ultimately fracturing the specimen. The effects of the microstructure on the observed dynamic crack behavior are discuss

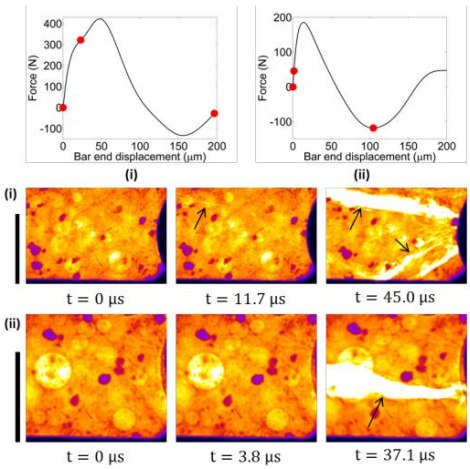

Fig.1 Force histories over displacement with corresponding high speed X-ray images for two representative concrete experiments.

References

[1] N. Parab, B. Claus, M. Hudspeth, J. Black, A. Mondal, J. Sun, *et al*. : *Int J Impact Eng*. 68(2014) pp8–14

[2] W. Chen, M. Hudspeth, B. Claus, N. Parab, J. Black, K. Fezza, *et al*.: *Philos Trans R Soc A*. 372(2015) 20130191

[3] M. Zbib, N. Parab, W. Chen, D. Bahr: *Powder Technol*. 283(2015) pp57–65

ID078: Explosive Sintering Tungsten Copper Alloy To Copper Surface

Xiang Chen[1], Xiaojie Li[2,a], Honghao Yan[1], Xiaohong Wang[1], Yusong Miao[1]

[1]Department of Engineering Mechanics, Dalian University of Technology, Dalian, Liaoning 116024, China

[2]State Key Laboratory of Structural Analysis for Industrial Equipment, Dalian University of Technology, Dalian, 116024, China

[a]m18740280150@163.com

Abstract: This paper proposes a method to sintering tungsten-copper alloy coating layer to copper plate surface. Sintering in the hydrogen after pre-compacted tungsten-copper alloy powder to the surface of the copper plate, compacted the pre-compacted powder by explosive sintering. Diffusion sintering at last in order to improve the coating layer density. The coating layer was up to 99.3% of the theoretical density. Microstructure characteristics indicated that tungsten copper powder well mixed. The size of the tungsten particles is larger than copper particles. The SEM fracture surface analysis is different from traditional fracture. Tungsten copper joint surface, analyzed by SEM, indicated that tungsten copper alloy sintered on the surface of the copper.

Keywords: Tungsten copper alloy coating layer, Explosive compaction, SEM fracture surface analysis

ID079: Influences of Crossover Tube Structures on Detonation Branching in a Pulse Detonation Engine with Liquid Hydrocarbon Fuel

Xiao Pan[1, a] , Chunsheng Weng[1, b] , Baoxing Li[1, c]

[1]National Key Lab of Transient Physics, Nanjing University of Science and Technology, Nanjing 210094, China

[a]panqey@163.com, [b]wengcs@126.com, [c]bestlibaoxing@163.com

The aim of this work is to numerically study the pre-detonation ignition of gas-liquid two-phase Pulse Detonation Engine (PDE). Based on the two-dimensional Conservation Element and Solution Element (CE/SE) method, different models of dual PDE and crossover tubes of varying configurations, using gasoline as fuel, are performed to find out the properties of detonation wave propagation in the whole system as shown in Fig.1. Compared to the driving PDE ignited by a traditional spark plug, the driven PDE achieves detonation with shockwave transferred from the crossover tube. Results show that at the entrance of crossover tube, detonation branching occurs. The shockwave pressure in crossover tube is higher than 0.8MPa and its velocity is about 1000m/s. When shockwave propagates into the driven PDE, its reflection on the detonation chamber wall generates a local high pressure area, which will affect oxidizer inflow in practical use. Detonation re-initiation accomplishes at the end of main detonation tube by pre-detonation ignition method as shown in Fig.2. Although different structures of crossover tube have little impact on the parameters of detonation wave achieved in the driven PDE, the detonation formation time and DDT distance can be shortened in varying degrees. Overall results and analyses show that to create the most efficient detonation ignition process, larger diameter crossover tubes should be used together with shorter length to decrease the total working cycle time of the driven PDE to perform at high frequency.

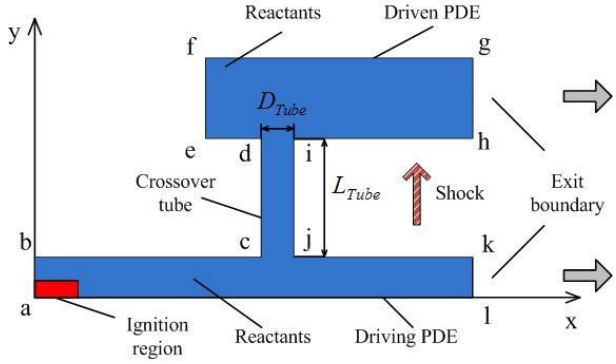

Fig.1 Simulation model of the dual PDE with crossover tube system

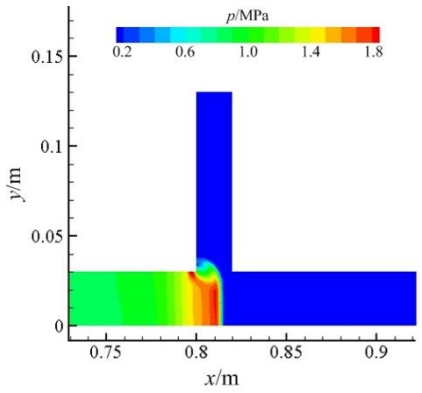

(a) t=0.677ms

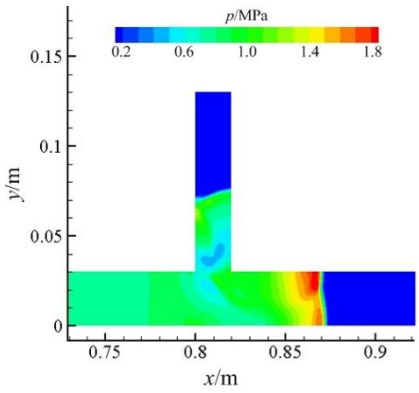

(b) t=0.721ms

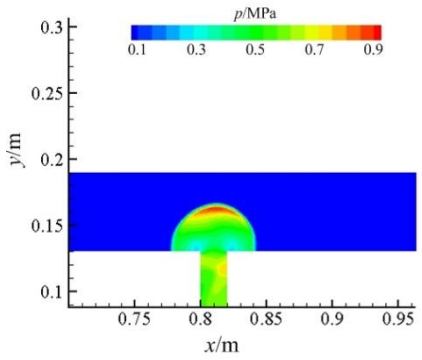

(c) t=0.807ms

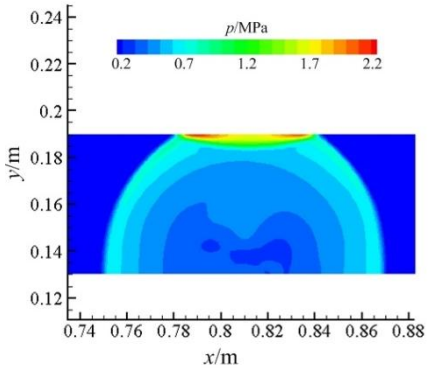

(d) t=0.842ms

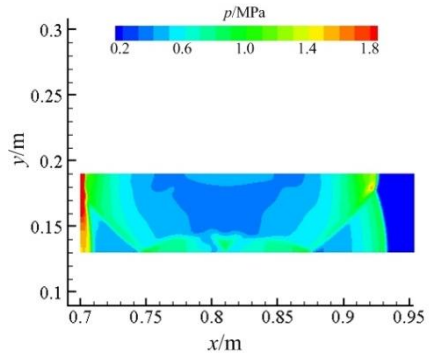

(e) t=0.912ms

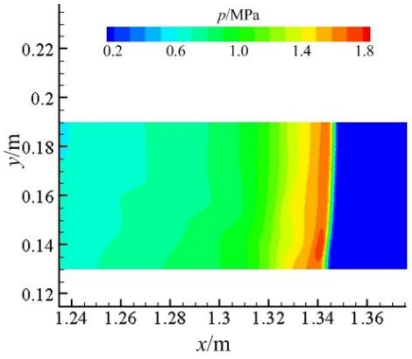

(f) t=1.260ms

Fig.2 Pressure contours of flow fluid in a dual PDE with crossover tube system

ID080: Numerical Simulations of Flow Field Outside Triple-tube Pulse Detonation Engine

Xiao-long Huang[1,a], Ning Li[1,b,*] Chun-sheng Weng[1,c]

[1]National Key Laboratory of Transient Physics, Nanjing University of Science & Technology, Nanjing, 210094, China.

[a]huang_xl@foxmail.com, [b]stokim@gmail.com, [c]wengcs@126.com.

Pulse Detonation Engine (PDE), as one of the most promising propulsive device in this century, has attracted a great attention due to its simple structure and higher thermal efficiency compared with existing aero engines under constant pressure combustion. Many researches show that a single pulse detonation tube would be insufficient to propel an aircraft alone, and multi-tube PDE would form a more practical propulsion system with higher overall engine frequency and the possibility of thrust vectoring was compared with which of the PDE with a single detonation tube.

The system with triple-tube PDE was designed and three tubes were arrayed as regular triangle, filled with the mixture of stoichiometric gasoline-oxygen. The space-time conservation element and solution element (CE/SE) method was deduced to simulate the flow field inside and outside of the PDE. Then, four firing patterns were performed to investigate the peak pressure of shock wave outside of the PDE. The three tubes were fired with different time delays in each firing patterns: (a) 0-0-0 ms, (b) 0-1-2 ms, (c) 0-2-4 ms, (d) 0-3-6 ms. The calculation result shows that the vortexes, shock and expansion waves were obtained in the flow field outside of the triple-tube PDE. The peak pressure of shock waves was largest when the tubes were fired simultaneous and decreased when each tube fired with longer delay time.

ID081: Effect of Graphene Nanoplatelets Content on Dynamic Compression Mechanical Properties of Titanium Matrix Composites

Xiaonan Mu[a], Hongmei Zhang[a*], Hongnian Cai[a], Qunbo Fan[a], Yan Wu[a]

[a]National Key Laboratory of Science and Technology on Materials under Shock and Impact, School of Materials Science and Engineering, Beijing Institute of Technology, Beijing 100081, China

*Corresponding author: Prof. H.-M. Zhang,

Tel.: +86 10 68913951 605; Fax. : +86 10 6891 3951 608

E-mail address: zhanghm@bit.edu.cn (H. Zhang)

Abstract: In this study, the titanium matrix composites（TiMCs）was fabricated by adding graphene nanoplatelets (GNPs). The dynamic compression test was carried out to study the effect of strain-rate and the GNPs content on dynamic mechanical properties of GNPs/Ti. Results show that the GNPs content (0wt%~0.8wt%) correspond to specific microstructure and affect the dynamic mechanical properties of the composites. Under high strain-rate ($3500s^{-1}$), the 0.4wt%GNPs/Ti has the highest dynamic stress (~1860MPa) and strain (~30%). The adiabatic shearing band (ASB) microstructure of GNPs/Ti with various GNPs content has been observed under $3500s^{-1}$ strain-rate and the ASB microstructure evolution of 0.4wt%GNPs/Ti under different strain rate is investigated in particular. The strain-rate sensitivity is also studied and results show that thermal softening paly a leading role to the composites.

Keyword: titanium matrix composites; graphene nanoplatelets; dynamic mechanical properties

GNPs is a two-dimensional nanomaterial which has been considered to be one potential new carbon material in the field of material science and engineering due to its remarkable electrical, thermal and mechanical properties [1-3].Powder metallurgy method was used to fabricated the GNPs (0wt%-0.8wt%) reinforced pure titanium matrix composites (GNPs/Ti)[4]. GNPs distribute uniformly in titanium matrix and combine firmly with α-Ti grains when the GNPs content is less than 0.4wt%. The 0.4wt%GNPs/Ti displays outstanding compression mechanical properties at high strain-rate because the GNPs can refine the grain size and block the deformation of the matrix at high strain-rate

[5].

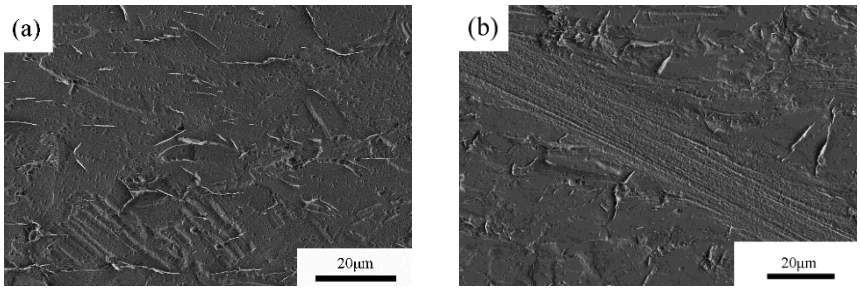

Fig.1. FSEM micrographs of 0.4GNPs/Ti composite: (a) before dynamic compression test (b) after dynamic compression test.

References

[1] A.K. Geim, K.S. Novoselov. The rise of graphene. *Nature materials* 6(2007), pp183–191.

[2] S. Park, R.S. Ruoff, Chemical methods for the production of graphenes. *Nature Nanotechnology* 5(2010), pp217–224.

[3] K.S. Novoselov, A.K. Geim, S.V. Morozov, D. Jiang, Y. Zhang, S.V. Dubonos, I.V. Grigorieva, A.A. Firsov. Electric field effect in atomically thin carbon films. *Science.* 306(2004), pp666–669.

[4] F.C. Wang, Z.H. Zhang, Y.J. Sun, Y. Liu, Z.Y. Hu, H. Wang, A.V. Korznikov, E. Korznikova, Z.F. Liu, S. Osamu. Rapid and low temperature spark plasma sintering synthesis of novel carbon nanotube reinforced titanium matrix composites. *Carbon.* 95(2015), pp396-407.

[5] S.E. Shin, H.J. Choi, J.H. Shin, D.H. Bae. Strengthening behavior of few-layered graphene /aluminum composites. *Carbon*. 82(2015), pp143-151.

ID082: Numerical Simulation on Cook-off Response of Fuse Explosive Train

Xin Tang[1,a], Junming Yuan[1,b], Yucun Liu[1], Wenzhi Tan[1], Zongren Xing[2] , Shuo Li [1] , Shangpeng Hao [1]

[1]School of Chemical Engineering and Environment, North University of China, Taiyuan 030051, China

[2]Institute of Chemical Materials, CAEP, mianyang621900, China

[a]494640136@qq.com,

[b] junmyuan@163.com

Abstract: The thermal cook–off response of fuse explosive train is not only important in the view of safety point, but also challenges our understanding of the explosive materials. When the explosive material was ignited, it was different from the primarily chemical and physical state in the case of slow and fast cook-off. To investigate the characteristics of the thermal reaction for JH-14C in the fuse explosive train, multi-point measured temperature cook-off tests were carried out at different heating rates. A 3D model of the fuse in medium and large caliber munitions was developed to simulate the thermal and chemical behavior in the thermal ignition at different heating rates which were calculated by FLUENT. The results of these numerical simulations are presented, together with some possible explanations of the behavior and discussion of the implications to modeling this response. The results show that the ignition temperature of the fuse explosive train is not much different and the ignition position is at the inner of booster charge of fuse explosive train on the condition of different heating rates. The ignition time decreases and the ignition position moves from the center to the end of the booster cylinder edge with the increase of the heating rate. The useful information can be provided to ensure the thermal reliability and safety of fuse in the storage and transportation.

Keywords: physical chemistry, fuse explosive train, Thermal decomposition kinetics, numerical simulation

References

[1] Chen L, Ma X, Lu F, et al. Investigation of the cook-off processes of HMX-based mixed explosives[J]. Central European Journal of Energetic Materials, 2014, 11.

[2] WANG W, WANG J, GUO W, et al. Influence of Al Content on the Detonation Pressure and Detonation Velocity of RDX-based Aluminized Explosive [J][J]. Chinese Journal of Explosives & Propellants, 2010, 1: 004.

[3] YANG J, JIA X, YU R, et al. Research on the Bullet Impact Characteristic of RDX Base Propellant[J]. Initiators & Pyrotechnics, 2011, 5: 005.

ID083: Laser Impact Welding of Aluminum/Copper Plates

Y.Iwamoto[1,a], R.Uchida[1], G.Kennedy[2], N.Thadhani[2] and K.Hokamoto[3]

[1]Graduate School of Science and Technology, Kumamoto University, 2-39-1 Kurokami, Chuo-ku, Kumamoto 860-8555, Japan

[2]School of Material Science and Engineering, Georgia Institute of Technology, Georgia, USA

[3]Institute of Pulsed Power Science, Kumamoto University, Kumamoto, Japan

[a]168d8202@st.kumamoto-u.ac.jp

Abstract: The process of Laser Impact Welding is that thin metal plate accelerated by laser-induced ablation collides with another plate at high speed having a collision angle similar to explosive welding. Recently, X.Wang et al. [1] suggested the possibility using such technique to weld a spot area for bonding dissimilar materials. In their experiment, two plates were fixed inclination angle for a making proper collision angle. On the other hand, our experiments tried to weld a thin aluminum foil (thickness; 50 and 100 μm) onto a copper plate (thickness; 1mm) with parallel set-up with a fixed stand-off distance at 50 and 100 μm, which means that there is no initial inclined angle between the two plates.

As a result of microstructural characterization, wavy interface, showing the evidence of tight bonding based on explosive welding mechanism, was confirmed at the edge of the welded spot area, and flat interface was confirmed at the center of the welded area. At the beginning of the welding at the center, collision angle is not high enough to cause waves, besides, the angle is considered more close to the edge of the welded spot area.

Reference

[1] Xiao Wang, Chunxing Gu, Yuanyuan Zheng, Zongbao Shen, Huixia Liu: Materials and Design 56 (2014), pp26-30

ID084: The Measurement of Overpressure of Shock Wave and Numerical Simulation to The Explosion Test of Steel Box Girder Scale Model

Yaling Liu [1,a], Shaobo Geng [1,b], Yucun Liu [2], Junming Yuan[2], Jianying Xue [1]

[1] School of Science ,North Univercity of China, Taiyuan 030051, China

[2] School of Chemical Engineering Environment, North Univercity of China,Taiyuan 030051,China

[a]liuyaling@nuc.edu.cn，[b]gengshaobo@nuc.edu.cn

Abstract: The overpressure of shock wave in a certain distance for the blast-resistant experiment of steel box girder scale model was measured. The TNT equivalent of the homemade composite explosive (TNT/RDX=40/60) and the overpressure values of corresponding location was analyzed and calculated **(1,2)**. The reasonable formulae of the calculation of shock wave overpressure for the experiment was found(3); the overpressure of shock wave of corresponding location is simulated by the finite element software AUTODYN, the measured values were compared with the theoretical calculation values and simulation values. Thus verified throung the rationality of the theoretical formula and the simulation parameters selection. Further, the condition 1 of the explosion test for steel box girder scale model was simulated, and a basis for the numerical simulation was provided for the next step to carry out the Steel box girder of blast-resistant performance.

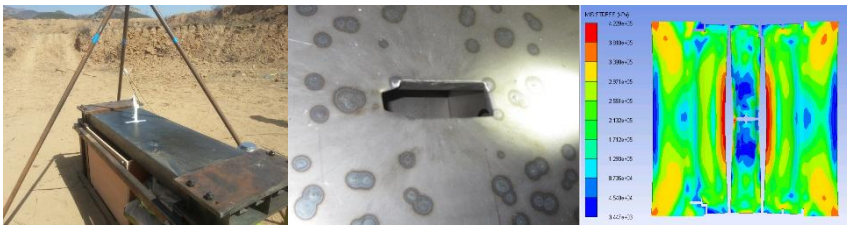

(a) (b) (c)

Fig.1 Experiment and simulation results

(a)Relative location of the overpressure sensor and explosive on the test site

(b)Breakage of Steel box girder (c) Stress nephogram under blast load

References

[1] Yulei Zhang etc.: The influence on the test method of overpressure to the result of explosives TNT equivalent calculation[J]， Chinese Journal of Explosives & Propellants37(2014),pp16-19

[2] Lin Zhou ,Xiangrong Zhang:Principle and Applications of Explosive Energy Transformation,Beijing ,National Defense Industry Press,2015

ID085: Discussion of Alumina Oxide/Nano-Diamond Composite Powders Preparation by Detonation

Yan Xianrong[1], Xiaojie Li [1, 2], Xiaohong Wang [1, 2], Honghao Yan [1, 2]

[1]Department of Engineering Mechanics, Dalian University of Technology, Dalian Liaoning 116024, China

[2] State Key Laboratory of Structural Analysis for Industrial Equipment, Dalian Liaoning 116024, China

[a]yxr05.ok@163.com

[b]dymat@163.com

Abstract: Nano diamond coated /nano aluminum oxide composite powders were prepared by detonation using Nano-diamond, boron anhydride, aluminum sols in this article. The testing ways as XRD, TEM, and SEM were brought to observe and analyze the detonation products. As the result of the high temperature and high pressure produced by the detonation of the explosive, the particle size of composite powders which have nano diamond in the center and nano aluminum oxide coated outside exist 40～130nm and the balls are uneven distribution.

ID086: Dynamic Mechanical Behaviors Under High Temperature and Constitutive Model of High-Nitrogen Austenitic Stainless Steel

Yanli Wang[1], Guzhai Jia[1, a], Wei Ji[1], Yanyun Liu[2], Xiaoming Mu[1], Yawei Zhou[1]

[1] No. 52 Institute of China Ordnance Industries, Yantai 264003, China

[2]North Micro-Electro-Mechanical Intelligent Group Corporation Limited, Beijing 101149, China

[a]jiaguzhai@yeah.net

Abstract: Dynamic tests of high-nitrogen austenitic stainless steel (HNS) with strain rates of 10^2~$10^3 s^{-1}$ were performed by split Hopkinson bar apparatus under different temperatures from 293K to 873K.Combined with quasi-static tests, strain rate effects and temperature effects of HNS were analyzed. The results show that dynamic mechanical behavior of HNS is great sensitive to strain rate and temperature. The increasing of flow stress over strain rate become strongly when strain rate reached $440s^{-1}$ or more; and also, as temperature decreases, the flow stress increases rapidly. The couple effects of strain rate and temperature to plastic behavior of HNS are investigated; and the results depicts that the thermal softening effect acted a key role in dynamic deformation under high temperature. Based on the classical Johnson-Cook constitutive model, a modified Johnson-Cook constitutive model was acquired. The modified Johnson-Cook constitutive model can describe the dynamic mechanical behavior of HNS correctly.

Keywords: High-nitrogenaustenitic stainless steel, strain rate, temperature,Johnson-Cook constitutive model

ID087: Experiment Investigation on Microvoid Nucleation and Analysis of Temperature Field for High Temperature Nickel Based Superalloy Under Thermal Shock Arisen as Laser Drilling

Xinchun Shang[1,2, a] , Yanting Xu[1, b] , Peifei Wu[1]

[1]National Center for Materials Service Safety, University of Science and Technology Beijing, Beijing 100083, China

[2]Department of Applied Mechanics, University of Science and Technology Beijing, Beijing 100083, China

[a]shangxc@ustb.edu.cn, [b]s20141372@xs.ustb.edu.cn

Abstract: The metal would overheat and even burn under the thermal shock arisen as laser drilling, which causes micro damage inside the metal. Void damage is the most important origin for crack propagation and failure of metal. To understand the damage mechanism in the heat affected zone of the high temperature nickel based superalloy DD6, a microvoid nucleation experiment was designed and implemented by laser drilling in DD6 sheet. The complex characteristics of micro-damage including micro-voids near the perforation were observed by scanning electron microscopy. An analytic solution of the temperature field in DD6 sheet for thermal shock arisen as laser drilling was obtained on the basis of the non-Fourier heat conduction theory. As a result, the minimum of peak temperature during the thermal shock in the zone of microvoid nucleation was estimated.

Keywords: microvoid damage, thermal shock test, laser drilling, non-Fourier heat conduction, analytical solution

Experiment for Microvoid Nucleation

The perforation at the center of a circle sheet made of high temperature nickel based superalloy DD6 was implemented by laser drilling. The diameter and thickness of the circle sheet are 50mm and 5mm, respectively. The light spot diameter of laser beam is 2mm, the power of fiber laser is 2kw and the irradiation time t_0 is 0.8s.

On the longitudinal section along the perforation, the micro-topography in the heat affected zone (HAZ) near the perforated surface was observed by scanning electron microscopy (SEM). As shown in the figure1, the complex micro-damage, such as micro-voids clusters, micro pits and micro cracks were found in the HAZ by SEM. It is clear that the HAZ with 100μm width is divided into two distinct areas: 1) the area of

30um-50um distant from perforated surface is oxidized, in which microvoid with bigger size distributes intensively and homogeneously and there are much more damage of micro pits and micro cracks. 2) the rest area has large number of sparse microvoid with smaller size and a few larger isolated microvoid. During the laser drilling, the DD6 material near the drilling position is suddenly heated up to a quite high temperature, meanwhile it would melt and vaporize. Such thermal shock will cause larger temperature gradient and higher triaxial thermal stresses, so that the nucleation and growth of microvoid occur in HAZ [1].

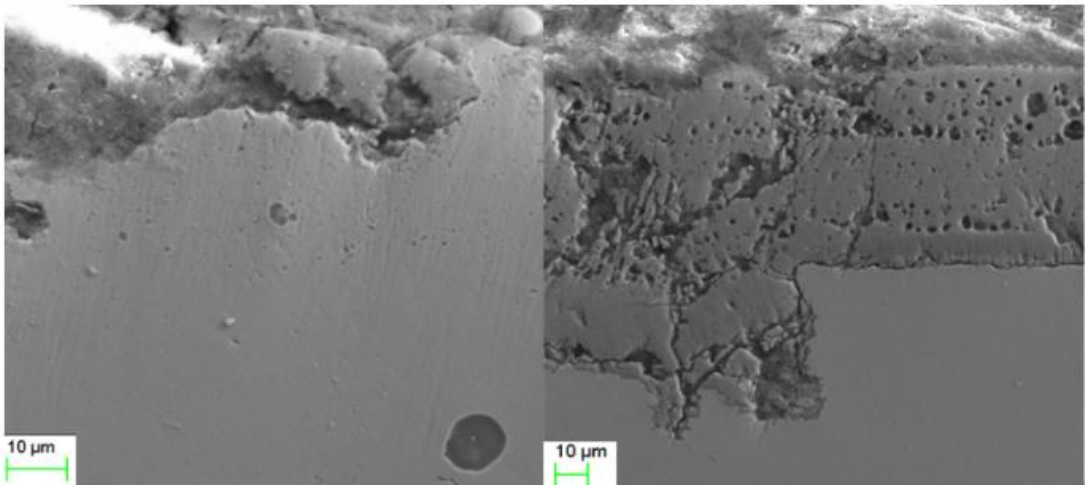

Fig1. Scanning electron microscopy of the HAZ near the perforated surface

Analysis of Temperature Field

For the ultrafast and ultra-conventional heat conduction like laser drilling, non-Fourier effect will be crucial. The mathematical modeling of the problem was built for temperature field, in which the governing differential equation contains a relaxation time [2]. The initial temperature in the sheet is the environment one, and the boundary conditions are adiabatic apart from the perforation surface where the change of temperature difference induced by laser drilling is described as $T = f(t) = (T_m - T_0)(t/t_0)\exp(1-t/t_0)$ (the DD6 melt temperature $T_m = 1370℃$). The Laplace transformation solution of the temperature field was obtained analytically by using the Bessel functions as follows:

$$\tilde{T} = \frac{I_0'(\theta_0 b)K_0(\theta_0 r) - K_0'(\theta_0 b)I_0(\theta_0 r)}{I_0'(\theta_0 b)K_0(\theta_0 a) - K_0'(\theta_0 b)I_0(\theta_0 a)}\,\tilde{f}(s)$$

By applying numerical algorithm of Laplace inverse transformation, the curve of the temperature versus time is plotted. As the edge of HAZ is about 100μm from the

perforated surface, the minimum of peak temperature in the edge of HAZ can be estimated roughly as nucleation temperature. The curve in Figure 2 indicates the nucleation temperature for DD6 sheet is about 1270℃, this result might be helpful to investigate the micro-damage of high temperature nickel based superalloy DD6 under thermal shock.

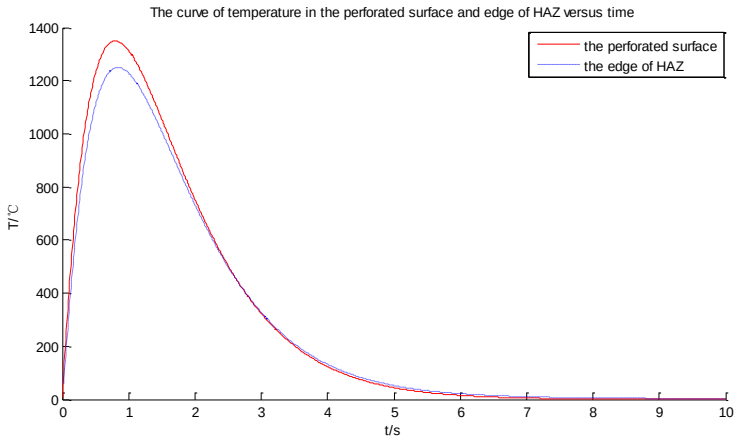

Fig2. The curve of temperature in the edge of HAZ versus time

Acknowledgment

The project supported by the National High Technology Research and Development Program of China (Grant No. 2012AA03A513), the National Natural Science Foundation of China (No. 10772024).

References

[1] Shang X C, Zhang Z B. Characterization of Microscopic Damage in Aluminum Alloy Materials Under Intense Thermal Shock[J]. Journal of Materials Engineering, 2011, 35(2):1-144.

[2] Zhang L, Shang X. Analytical solution to non-Fourier heat conduction as a laser beam irradiating on local surface of a semi-infinite medium [J]. International Journal of Heat & Mass Transfer, 2015, 85:772-780.

ID088: A New Mathematical Method for Optimizing the Process of Exploding Foil Initiators Drive a Plane Flyer

Yaqi Zhao[1, a], Xinping Long[2], Qiubo Fu[3, b], Daojian Jiang[4]

[1]Graduate school of Chinese academy of engineering physics, Mianyang, Sichuan, 621900, China

[2]China Academy of Engineering Physics, Mianyang, Sichuan, 621900, China

[3]Institute of Chemical Materials, China Academy of Engineering Physics, Mianyang, Sichuan, 621900, China

[4]Institute of Applied Electronics, China Academy of Engineering Physics, Mianyang, Sichuan, 621900, China

[a] zhaoyq09@buaa.edu.cn, [b] fuqiubo@caep.cn

Exploding foil initiator, also called slapper detonators as a new igniter for insensitive high energy weapons, is highly insensitive to mechanical shock and electromagnetic interference because a special high pulse current is needed for initiation. This paper briefly introduces the physical model of EFI, then systematically analyzes the relationship between each component of EFI and the ability of flyer which is driven by EFI system. A new structure of foil is designed (Fig. 1). Based on this new structure, our team has done a series of experiments to analyze the ability of flyer driven. Compared to the classical bridge foil with a quadrate shape, new experimental results show that annular foil need lower ignition energy and can generate stronger shock wave pressures.

Fig.1 Structure of annular foil

Table 1. The comparison of annular foil and classical foil

No.	Diameter of annular exploding foil Mm	width of annular mm	dimension of barrel mm	area of exploding foil mm	velocity of flyer m s^{-1}	kinetic energy of flyer mJ
1#	0.4/0.8	0.20	Φ0.8×0.4	0.6×0.6	4137	0.304
2#	0.4/0.8	0.20	Φ0.8×0.4	0.6×0.6	4163	0.308
3#	0.6×0.6	-	Φ0.8×0.4	0.6×0.6	3027	0.163

Meanwhile, as we all know that meshes generation is the key to numerical solution of partial differential equations. The quality of meshes undoubtedly affects the simulation results. In terms of numerical simulation, adaptive grid method ' Delaunay algorithm ' (Fig. 2) has been applied to mesh for the purpose of precisely catching the transformation of each variable during the whole process of exploding foil initiators ' burst.

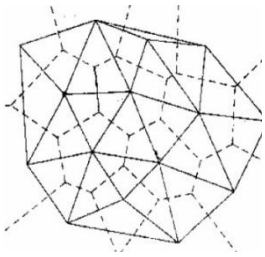

Fig. 2 Voronoi (dotted line) and Delaunay triangle (solid line)

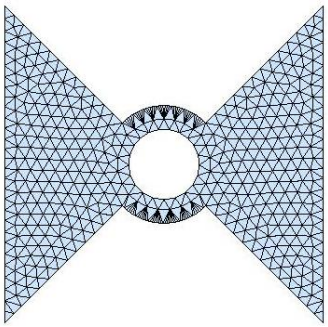

Fig. 3 Delaunay mesh grid result

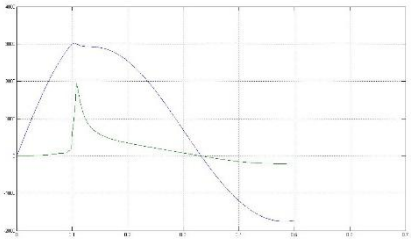

Fig. 4 U-I relationship during burst process

References

[1] J. D. Logan, R. S. Lee, R. C. Weingart, and K. S. Yee. Calculation of heating and burst phenomena in electrically exploded foils. Journal of Applied Physics, Vol. 48, No. 2, February 1977.

[2] G. R. Gathers. Thermophysical Properties of Liquid Copper and Aluminum. International Journal of Thermophysics, Vol. 4, No. 3, 1983

[3] Carlton M. Furnberg. Computer Modeling of Detonators. 0-7803-2428-5195 $4.00 0 1995 IEEE.

[4] Per-Olof Persson. Mesh Generation for Implicit Geometries.

ID089: Understanding Scaling Deviations of Diameter and Thickness Effects

Yehuda Partom[1,a]

[1]Retired from RAFAEL, ISRAEL

[a]ypartom@netvision.net.il

One way to characterize the sensitivity of explosives (in the sense of reaction rate) is through size effect tests. Using cylinders it is called diameter effect test, and using plates it is called thickness effect test.

From the equations of motion for the two test configurations it can be deduced that the two test configurations scale as:

$$d(D) = 2h(D) \quad or \quad r(D) = h(D) \tag{1}$$

where d=rod diameter, r=rod radius, h=plate thickness, and the scaling holds for the same steady detonation velocity D.

But tests with various explosives show deviations from the scaling expressed by Eq. (1) (perfect scaling) [1-4]. The results of these tests show that sometimes r/h<1 and other times r/h>1, and that deviations from perfect scaling may be as high as 10%.

Until now no explanation to these deviations has been given, and here we suggest such an explanation. Our explanation is based on our work in [5], where we show that a boundary layer of partial reaction usually forms for a detonation wave grazing a free boundary. Denoting the equivalent thickness of such a boundary layer by Δ_r for a rod, and by Δ_h for a plate we have:

$$\frac{r-\Delta_r}{h-\Delta_h} = 1 \qquad \frac{r}{h} = 1 - \frac{2\Delta_h - \Delta_r}{h} \tag{2}$$

So that:

$$\frac{r(D)}{h(D)} < 1 \quad for \quad 2\Delta_h > \Delta_r$$

$$\frac{r(D)}{h(D)} > 1 \quad for \quad 2\Delta_h < \Delta_r \tag{3}$$

On this basis we suggest that scaling deviations of the diameter effect from the thickness effect are related to the partially reacted boundary layer phenomenon. To further establish this suggestion we run direct numerical simulations with our reactive flow code TDRR [6]. As shown in [5] TDRR reproduces the partially reacted boundary layer. It

follows that if TDRR reproduces the scaling deviations as well, this would strengthen our suggestion for the origin of the scaling deviations.

The material parameters in our simulations are those of PBX 9502, but without the slow reaction component. This is why we don't quite reproduce diameter effect data. The rod radius is between 5 and 10mm, and the plate thickness is between 5 and 12mm. We show the simulation results in figure 1.

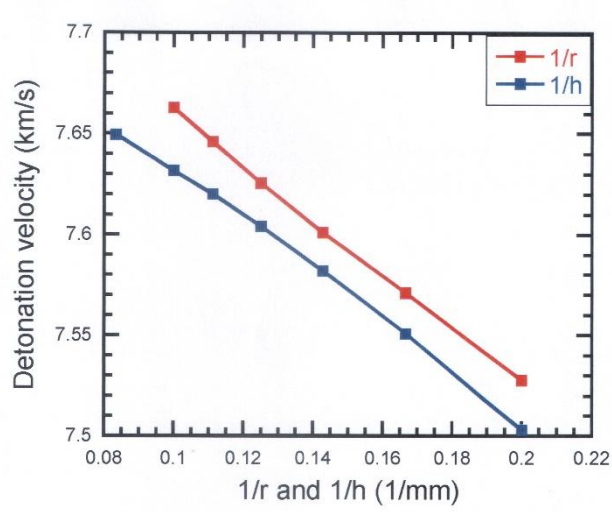

Fig.1 Simulated radius and thickness effect curves

We see from Fig. 1 that r(D)/h(D) is between 0.78 for the highest detonation velocity and 0.9 for the lowest velocity, which is the correct order of magnitude.

In figure 2 we show maps with lines of equal reaction progress parameter after 60mm into a rod of radius 10mm and a plate of thickness 10mm, where we lowered in the simulations the reaction rate by 22%. The plate run is for half the thickness because of the symmetry.

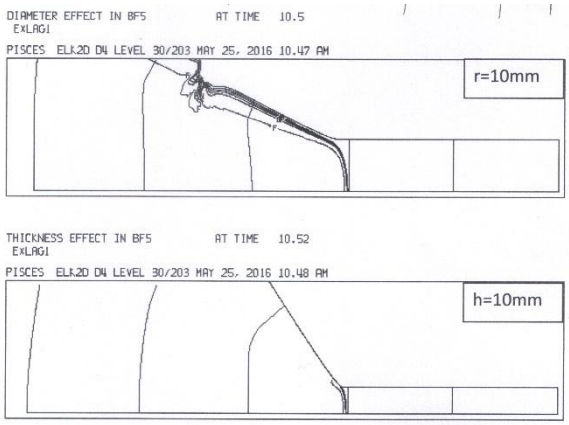

Fig.2 Maps with lines of equal reaction progress parameter after 60mm into the rod or plate, and for a reaction rate lowered by 22%.

References

[1] S.I. Jackson and M. Short: 18th APS-SCCM and 24th AIRAPT conference, J. of Phys. Conference series 500 (2014) 052020

[2] O. Petel, D. Mack, A. Higgins, R. Turcotte and S. Chan: J. Loss Prevent. Proc. 20 578–8 (2007)

[3] V. V. Silvestrov, A. V. Plastinin, S. M. Karakhanov and V. V. Zykov: Combust. Explo. Shock 44 354–9 (2008)

[4] A. Higgins: AIP Conf. Proc. 1195 193–6 (2009)

[5] Y. Partom: 18th APS-SCCM and 24th AIRAPT conference, J. of Phys. Conference series 500 (2014) 052034

[6] Y. Partom: APS-SCCM conference, Atlanta GA, 460-463 (2001)

ID090: Experimental Study and Computational Simulation for Shock Characteristics Estimation of Okinawa's Soils "*Jahgaru*"

Yoshikazu Higa[1, a], Hirofumi Iyama[2, b], Ken Shimojima[1], Masatoshi Nishi[2] and Shigeru Itoh[3]

1 Dept. Mechanical Systems Engineering, National Institute of Technology, Okinawa College, 905 Henoko, Nago, Okinawa 905-2192, Japan

2 Dept. Mechanical & Intelligent System Engineering, National Institute of Technology, Kumamoto College, Kumamoto 866-8501, Japan

3 Professor Emeritus, Kumamoto University & National Institute of Technology, Okinawa College

[a]y.higa@okinawa-ct.ac.jp, [b]eyama@kumamoto-nct.ac.jp, [c]k_shimo@okinawa-ct.ac.jp, [d]nishima@kumamoto-nct.ac.jp, [e]itoh_lab@okinawa-ct.ac.jp

To clarify the shock characteristics of Okinawa's unique soils "*Jahgaru*" that is widely distributed in southern part of Okinawa Main Island [1], an experimental investigation of dynamics properties such as shockwave propagation, pressure and particle velocity have been performed using impedance matching method [2]. Therefore, we have also obtained the Hugoniot date of "*Jahgaru*". And then, to reveal a validity of the material characteristics, a computational model for the experimental procedure using ALE simulation [3] have been developed. A comparison between numerical results and experimental ones, the capability of proposed method through the numerical simulations have been confirmed.

References

[1] Okinawa Prefecture Agricultural Experiment Station: *Soils in Okinawa prefecture and measures to improve their quality*, Okinawa, Japan: (1999), Okinawa International Center, Japan International Cooperation Agency

[2] K. Tanaka: *Sci. Tech. of Energetic Mater.* Vol.37, No.6 (1976), pp.277-290

[3] C.W. Hirt, A.A. Amsden and J.L. Cook: *J. Comput. Phys.* Vol.14, No.3 (1974), pp.227-253

ID091: Numerical Simulation of Electrical Discharge Characteristics Induced by Underwater Wire Explosion

Ryo Henzan[1,a], Yoshikazu Higa[2,b], Osamu Higa[3,c], Ken Shimojima[2,d] and Shigeru Itoh[4,e]

1 Creative System Engineering Advanced Course, National Institute of Technology, Okinawa College, 905 Henoko, Nago, 905-2192, Japan

2 Dept. Mech. Sys. Engng., Nat. Inst. Tech., Okinawa Coll.

3 Sci. & Tech. Division, Nat. Inst. Tech., Okinawa Coll.

4 Emeritus Prof., Kumamoto Univ. & Nat. Inst. Tech., Okinawa Coll.

[a]ac164507@edu.okinawa-ct.ac.jp, [b]y.higa@okinawa-ct.ac.jp, [c]osamu@okinawa-ct.ac.jp, [d]k_shimo@okinawa-ct.ac.jp, [e]itoh_lab@okinawa-ct.ac.jp

Underwater shock wave phenomenon is applied to various fields such as manufacturing, food processing and medical equipment, and has been investigated with many experiment and numerical analysis in the past [1]. The underwater shock wave is produced by various methods e.g., underwater wire explosion and pulse gap electrical discharge. Therefore, it is extremely important to clarify the shock characteristics depending on the stored electrical energy, wire dimension and material. However, it is hard to predict a pressure and its distribution induced by underwater electrical wire explosion because the phenomena associated with an elementary process is significantly complicated.

In this study, to predict a discharge characteristics induced by underwater electrical wire explosion, the numerical simulation based on the "simplified model of underwater electrical discharge"[2] has been performed. The numerical results show good agreement with experimental ones.

References

[1] S. Itoh: *Materials Science Forum* Vol. 556 (2008), pp361-372

[2] V. Ts. Gurovich, A. Grinenko, Ya. E. Krasik, and J. Felsteiner: *Phys. Rev*. E69, 036402 (2004)

ID092: Numerical Simulation of Dynamic Brazilian Splitting by the Discontinuous Deformation Analysis Method

Zheng Yang[1], Youjun Ning[1,*], Ge Kang[2]

[1]School of Manufacturing Science and Engineering, Southwest University of Science and Technology, Mianyang 621010, P. R. China

[2]State Key Laboratory of Explosion Science and Technology, Beijing Institute of Technology, Beijing 100081, China

[*]cnningyj@foxmail.com

Abstract: The discontinuous deformation analysis (DDA) method is adopted to numerically simulate the dynamic Brazilian splitting test of rock. When trapezoid dynamic compressive loads with different amplitudes are applied to the rock disk, the splitting failure process of the disk shows different features and forms different ultimate failure patterns. It is indicated that the failure pattern and failure mechanism of rock under dynamic loading is closely related to the propagation of the stress waves in the rock. The numerical simulation results are beneficial for the study of the failure pattern and failure mechanisms resulting from the propagation of stress waves in rock-like materials.

ID093: Adaptive Aiming of Asymmetrically Initiated Warhead

Yuan Li[a], Yuquan Wen[b], Yanhua Li, Chen Liu

State Key Laboratory of Explosion Science and Technology, Beijing Institute of Technology, Beijing 100081, China

[a]panshi-boshi@163.com, [b]wyquan@bit.edu.cn

Abstract: Asymmetrical initiation is an effective way to alter the lethality direction, but the aiming precision is still not enough and it may cause fuze/warhead corporation problems. For more precise control of the lethality elements, numerical simulation is used to study the influence of circumferential delay initiation and axial delay initiation on the cylindrical and hexagonal prism warheads' lethality distribution. The results show that as the circumferential initiation delay increases, the aiming direction changes much. The maximum change of cylindrical warhead is considerable, but that of the hexagonal prism warhead is only 2.3° due to structural constraint. The axial ejection angle similarly changes along with the axial initiation delay, and the maximum angle changes of cylindrical warhead and hexagonal prism warhead are 6.6° and 8.4° respectively. The delay initiation of multi-point is proved to be an effective way to re-aim the aiming direction of aimable warhead.

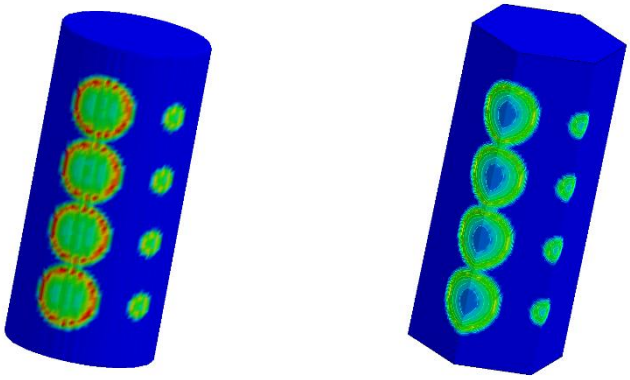

(a) Cylindrical warhead (b) Hexagonal prism warhead

Fig.2 Detonation pressure of multi-point delay initiation

ID094: Fabrication of Unidirectional Porous Metal With Spacers Through Explosive Compaction using Cylindrical Geometry

Yudai Kunita[1, a], Koshiro Shimomiya[1], Masaki Oshita[1], Matej Vesenjak[2], Zoran Ren[2], Kazuyuki Hokamoto[3]

[1]Graduate School of Science and Technology, Kumamoto University, Kumamoto 860-8555, Japan

[2]Faculty of Mechanical Engineering, University of Maribor, Maribor, Slovenia

[3]Institute of Pulsed Power Science, Kumamoto University, Kumamoto, Japan

[a]zlatan1028@outlook.com

Abstract: The fabrication process for making unidirectional porous metal using explosive compaction has been intensively investigated over the recent years [1-3]. The high pressure induced during explosive compaction results in welding between the surfaces of tightly packed small pipes inserted into a larger outer pipe.

In the present study, the fabrication of unidirectional porous copper by inserting thin spacers between the outer and inner pipes was attempted to improve the quality of explosive welding. The spacers contribute to obtain higher collision velocity between the pipes. Metallographic analysis and mechanical tests of produced samples suggest that the quality of explosive welding seems to be improved by inserting the spacers. The compression tests showed high value of the plateau stress, indicating improved quality of the explosive welding.

Reference

[1] K. Hokamoto, M. Vesenjak, Z. Ren: *Materials Letter* 137 (2014), pp323-327

[2] M. Vesenjak, H. Hokamoto, S. Matsumoto, Y. Marumo, Z. Ren: Materials Letter 170 (2016), pp39-43

[3] M. Vesenjak, H. Hokamoto, M. Sakamoto, T. Nishi, L. Krstulović-Opara, Z. Ren: Materials and Design 90 (2016), pp867-880

ID095: Munroe Effect Based on Detonation Wave Collision

Yusong Miao[1, a], Xiaojie Li[2], Xiaohong Wang[1], HonghaoYan[1], Xiang Chen[1]

[1]Department of Engineering Mechanics, Dalian University of Technology, Dalian, Liaoning 116024, China

[2]State Key Laboratory of Structural Analysis for Industrial Equipment, Dalian University of Technology, Dalian, 116024, China

[a]miaoyusong_1986@126.com

Abstract: Munroe effect has been more and more used in blasting engineering and most assembling energy technologies use shaped charge device to achieve detonation wave collision. In this paper, a new method is used to achieve detonation wave collision by detonating cord initiation common ammonium nitrate explosive. A numerical simulation using LS-DYNA on Munroe effect is implemented，detonation wave propagation and collision process caused by different initiation forms are compared. Numerical results show that peak pressure by this new method can reach 2.42 times than traditional method, and the growth of specific impulse at the explosive bottom is 49% compared to early results. Based on this numerical simulation, an experiment of explosive-determination of power be implemented, the experiment result can verify the simulation result well.

Keywords: Munroe effect, Detonation wave collision, Detonation wave, Mach reflection, Lead block method

ID096: Blast Wave Mitigation From the Straight Tube by Using Water Part II –Numerical Simulation–

Yuta Sugiyama[1, a], Tomotaka Homae[2], Kunihiko Wakabayashi[1], Tomoharu Matsumura[1], Yoshio Nakayama[1]

[1]National Institute of Advanced Industrial Science and Technology, Central 5, Higashi 1-1-1, Tsukuba, Ibaraki, Japan

[2]National Institute of Technology, Toyama College, 1-2 Ebie-neriya, Imizu, Toyama 933-0293, Japan

[a]yuta.sugiyama@aist.go.jp

Abstract: High-energetic materials are used widely in industrial technologies, because even a little explosive releases powerful energy instantly. After an explosion of high-energetic materials generates a shock wave inside a tunnel, it propagates in a passageway and expands as a blast wave from the exit into an open space. It is well known that the shock pressure at the exit determines the blast wave strength. Therefore, it is important to reduce the strength of the shock wave inside a tunnel.

Homae et al. (2016) conducted the explosion experiments of a magazine and showed that some water inside the magazine remarkably reduces the peak overpressure on the ground. However, in this study, shock wave complexly propagated between the wall and water surface, and water splashed inside the magazine. Therefore, it is difficult to understand the mitigation mechanism of the blast wave by water. In the present study, we newly investigate the mitigation mechanism of the blast wave and use a simple system, in which the shock wave generated by the explosion propagates on the water inside a square duct (30 x 30 x 330) as shown in Figure 1. High explosive (H.E.) is located near the end wall of the square duct. When water is considered, its depth is 5 mm. The peak overpressure along the exit direction outside the duct is obtained to discuss the blast wave mitigation by water.

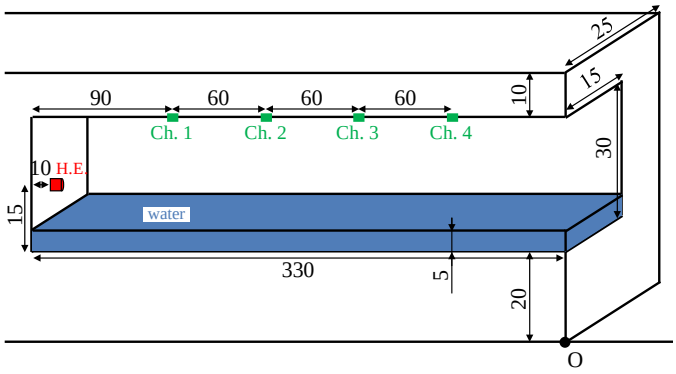

Fig. 1 Calculation target in the case with water. Cylindrical high explosive (H.E.) is located near the end.

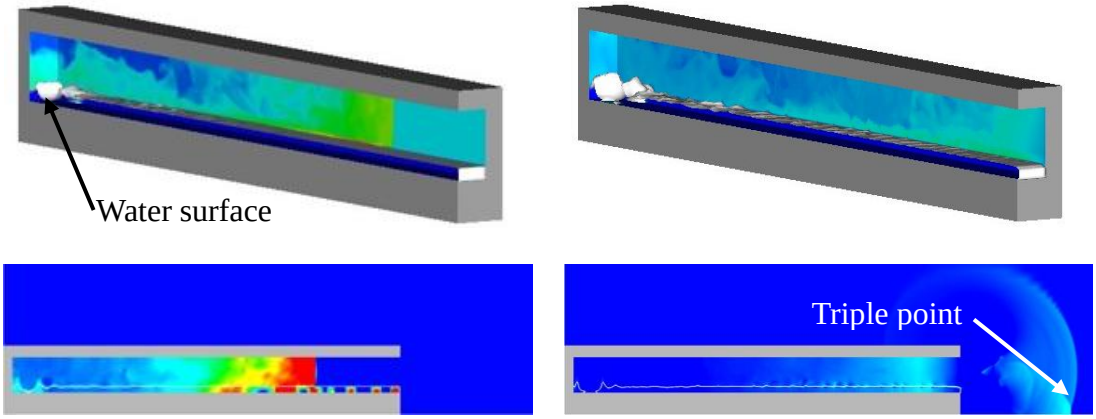

(a) 277 μs (b) 597 μs

Fig.2 Distributions of density on the inner wall and water surface for upper pictures and of pressure at the central cross section of square duct in the case with water. White surface denotes the water surface.

In Fig. 2, after the explosion, shock wave propagates to the exit, and water splash is generated and grows especially around the region above which high explosive is located in Fig. 2. After the shock wave expands from the exit, it reflects off the ground, which generates the triple point on the blast wave front as shown in Fig. 2b. Figure 3 shows the peak overpressure distribution in the case with and without water. Our numerical data agrees with the experimental ones, and water decreases the peak overpressure by 30 %. We discuss the mitigation effect of the blast wave quantitatively from the viewpoint of the energy increment of water. Here, we obtain the time history of increment ratio of internal and kinetic energies of water as shown in Fig. 4. 100 % denotes the total energy of H.E. in Fig. 1 (130 J). In Fig. 4, the increment ratio of kinetic energy becomes only around 1 %. On the other hand, the increment ratio of internal energy becomes around 50 %. Therefore,

internal energy absorption of water is dominant for the mitigation on the blast wave on the ground as shown in Fig. 3.

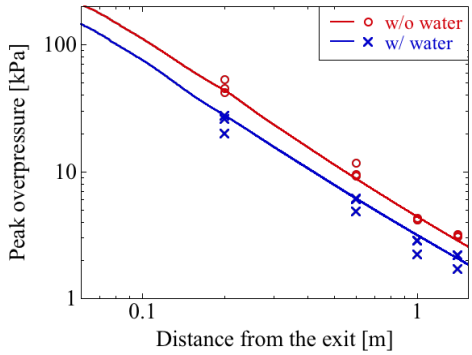

Fig. 3 Peak overpressure distribution the exit direction in the case with (w/) and without (w/o) water.

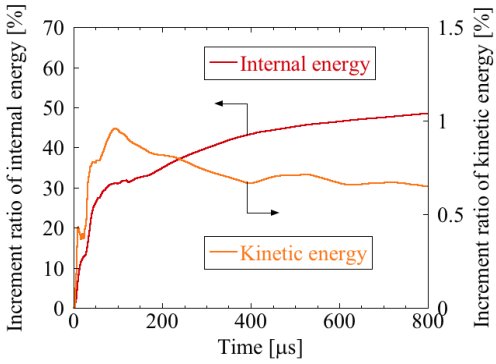

Fig. 4 Time history of increment ratio of along internal and kinetic energies of water. 100 % denotes the total energy of H.E.

References

[1] T. Homae, Y. Sugiyama, K. Wakabayashi, T. Matsumura and Y. Nakayama: *Science and Technology of Energetic Materials* 77, (2016) pp18-21.

ID097: On Fracture Patterns of Laminated Tempered Glass Exposed to Blast loads

Zhiqiang Li[1, a] , Shengjie Li[1] , Zhihua Wang[1]

[1]Shanxi Key Laboratory of Material Strength & Structural Impact, Taiyuan

[a]lizhiqiang@tyut.edu.cn

Laminated glass (LG), which consists of two or more layers tempered glass plates bonded by one or more polymer interlayers such as PVB, EU and PU , has been widely adopted as a kind of more safety part in the building facade and automotive windshield than monolithic glass[1-3]. LG is terribly prone to generate cracks and even flying fragments on glass plies that can constitute injury to resident subject to particularly extreme loads, i.e. impact and blast loads. Many researchers conducted the coupled experimental and numerical study on the crack patterns of LG under quasi-static and low level impact[4-7]. However, few scholars investigated the evolution of cracks and the formation of fragments in LG acted by blast loads. In this work, we study the influences of TNT charge and stand-off distance on the fracture patterns of $300\times300mm^2$ double layered PVB LG with 5mm thick tempered glass and 1.52mm thick PVB using 3D nonlinear explicit code LS-DYNA3D. In finite element models, JH-2 criteria used to model the damage behavior of tempered glass, and PVB is modeled by Mooney-Rivlin constitutive for hyper elastic material. Empirical explosion loads are exerted on the surface of outer glass ply through key words of *blast_load in LS-DYNA input file. All simulations are categorized into two groups referring to considered influence factors. In group 1, TNT mass ranges from 15g to 45g at 5g increment remaining the constant stand-off distance of 200mm. In group 2, stand-off distance varies in the range of 200mm to 500mm at 50mm interval maintaining the fixed TNT of 40g . Fig.1 are the resulting fracture patterns from different TNT charge under the same stand-off distance, which show that cracks initiate at the center of glass plies and subsequently extend to the edge in a radial shape, and the numbers of radial cracks increase with TNT charge. It is also seen in Fig.1 that the circumferential cracks which appear only at the center with a small amount, are unobvious in the cases of less than 35g TNT, and that the numbers of concentric cracks gathering at the center grow in the both cases of 40g and 45g TNT, and breakage area is larger in

outer glass ply marked by red than in inner glass ply by green due to the action of impact pressure wave.

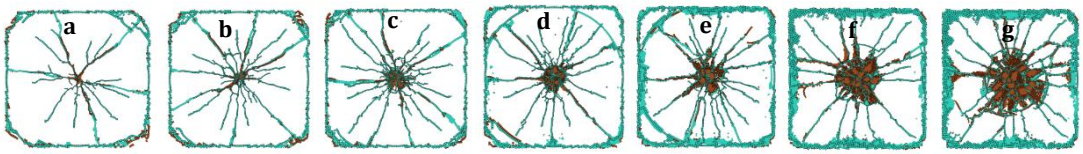

Fig. 1 The fracture patterns in LG under differnt TNT charges at the invaried stand-off distance of 200m:

a) 15g; b) 20g;c) 25g;d) 30g;e) 35g;f) 40g; g) 45g

Fig.2 exhibits the eventual facture patterns in LG loaded by the constant TNT charge of 40g at the varied stand-off distance from 200mm to 500mm. We find that the numbers of cracks which are majority in radial direction and minority in circular direction, decrease inversely with the stand-off distance. Particularly at the stand-off distance of 450mm and 500mm, it is clear that cracks occurs only in the boundary of LG.

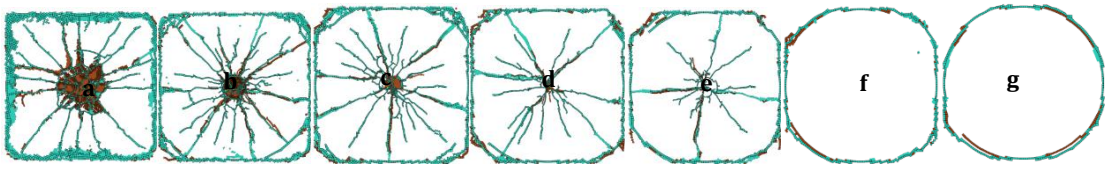

Fig. 2 The crack patterns in LG loaded by 40g TNT under different stand-off distance:

a) 200mm; b) 250mm;c) 300mm;d) 350mm;e) 400mm;f) 450mm; g) 500mm

References

[1] D. Weggel, B. Zapata:*Journal of Structural Engineering*134(2008),pp.466-477.

[2] Hooper, R. Sukhram, B.Blackman,J. Dear: *International Journal of Solids and Structures*49(2012),pp 899-918.

[3] X.Zhang,H.Hao,Z.Wang: *International Journal of Impact Engineering* Vol.78(2015),pp1-19.

[4] C. Chaichuenchob, P.Aungkavattana, S. Kochawattana: *Key Engineering Materials* 608 (2014), pp 316-321.

[5] J. Xu, Y. Sun, B. Liu, M. Zhu, X. Yao, Y.Yan, Y. Lia, X. Chen: *Engineering Failure Analysis* 18 (2011),pp 1605–1612.

[6] D.Mocibod,J.Belis:*EngineeringStructures*32(2010),pp753–761.

[7] T. Pyttel,H. Liebertz, J. Cai: *International Journal of Impact Engineering* 38 (2011), pp252-263.

ID098: Projectile Impact Testing Aluminum Corrugated Core Composite Sandwiches using Aluminum Corrugated Projectiles: Experimental and Numerical

İ. Kutlay Odacı[1], C. Kılıçaslan[1], A. Taşdemirci[1], M Güden[1,a] and A.G. Mamalis[2,b]

[1]Dynamic Testing and Modeling Laboratory, Department of Mechanical Engineering,Izmir Institute of Technology, Izmir, Turkey

[2]Project Center for Nanotechnology and Advanced Engineering, NCSR "Demokritos", Athens, Greece

[a]mustafaguden@iyte.edu.tr;

[b]a.mamalis@inn.demokritos.gr

E-glass/polyester composite plates and 1050 H14 aluminum trapezoidal corrugated core composite sandwich plates were projectile impact tested using 1050 H14 aluminum trapezoidal fin corrugated projectiles with and without face sheets. The projectile impact tests of the composite and corrugated core composite sandwich plates were modelled in LS-DYNA. The MAT_162 material model parameters of the composite were determined and optimized through both the quasi-static and dynamic tests. Non-centered projectile impact test models were validated by comparing the experimental and numerical back face displacements of the plates. Then, the centered projectile impact test models were developed and the resultant plate displacements were compared with those of the TNT mass equal Conwep simulations. The projectiles with the face sheets induced similar plate displacement with the Conwep blast simulation, while the projectiles without face sheets underestimated the Conwep displacements, which was attributed to more uniform pressure distribution on the composite plate with the use of the projectile with the face sheets.

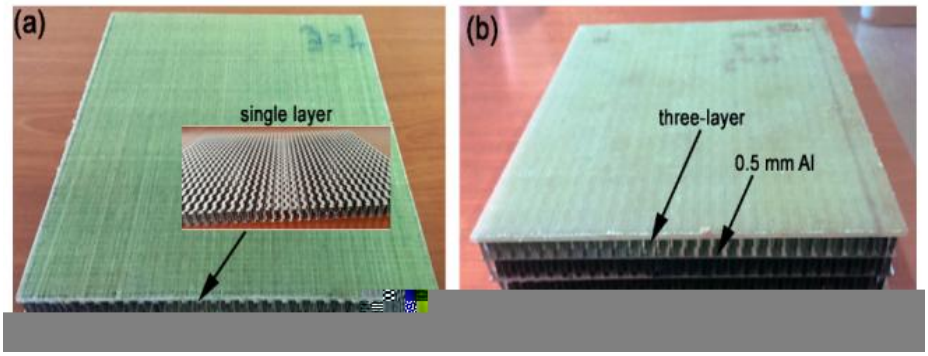

Fig. 1 Corrugated core composite sandwich plates with the core of (a) single and (b) 3-fin layer

with the presence of rubber lay on back panel. The response of measuring point of back panel and front panel had the same trend, see Fig.16. When there was no rubber on the sandwich plate, measuring displacement was 82.2mm. When the sandwich plate had rubber layer, measuring displacement was 76.0mm. From the measuring displacement, the anti-knock performance was consistent when different thickness hyperelastic material on sandwich plate.

3.3 Response of sandwich plate with rubber layer on core

When the explosive distance was 500mm. Properties of core material laid on different thicknesses of rubber of sandwich plate were analyzed. According to the thickness of the core material, rubber layer thicknesses were taken 6mm and 12mm, response of sandwich plate laid with rubber under cabin explosive load were calculated.

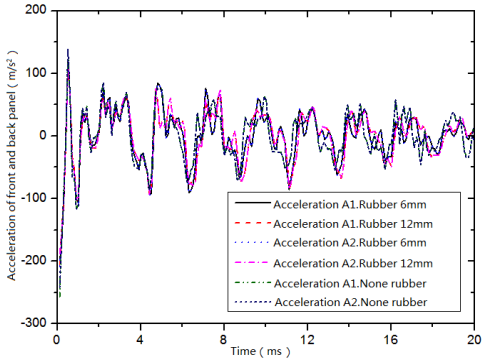

Fig.17 Acceleration curves of points

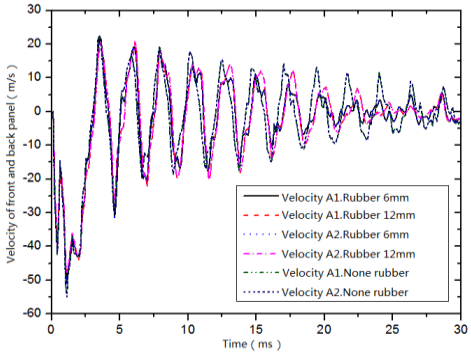

Fig.18 Velocity curves of points

Acceleration response of measuring points on front and back panel of sandwich plate were shown in Fig.17. The initial acceleration peak are almost the same when the sandwich plate with or without rubber under explosive loading. Acceleration curves substantially coincided on loading before 5ms. Acceleration curves of measuring point of different rubber layers become different after 5ms. It indicated that the rubber layer of core material had a certain effect on the explosive response.

Velocity response of measuring points on front and back panel of sandwich plate were shown in Fig.18. Within 5ms after explosion, velocity response curve of measuring point was consistent when the sandwich plate with or without rubber layer. After 5ms, curve oscillation peak of velocity response of measuring point with rubber layer was slightly smaller than without rubber layer. It indicated that rubber layer of core had a role in reducing the response of measuring point.

Displacement curves time-history of measuring point at the center of the front panel and back panel was shown in Fig.19. Displacement curves are almost the same when core material with or without rubber layer. The rubber lay of core could effectively reduce the oscillation peak of displacement response after 15ms.

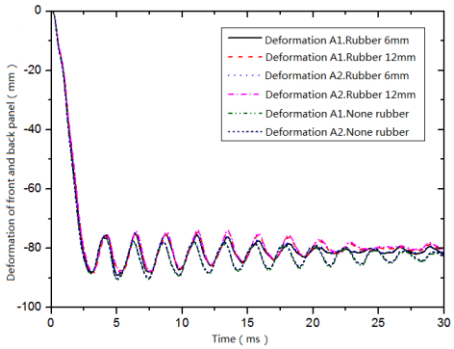

Fig.19 Deformation curves of point

4. Conclusion

Firstly, the reliability the numerical method to calculate cabin explosive loading was verified. According to orthogonal optimization method, the general stiffened plate was optimized to be sandwich plate with better anti-knock properties. When the rubber was laid different location, the response of displacement, velocity and acceleration was calculated by nonlinear numerical method, the conclusions as follows:

(1) The response of acceleration, velocity, displacement and oscillatory phenomenon could be reduced by laying rubber in the sandwich plate. When rubber was laid on the front panel, back panel and core material, the response of acceleration, velocity and displacement of each case were compared and analyzed. It indicated that the rubber laid on the front panel could better improve the anti-knock properties of sandwich plates.

(2) From oscillation period know that the rubber layer could extend the response period. With the increase of thickness of the rubber layer, the response of sandwich plate period was more durable. When sandwich plate filled with thicker rubber, the loading can be better transferred from front panel to back panel. So the acceleration difference between front panel and back panel decreased.

Reference

[1] A. Zyskowski, I. Sochet, G. Mavrot, P. Bailly, and J. Renard: *Journal of Loss Prevention in the Process Industries* 17.4(2004), pp291-299

[2] C. Wu, M. Lukaszewicz, K. Schebella, and L. Antanovskii: *Journal of Loss*

Prevention in the Process Industries 26.26(2013), pp737-750

[3] H. Wadley, K. Dharmasena, Y. Chen, P. Dudt, D. Knight, and R. Charette: *International Journal of Impact Engineering* 35.9(2008), pp1102-1114

[4] L.F. Mori: *Dissertations & Theses – Gradworks* (2008)

[5] K.P. Dharmasena, H.N.G. Wadley, Z. Xue, and J.W. Hutchinson: *International Journal of Impact Engineering* 35.9(2008), pp1063-1074

[6] K.P. Dharmasena, H.N.G. Wadley, K. Williams, Z. Xue, and J.W. Hutchinson: *International Journal of Impact Engineering* 38.5(2011), pp275-289

[7] Z.L. Wang, Y.C. Zhang, J.L. Gu: *Ship Science and Technology* 32.1(2010), pp22-27

[8] P. Zhang, J. Liu, Y. Cheng, H. Hou, C. Wang, and Y. Li: *Materials & Design* 65.65(2015), pp221-230

[9] P. Zhang, Y. Cheng, J. Liu, C. Wang, H. Hou, and Y. Li: *Marine Structures* 40(2014), pp225-246

[10] R. Alberdi, J. Przywara, K. Khandelwal: *Engineering Structures* 56.6(2013), pp2119-2130

[11] H. Yu, Z.H. Bai, X.L. Yao: *Chinese Journal of Ship Research* 7.2(2012), pp60-64

[12] Z.H. Zhang, Y. Shen, H.X. Hua, W. Yu, Z.Y. Zhang, and X.C. Huang: *Journal of Vibration and Shock* 31.5(2012), pp132-134+143

[13] H.F. Cheng: *Journal of Gansu University of Technology* 29.4(2003), pp38-40

[14] Y. Chen, Z.Y. Zhang, Y. Wang: *Thin-Walled Structures* 47.12(2009), pp1447-1456

[15] Z.Y. Mei, X. Zhu, R.Q. Liu: *Explosion and Shock Waves* 24.1(2004), pp80-84

[16] H.L. Hou, C.L. Zhang, X. Zhu: *Ordnance Material Science and Engineering* 35.4(2012), pp1-4

[17] R.W. Ogden R W: *Proceedings of the Royal Society of London* 326.2(1972), pp565-584

ID125: Shock Induced Preparation of Ag/TiO_2 Heterojunction Photocatalyst

Chunxiao Xu[1], Pengwan Chen[2, *], Jianjun Liu[3], Yazhu Lan[1]

[1]School of Materials Science and Engineering, Beijing Institute of Technology, Beijing 100081, China

[2]State Key Laboratory of Explosion Science and Technology, Beijing Institute of Technology, Beijing 100081, China

[3]State Key Laboratory of Chemical Resource Engineering, Beijing University of Chemical Technology, Beijing 100029, China

[*]pwchen@bit.edu.cn

Shock wave action combined with shock-induced modification and phase transition will cause obvious changes of chemical and physical properties of materials. Using metatitanic acid (H_2TiO_3) and silver nitrate ($AgNO_3$) as titanium precursor and silver source respectively, a visible-light responsible Ag/TiO_2 heterojunction photocatalyst is successfully prepared by shock loading. X-ray powder diffraction (XRD), transmission electron microscopy (TEM), X-ray photoelectron spectroscopy (XPS) and UV-visible diffuse reflectance spectroscopy (UV-Vis DRS) are employed to characterize the crystalline structure, morphology, chemical composition and optical property of recovered samples. The results indicate the metatitanic acid could transform to either pure anatase or pure rutile TiO_2 phase under different load condition. Ag nanoparticles cover on the surface of TiO_2 uniformly and a nanojunction structure is formed efficiently. Furthermore, due to the further enhanced separation for photogenerated charges resulting from close interfacial contact of the hetero structure, the obtained Ag/TiO_2 photocatalyst exhibit remarkably improved photocatalytic activities than that of P25 and shock induced pure TiO_2 for the degradation of Rhodamine B under simulated sunlight irradiation.

ID126: Synthesis of Carbon-encapsulated Metal Nanoparticles by Heating Explosives and Metallic Compounds

Liyong Du[1], Pengwan Chen[2,*], Chunxiao Xu[1], Yazhu Lan[1], Jianjun Liu[3]

[1]School of Materials Science and Engineering, Beijing Institute of Technology, Beijing 100081, China

[2]State Key Laboratory of Explosion Science and Technology, Beijing Institute of Technology, Beijing 100081, China

[3]State Key Laboratory of Chemical Resource Engineering, Beijing University of Chemical Technology, Beijing 100029, China

[*]pwchen@bit.edu.cn

A one-step, catalyst-free detonation of explosives sealed in a vacuum stainless steel vessel method was developed to synthesize nano materials, such as graphene, CNTs (carbon nanotubes). Recently, we used this method to synthesize carbon-encapsulated metal nanoparticles successfully, by heating the mixture of explosives (2,4,6-Trinitrotoluene and Cyclotrimethylene trinitramine) and metallic compounds. The products were taken out after the vessel was cooled down to room temperature. The obtained samples were characterized using various techniques such as transmission electron microscopy(TEM), high resolution TEM (HRTEM), and X-ray diffraction(XRD). The carbon-encapsulated metal nanoparticles we got have clear core-shell structure, that the metal nanoparticle is covered by several graphitic layers. Furthermore, it was found that the mass ratio of explosives and metallic compounds was essential factor to obtain the core-shell structure, as well as the number of the graphitic coating layers and the size of particles.

ID127: A Gradient Metallic Alloy Rod with Unique Dynamic Mechanical Behaviour

Jitang Fan[1,2*]

[1]State Key Laboratory of Explosion Science and Technology, Beijing Institute of Technology, Beijing 100081, China

[2]Advanced Research Institute for Multidisciplinary Science, Beijing Institute of Technology, Beijing 100081, China

Abstract: A 7mm-diameter ZrCu-based alloy rod, cast by fast cooling rate technology, is characterized with a gradient microstructure of ductile amorphous and ZrCu phases in the outer surface and brittle Zr_2Cu and $Cu_{10}Zr_7$ phases in the center. Compressive mechanical tests at various strain rates illustrate the rate-dependent characteristics of yield stress and strain hardening after yielding. Post-test SEM observation and XRD analysis reveal the shearing, vein-like structuring, temperature-rise-induced melting, martensite transforming and lamellar cracking under the dynamic loading. A modified Johnson-Cook constitutive model was used to investigate the mechanisms of temperature-rise-induced softening at lower strain rate and martensite-transformation-induced hardening at higher strain rate, as well as the resultant phenomena of rate dependency. The mixed dynamic damage and fracture mechanisms of ductile and brittle models are discussed for the strength-toughness combination. Laminar cracking is addressed for developing a 'self-sharpening' high-performance penetrator.

* Corresponding authors: Jitang_fan@hotmail.com (J.T. Fan)

ID129: Dynamic Behavior of Shock-treated Pure Titanium

Ling Li[1, a], Pengwan Chen[1, b], Qiang Zhou[1], Chun Ran[1], Wangfeng Zhang[2]

[1]State Key Laboratory of Explosion Science and Technology, Beijing Institute of Technology, Beijing 100081, China

[2]Beijing Institute of Aeronautical Materials, Beijing 100095, China

[a]a5207721@126.com, [b]pwchen@bit.edu.cn

Abstract: Commercial purity titanium is widely used in various fields, especially in the aviation and aerospace filed, due to its excellent mechanical physical properties such as high plasticity, good formability excellent corrosion resistance and biological compatibility. In fact, because of the overall features of many of its applications, pure titanium is frequently subjected to dynamic impact loading during the course of its service life [1]. Therefore, split Hopkinson pressure bar (SHPB) has been used as an efficient experimental technique to obtain its dynamic stress-strain curves and dynamic flow behavior by some famous researchers such as Chichili [2]. Explosive can release a huge amount of energy in a very short time (10^{-9}~10^{-6}sec), and form the extreme conditions, which may greatly affect the properties of the material. The effects of high pressure due to explosive detonation on material such as copper have been investigated (Gumruk et al. [3]; Murr L E et al. [4]; Kommel et al. [5]), but relatively little attention has been directed towards other material, especially titanium.

In the present research, a device was designed to process pure titanium by means of explosion. The steel whose density is 7.8g/cm^3 is selected as flyer tube, because it's widely used in explosion welding. Titanium bar is placed in the center of the whole device to absorb explosive energy. The powder explosive expanded ammonium nitrate whose detonation velocity is 2300m/s has been used for this explosive treatment experiment. The Vickers hardness (HV 10) of pure titanium with and without explosive shock treatment at room temperature which listed in table 1 show that the hardness enhances about 30% by explosive shock treatment on the interface of flyer tube and pure titanium rod (In this paper, 0# and 3# denote the specimen without and with explosive shock treatment). Quasi-static compression was performed by INSTRON 5985 material testing machine. On the other hand, dynamic testing was conducted using a split Hopkinson pressure bar at the strain rates from1000/s to 3500/s.

Table 1. The Vickers hardness (HV10) of pure titanium with and without explosive treatment

No.	distance from the edge								
	1mm	2mm	3mm	4mm	5mm	6mm	7mm	8mm	9mm
0#	193	192	192	195	194	197	197	198	196
3#	260	243	225	217	204	199	195	199	198

The typical stress vs. strain curves for with and without explosive shock treatment under quasi-static compression conditions and dynamic compression (different strain rate) conditions are shown in Fig. 1 and Fig 2 respectively. As shown in figure 1, under quasi-static compression conditions, the value of the yield stress for 3# is up to 700MPa, which is about 50% higher than that for 0# (470MPa). And during the whole loading process, the strength for 3# is about 200MPa higher than that for 0#. As shown in Fig. 2, the yield stress of 3# is always higher than that of 0# when strain rate increases from 1000s-^{1} to 3500s^{-1}. Due to the difference of strain rate effect between with and without explosive shock treatment, the maximum stress of 3# is consistent with 0# when strain rate is 2500s^{-1}. When strain and strain rate hardening effect weaker than thermal softening effect, thermoplastic instability will occur in the specimen, which means the failure of material to some extent. From Fig. 2, hardening effect is greater than thermal softening effect for 0# during the whole loading process when strain rate is below 3500s^{-1}, while significant thermal softening occurs when strain rate equals to 3000s^{-1} for 3#. Based on the recovered experimental samples, the experimental results are consistent with the Fig. 2.

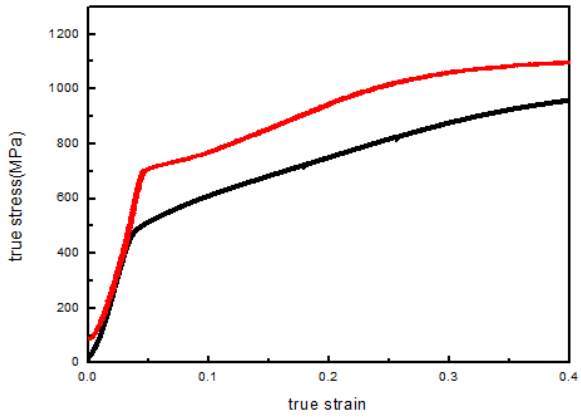

Fig.1 Quasi-static compressive stress-strain curves with and without explosive treatment

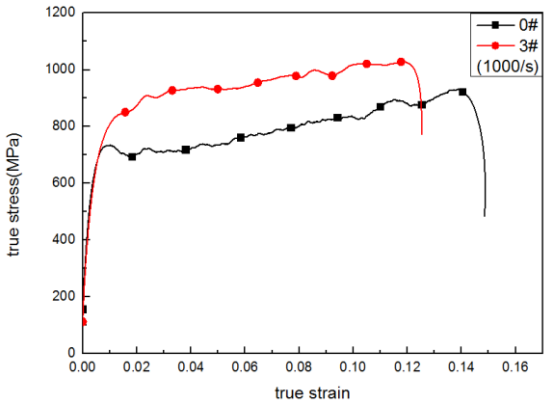

(a) 1000/s

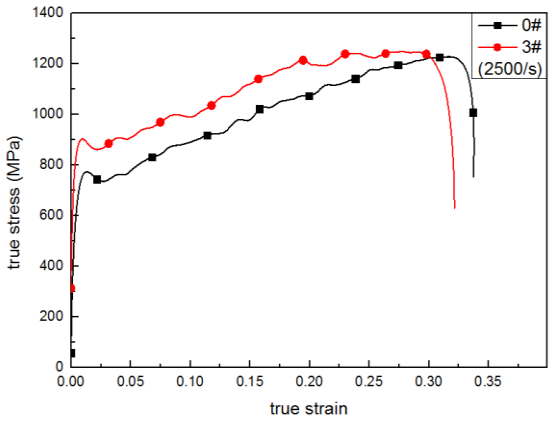

(b) 2500/s

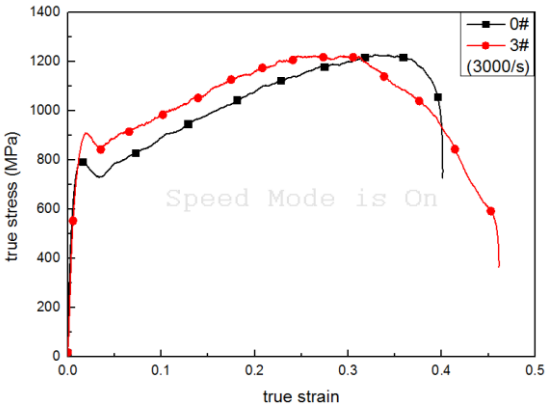

(a) 3000/s

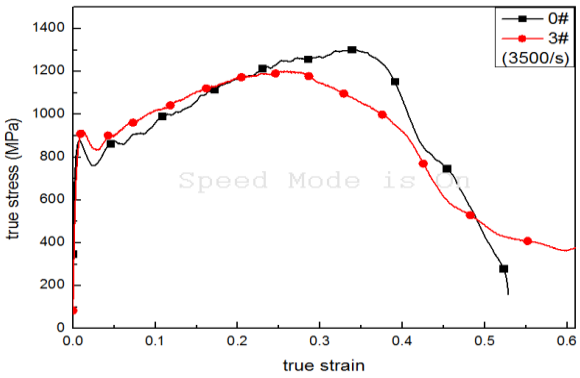

(b) 3500/s

Fig.2 Dynamic compressive stress-strain curves with and without explosive treatment at different strain rate.

In this research, pure titanium rod was processed by means of explosion. The results of quasi-static and dynamic compression testing of pure titanium with and without explosive shock treatment which studied by material testing machine and split Hopkinson pressure bar show that the mechanical properties of pure titanium are affected by explosion treatment. The yield strength increased about 50% under quasi-static condition. Consistently, the yield strength is always higher when the strain rate ranges from 1000 to 3500s^{-1} after explosive shock treatment. But the specimen with explosion treatment will failure at lower strain rate than original pure titanium, which means the resistance of strain rate is reduced by explosive shock treatment.

References

[1] S X Zhang, Y C Wang, P Zhilyaev Alexander: *Materials Science & Engineering A* 641(2015) 29-36

[2] D R Chichili, K T Ramesh, K J Hemker: *Acta Mater*46 (1998) 1025-1043

[3] R Gumruk, R A W Mines, S Karadeniz: *Materials Science & Engineering A* 586 (2013) 392-406

[4] L E Murr, E V Esquivel: *Journal of Materials Science* 39 (2004) 1153-1168

[5] L Kommel, I Hussainova, O Volobueva: *Materials & Design* 28 (2007) 2121-2128

ID130: A Preliminary Study of Dynamic Deformation Behavior of Ti-6Al-4V Titanium Alloy

Chun Ran[1,a], Pengwan Chen[1,b], Kaida Dai[1], Baoqiao Guo[1], Ling Li[1],Wangfeng Zhang[2], Haibo Liu[1]

[1]State Key Laboratory of Explosion Scien0ce and Technology, Beijing Institute of Technology, Beijing 100081, China

[2] Beijing Institute of Aeronautical Materials, Beijing 100095, China

[a]rangle123@163.com, [b]pwchen@bit.edu.cn

Titanium alloys have been wildly utilized in the field of aerospace as key structure components due to their high strength-to-weight ratio, excellent combinations of corrosion, toughness and crack growth resistance [1]. Among them, Ti–6Al–4V, an α+β titanium alloy, is one of the most commonly used. Hence, the increasing attention has been received with respect to TC4 titanium alloy by many material researchers over the last few decades. Rittel et al [2] proposed a new failure criterion based on mechanical energy (the stored energy of cold work as the driving force for microstructural rearrangement by DRX) rather than a critical strain proposed by Recht [3]. A series of corresponding work have been carried out by Xue et al.[4], Lee et al.[5], Peirs et al.[6].

Hat-shaped (HS) specimen was invented in 1977 by Hartmann and Meyer at the Fraunhofer Institute (IFAM, Bremen, Germany) [7]. Due to the unique geometry of HS specimen, extremely high strains at high strain-rate can be reached. However, in fact, the shear stress measurement is influenced by edge effect, and it is impossible to track the shear band, detect its temperature and measure the local strain. To reduce edge effect and measure the temperature rise during the deformation, the Flat Hat-shaped (FHS) specimen was designed by Clos [8].

This research aims at obtaining an insight into a) mechanical response, b) distribution of the local shear deformation based on DIC technology.

The paper is organized as follows: First, introduce the experimental techniques, next, experimental results and discussion is presented, followed by concluding remarks.

The split Hopkinson pressure bar technique is used to load the specimens dynamically. The schematic of split Hopkinson pressure bar used in this study is shown in Fig. 1, the FHS specimen is sandwiched between two bars. An impact pulse is provided with a

striker driven by a light gas gun. It should be noted that the setup used in this work is nickel (18Ni) bars with diameters of14mm and the lengths of the striker, incident and transmission bar are 0.2m, 1.2m, 1.2m, respectively. The in-plane dimensions of the FHS specimen used in this study are based on Ran et al. [9]. The specimen can be divided into three parts: the upper hat part, the lower edge part and the shear region where extremely high strain rate, strain and temperature generate and propagate.

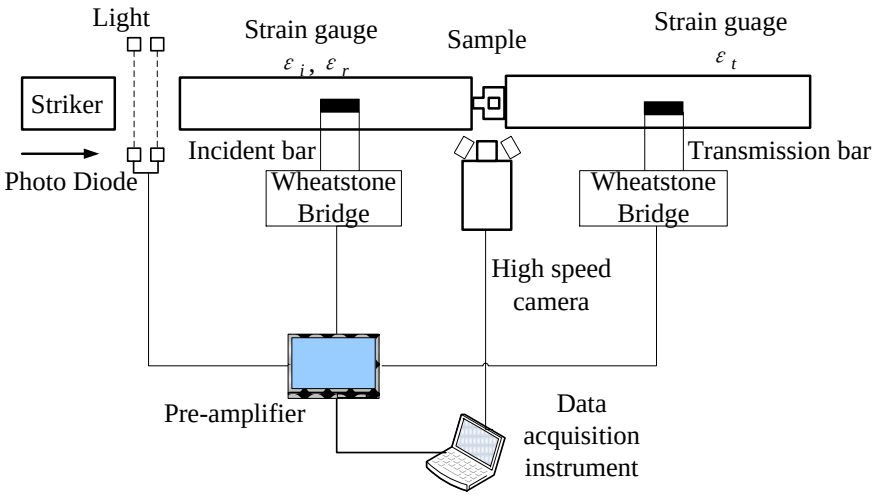

Fig.1 A schematic of split Hopkinson pressure bar setup

The velocities of the striker calculated by the signal recorded by photo diode are listed in table 1.

Table 1 Velocities of the striker

No.	1#	2#	3#	4#	5#	6#	7#
v/ms^{-1}	19.42	17.92	15.78	16.24	14.65	13.22	12.21

Based on Ran et al [16], the shear stress and average shear strain can be approximately estimated as:

$$\tau \approx \frac{\pi E_0 r_0^2 \varepsilon_t(t)}{2ht} \tag{1}$$

$$\gamma \approx \frac{-2C_0 \int_0^t \varepsilon_r(t)\,dt}{h} \tag{2}$$

Where E_0 and C_0 are Young's Modulus and elastic bar wave speed in the bar material, respectively. r_0 is the radius of the Hopkinson bars, h and t are height and thickness of the shear region, and $\varepsilon_t(t)$ and $\varepsilon_r(t)$ represent transmitted and reflected strain histories in the bars at the specimen ends, respectively.

Typical resulting stress-displacement curves of the dynamic experiments are presented in

Fig. 2. It should be noted that the arrows indicate the maximum stress.

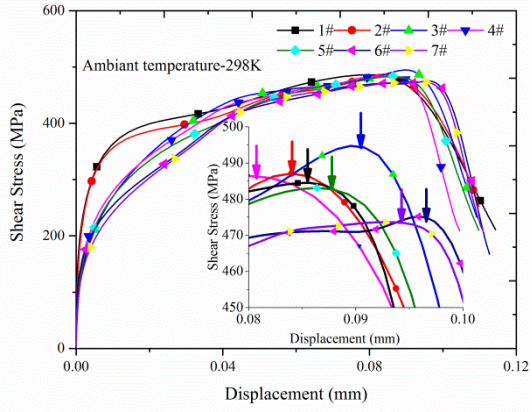

Fig. 2 Typical shear stress vs. displacement curves for different velocities of the striker

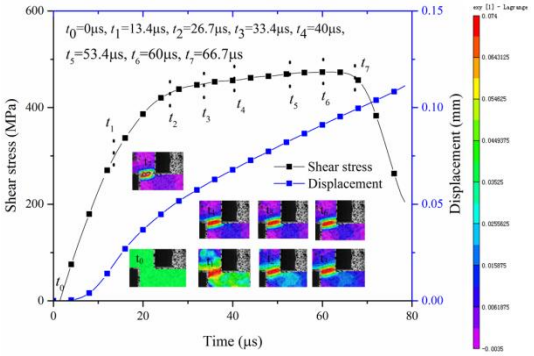

Fig. 3 The strain field measured by DIC on the surface of FHS specimen

Typical curve of dynamic shear stress and displacement response for FHS specimen is shown in Fig. 3, and the evolution of strain field of the shear region obtained by DIC technique is also presented.

A series of dynamic compression tests on FHS specimens have been performed by split Hopkinson pressure bar setup combined with DIC technique. The experimental results demonstrated that a) The higher the strain rate, the higher the flow stress, and b) The flow stress increases with increasing the true strain under quasi-static loading condition during the plastic deformation.

This research was financially supported by the National Natural Science Foundation of China (Grant No.11472054) and the Opening Project of State Key Laboratory of Explosion Science and Technology (Beijing Institute of Technology) with Grant No. KFJJ16-02M.

References

[1]. Boyer, R.R., Materials Science and Engineering: A, 1996. 213(1): pp. 103-114.

[2]. Rittel, D., Wang, Z. and Dorogoy, A.. International Journal of Impact Engineering, 2008. 35(11): pp. 1280-1292.

[3]. Recht, R., Journal of Applied Mechanics, 1964. 31(2): pp. 189-193.

[4]. Xue, Q., Meyers, M. and Nesterenko, V.. Acta Materialia, 2002. 50(3): pp. 575-596.

[5]. Lee, W.-S., Liu C.-Y., and Chen T.-H.. Journal of Nuclear Materials, 2008. 374(1–2): pp. 313-319.

[6]. Peirs, J., et al., International Journal of Impact Engineering, 2010. 37(6): pp. 703-714.

[7]. Hartmann K.H., Kunze, H.D. and Meyer, L.W.. Metallurgical effects on impact loaded. in Shock waves and high-strain-rate phenomena in materials, ed. Marc A. Meyers and L.E. Murr. 1981, New York: Plenum Press. pp. 325-337.

[8]. Clos, R., Schreppel, U., and Veit, P.. Journal de Physique IV, 2000. 10(PR9): pp 257-262..

[9]. Ran C., Chen P., Li L. et al., in 2016 3rd international conference on mechanics and mechatronics research. 2016: Chongqing, China. (in press).

ID131:Dynamic Mechanical Behavior and the Damage Analysis of CFRP Under the Blast Shock

Yi Li, Baoqiao Guo*, Pengwan Chen, Wenbin Liu

State Key Laboratory of Explosion Science and Technology, Beijing Institute of Technology, Beijing 100081, China

Abstract: To study the dynamic mechanical response of carbon fiber reinforced polymer (CFRP) under air blast loading, the explosion shock tests of two ply stacking sequence, $[0/90/90/0]_{2s}$ and $[45/-45/90/0]_{2s}$, of CFRP are performed by 3D-DIC system and small scale explosion vessel. The detonator is parallel or perpendicular to the back-surface of the sample. The explosion shock resistance of the two kinds of laminates is compared, and the failure mode and damage process of the laminates during the explosion shock are discussed. Simultaneously, the vibration response of the laminates is analyzed. The experimental results indicate that a) when the detonator is perpendicular to the sample, the explosion shock wave loads the specimen directly, and the specimen is cut along the flange, meanwhile, the failure mode of the edge is shear fracture and fiber debonding; b) when the detonator is parallel to the sample, the decompression of the vessel is caused by the holes formed by the fragments of the detonator. And large scale of plastic deformation of the sample occurs rather than cut along the flange. And the non-deformability of sample, $[45/-45/90/0]_{2s}$, is superior to $[0/90/90/0]_{2s}$ under explosion shock loading conditions.

Key words: carbon fiber reinforced polymer, blast shock, dynamic damage

ID132: The Study on Spall and Damage of OFHC in Convergent Geometry

Xiaoyang Pei[1,a], Hui Peng[1], Hongliang He[1], Ping Li[1], Jidong Yu[1], Jingsong Bai[1] Suyang Zhong[1]

[1]Institute of Fluid Physics, China Academy of Engineering Physics, Mianyang 621900, China

[a]peixiaoyang2000@sina.com

Abstract: Spallation damage in ductile materials is the process of void nucleation, growth and coalescence due to states of high tensile stress. Typical experiments are conducted in a planar, uniaxial stress configuration[1]. Here, the effect of convergent geometry on the properties of dynamic damage evolution of OFHC are investigated. The spall fracture experiments were conducted using explosive generators. The damage evolution process are studied using the time-resolved free-surface velocity interferometry, post-experiment metallurgical analysis of the soft recovered samples and similation. It indicated that, the convergent effect is a very important factors for the spallation damage, and the distinct differences are observed in the damage pattern between planar and convergent experiment.

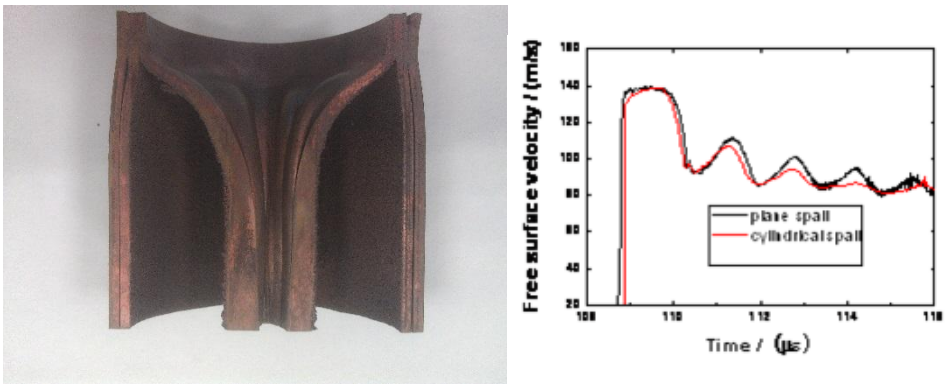

(a) the recovered sample (b)the free surface velocitiies profiles

Fig.1 The results of spall experiment in convergent geometry

Keywords: spall fracture, peak stress, dynamic damage evolution

References

[1] Antoun T H, Seaman L, Curran D R, et al. Spall Fracture [M]. New York: Springer, 2003.

ID134: Shock Induced Conversion of Carbonate to Multi-layer Graphene

Hao Yin[a], Qiuhua Du[a], Chao Li[a], Pengwan Chen[b]

[a]Institute of Systems Engineering, China Academy of Engineering Physics,Mianyang 612900, Sichuan Province, China

[b]State Key Laboratory of Explosion Science and Technology, Beijing Institute of Technology, Beijing 100081, China

Abstract: Using Carbonate as the carbon source, multi-layer graphene sheets were synthesized instantaneously by reduction of Carbonate with magnesium under shock wave loading. In addition, by adding ammonium nitrate or urea to the reaction system, nitrogen-doped graphene material was formed in this one-step shock treatment. The recovered samples were characterized using various techniques such as transmission electron microscopy, scanning electron microscopy, Raman spectroscopy and X-ray photoelectron spectroscopy. Shock-synthesized nitrogen-doped graphene material was demonstrated to act as a metal-free electrode with an efficient electrocatalytic activity and long-term operation stability for the oxygen reduction reaction via two- and four-electron pathways in alkaline fuel cells.

ID135: Steady Shock Waves in Heterogeneous Media: the Relationship Between Material Structure and Shock-layer Structure

Alain Molinari, Christophe Czarnota, Sébastien Mercier
LEM3, University of Lorraine, Ile du Saulcy, 57045 Metz, France

In this presentation we analyze steady shock waves in heterogeneous materials. Three different configurations are considered:

- highly nonlinear granular chains
- steel–polymer laminate composites
- porous metals

In each case the shock layer turns out to be mainly structured by the interaction of inertia with the internal-structure of the material (wave dispersion due to heterogeneities, local acceleration fields due to the collapse of micro-voids, etc ..).

Firstly, we recall results obtained by Molinari and Daraio (2009) for steady shocks in periodic heterogeneous highly nonlinear granular chains governed by a power-law contact interaction. The shock-width appears to be scaled by the cell-size (particles periodicity) and the theoretical results (analytical and numerical) are found to be in good agreement with experiments. We refer also to Nesterenko (2001) for other fundamental aspects related to shock waves in granular chains.

Then, considering the work Molinari and Ravichandran (2006), we concentrate on steady plastic shocks generated by planar impact on steel–polymer laminate composites. The laminate material has a periodic structure with a unit cell composed of two layers of different materials. Using gradient plasticity theories it is found that, for a given shock intensity, the shock width is proportional to the cell size. Theoretical predictions are compared with experiments for different cell sizes and various shock intensities.

Finally, we present recent results for steady shocks in porous metals, Czarnota et al (2016). Porosity is assumed to be moderate and voids are not connected (foams are not considered). When the shock front moves in the porous medium, voids are facing a rapid collapse. Material particles are subjected to very high acceleration in the vicinity of voids, hence generating important acceleration forces at the microscale that influence the overall response of the porous material. Micro-inertia effects can be embedded in the constitutive response of the porous material following the work of Carroll and Holt (1972) for spherical loading. Micro-inertia effects for general loading conditions and general

viscoplastic behaviors have been considered by Molinari and Mercier (2000), Czarnota *et al* (2006-2008) and Jacques *et al* (2010).

We analyze how stationary shocks in porous metals are influenced by micro-inertia effects. Following the constitutive framework developed by Molinari and Ravichandran (2004) for dense metals, an analytical approach of steady state plastic shocks in porous metals is proposed. For a given initial porosity, the void size appears as the characteristic internal length that scales the overall dynamic response, thereby contributing to the shock front structure. This key feature is not captured by standard damage models where the porosity stands for the single parameter characterizing the damage with no contribution of the void size. The results obtained in this work provide a new insight in the fundamental understanding of shock waves in porous media.

References

[1] Carroll, M. M., Holt, A. C., 1972a. Static and dynamic pore collapse relations for ductile porous materials. J. Appl. Phys. 43 (4), 1626–1636.

[2] Czarnota, C., Mercier, S., Molinari, A., 2006. Modelling of nucleation and void growth in dynamic pressure loading, application to spall test on tantatum, Int. J. Fracture, 141, 177-194.

[3] Czarnota, C., Jacques, N., Mercier, S., Molinari, A., 2008. Modelling of dynamic ductile fracture and application to simulations of plate impact tests on tantalum, J. Mech. Phys. Solids, 56, 1624-1650.

[4] Czarnota, C., Molinari, A., Mercier, S., 2016. The structure of steady shock waves in porous metals, to be published.

[5] Jacques, N., Czarnota, C., Mercier, S., Molinari, A., 2010. A micromechanical constitutive model for dynamic damage and fracture of ductile materials. Int. J. of Fracture, 162, 159-175.

[6] Molinari, A., Mercier, S., 2001. Micromechanical modelling of porous materials under dynamic loading. J. Mech. Phys. Solids, 49, 1497-1516.

[7] Molinari, A., Ravichandran, G., 2004. Fundamental structure of steady plastic shock waves in metals J. of Applied Physics, 95, 1718-1732.

[8] Molinari, A., Ravichandran, G., 2006. Modeling plastic shocks in periodic laminates with gradient plasticity theories. J. Mech. Phys. Solids, 54, 2495-2526.

[9] Molinari, A., Daraio, C., 2009. Stationary shocks in periodic highly nonlinear granular chains. Phys. Rev. E, 80, 056602.

[10] Nesterenko, V. F., 2001. Dynamics of Heterogeneous Materials, Springer, 2001.

ID136: Investigation on Mie-Grüneisen Type Shock Hugoniot Equation of State for Concrete

Masahide KATAYAMA[1, a], Atsushi ABE[1], Atsushi TAKEBA[1]

[1]Science & Engineering Systems Division, ITOCHU Techno-Solutions Corporation, 3-2-5, Kasumigaseki, Chiyoda-ku, Tokyo 100-6080, JAPAN

[a]masahide.katayama@ctc-g.co.jp

It is generally known that geological materials including mortar and concrete as artificial structural components indicate specific bilinear Hugoniot characteristics (U_s-u_p relationship) as shown in Fig. 1 [1]. Especially, they are featured as V-shaped bilinear relationship; i.e. with *negative* gradients in the lower particle velocity region and positive ones in the higher region. Thomas J. Ahrens et al. concluded that this negative gradient regime is caused by a transition via dynamic yielding to a quasi-hydrostatic state [2]. This paper presents that V-shaped bilinear shock Hugoniot equation of state enable us successfully to model the plasticizing process of concrete for high-velocity impact problems. The negative gradient of the bilinear Hugoniot for low particle velocity regime can simulate the process that the porosity of concrete may be compressed to form shock wave in concrete, through a series of numerical analyses.

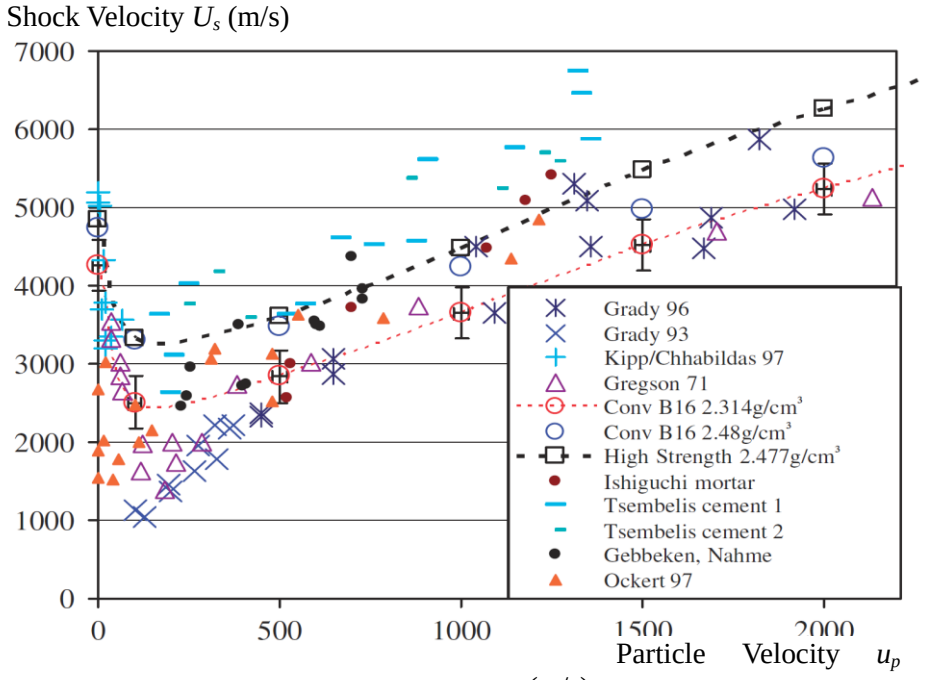

Fig.1 Comparison of Hugoniot relations of concretes[1].

References

[1] W. Riedel, M. Wicklein, K. Thoma, *Int. J. of Impact Engng.*, **35** (2008), pp155-171

[2] T. J. Ahrens, M. L. Johnson, *A Handbook of Physical Constants*, **3** (Ed.: T. J. Ahrens), American Geophysical Union, Washington, D. C., (1995), pp35-44

ID137: The Mechanical Performance of Polymer Bonded Explosives at High Strain-Rates

William G. Proud

Institute of Shock Physics, Blackett Laboratory, Imperial College London, London, SW7 2AZ, UK

e-mail address: wproud@imperial.ac.uk

Polymer-based systems have non-linear mechanical properties which are highly-temperature dependent and strain-rate sensitive. In this presentation a number of low to high-rate characterisation techniques are described. A description of the output obtained is described with reference to a range of polymer-bonded explosives (PBX) and sugars (PBS): this last of material type is used as inert mechanical and density simulants. The field of high strain-rate experimentation has expanded greatly in recent years, the increase in high-speed diagnostics allowing sub-microsecond resolution to become commonplace. Increased use of predictive modelling has provided a significant drive for well controlled experiments. This forms a development circle involving experiment, theory and numerical methods. The use of multiple diagnostic systems on a single experiment, e.g. stress gauges, high-speed photography and flash X-ray systems Some of the more widely used techniques are reviewed applied to a wide range of materials has been reviewed by the author and colleagues elsewhere[1].

The main effect of increasing the strain rate is that the transient stress levels increase and the sudden delivery of energy allows processes with high activation energies to be accessed. Processes, which operate on long time scales, e.g. thermal diffusion, which are significant under quasi-static loading, do not have time to occur. It is generally found that yield and fracture stresses increase with increasing strain rate [2]. The increase in failure stress is very marked at strain rates above 10^3 s^{-1} and the effect of inertia becomes significant. Ultimately the response changes from one where the sample can be assumed to be in stress equilibrium to one of a wave with associated 1-D strain moves so quickly that the material does not have time to move laterally, as seen in shock waves.

In addition techniques, such as differential thermo-mechanical analysis (DMTA) are widely used in the polymer community and provide insight into the molecular-level processes occurring in the polymer system. Historic spring-dashpot models are used with

some degree of success in some areas, there are numerous semi-empirical models, however, there is a great drive to use models which are based on the fundamental structure of the polymer as in the group interaction model [3] is proving a fruitful area

In the mid 2000's the effect of grain size on the high rate mechanical properties of an ammonium perchlorate (AP)/hydroxyl-terminated polybutadiene (HTPB) PBX was studied. This PBX consisted of 66% AP and 33% HTPB by mass. The AP was available in four different crystal sizes: 3, 8, 30 and 200–300 mm. The effect of grain size was most clearly seen at low temperatures (figure 1a) the effect of particle size on the flow stress of the material is linear in $1/d^{1/2}$; where d is the particle size (figure 1b). This has been subject to further investigation to determine if the particle size or the particle separation is dominant [4].

The use of DMTA in combination with data across a wide range of strain rates has resulted in a consistent view, in a qualitative sense of the response and damage processes in these composite systems. This is illustrated by Drodge *et al.*[4] in this paper the effect of the binder, its thermal and mechanical properties is compared with those for a granular composite. Overall this illustrates the utility of frequency time shifts linked to strain rate effects in this area of research.

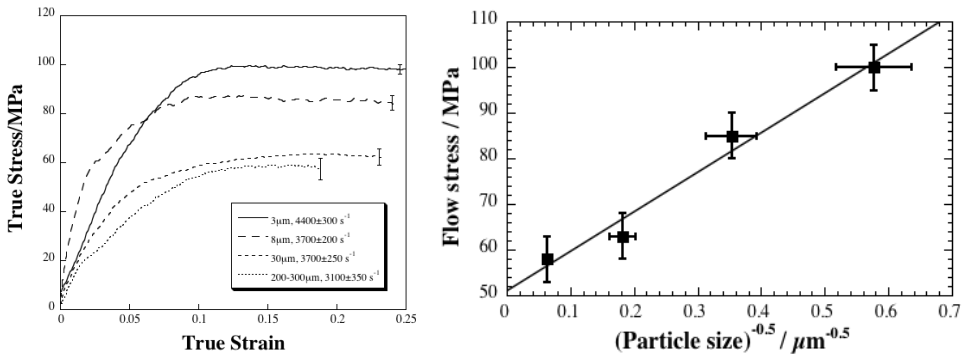

Figure 1(left) Effect of particle size on yield stress at -60oC (right) Plot of the flow stress versus the reciprocal of the square root of particle size.

At very high strain-rates, shock wave loading, ~20GPa, the energy deposited is sufficient to cause many polymers to chemically decompose. For some polymers a "kink" can be seen in the shock velocity – particle velocity Hugoniot. For poly(styrene). Porter and Gould [5] proposed that this kink is due to an activated change in structure whereby the aromatic ring transforms into a triangular prism. Molecular mechanics can predict the equation of state of polymers from their structure alone [6] and this technique has

been used to predict pressure-volume for the two structures: aromatic ring and triangular prism. The prediction is compared with experimental data in Figure 2. Molecular mechanics also allows prediction of the activation energy of such a structural change, via an energy density, and this equates to a pressure of around 20 GPa [5].

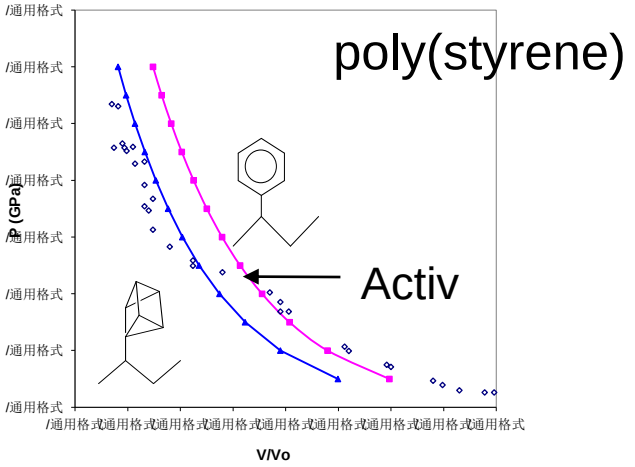

Figure 2: Comparison between predicted pressure-volume behaviour of two structures in poly(styrene) and measured data

Significant effort has been made to understand the material response both in terms of the strain-time records seen and also in the recovery of shocked samples for post impact analysis [7]. Here both strain-rate hardening and softening was seen in PTFE samples, depending on the conditions used, re-shocking of the sample material had a significant effect and there was a marked difference in the crystallinity of the recovered material.

Similar effort has been made into the variation of temperature and strain rate on the response of polymers and PBXs. This allows the polymer behaviour to be explained in a coherent fashion thus leaving the processes of fracture and damage more visible in the data. This can be illustrated by considering the temperature time response of a polymer bonded energetic system. One of the few that represents a complete study across a wide range of strain rates and temperatures is reported in [8] for the energetic composition EDC37, over a range of strain rates from 10^{-8} to 10^{3} s^{-1}, and at a strain rate of 10^{-3} s^{-1} for the temperature range 208 to 333 K. Figure 3 shows the main experimental results used in this study: the similarity in trends is obvious.

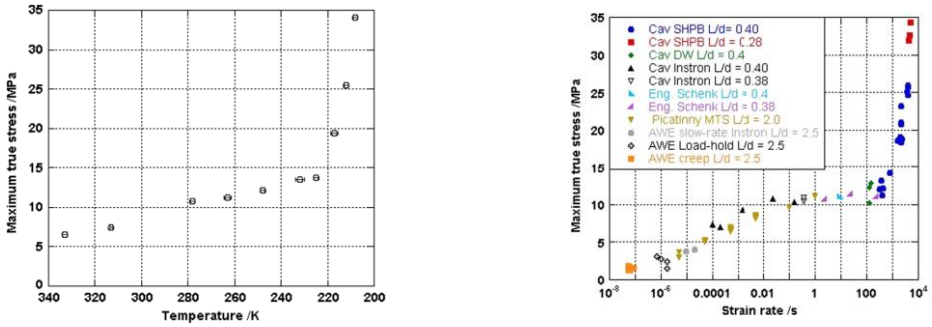

Figure 2. Yield strength of a granular composite at (left) a fixed 10^{-3} s^{-1} strain rate, varying temperature (right) failure stress as a function of strain rate tested at 293 K.

Acknowledgements

The Institute of Shock Physis acknowledge the support of AWE, Aldermaston, UK and Imperial College London. Significant long-term support was provided by QinetiQ, UK MoD, AWE and EPSRC. Drs. D. Williamson, S.M. Walley, C. Siviour, S. Grantham, T. Goldrein and Mr SJJP Palmer contributed significantly to the research presented here. Prof. J.E. Field is thanked for his on-going support and tutelage of research in this area.

References

[1] Field JE, Walley SM, Proud, WG, Goldrein, HT, and Siviour, CR,. IJIE, 30 (2004),, 725-775. [2] Meyers, MA, Dynamic Behavior of Materials. New York, Wiley Interscience. 1994

[3] D. Porter, P.J. Gould, IJSS 46 (2009) 1981–1993

[4] D.R. Drodge, D.M. Williamson, S.J.P. Palmer, W.G. Proud and R.K. Govier, The Mechanical Response of a PBX and its binder: combining results across the strain-rate and frequency domains, J. Phys. D.: Appl. Phys. 43 (2010) 335403.

[5]. D Porter, P.J. Gould, J. Phys. IV France, 110 (2003), pp. 809-814.

[6] Porter, D., Gould, P.J., 2006. A general equation of state for polymeric materials. Journal de Physique IV France 134 (2006), 373–378.

[7] E.N. Brown, C.P. Trujillo, G.T. Gray III, P.J. Rae and N.K. Bourne, "Soft Recovery of polytetraflouroethlyene shocked through the crystalline phase II-III transition, J. Appl. Phys 101 (2007) 0249916

[8] D M Williamson, C R Siviour, W G Proud, S J P Palmer, R Govier, K Ellis, P Blackwell and C Leppard, Temperature–time response of a polymer bonded explosive in compression (EDC37), J. Phys. D: Appl. Phys. 41 (2008) 085404

ID138: Recent Experimental and Numerical Study on Reacted Materials of the Double-Layer Liner in Shape Charges

See Jo Kim[1, a], Sang Ho Mun[1], Chang Hee Lee[2], Seong Lee[3]

[1]Department of Mechanical Design Engineering, Andong National University, Andong, 1375, Korea

[2]Division of Materials Science & Engineering, College of Engineering, Hanyang University, Seoul, 04763, Korea

[3]The 4th Research and Development Institute, Agency for Defense Development, Daejeon, 34060, Korea

[a] Corresponding Author: sjkim1@anu.ac.kr

In general, a Cu liner is used for shaped charge ammunition in military applications. New study on the concepts of double-layer shaped charge liners is increasing using highly reactive materials (e.g., Al, Mg, and self-propagating high temperature synthesis materials). This double-layer liner can be to effectively neutralize the enemy's attack power concealed in the armored vehicles. A double-layer liner is one of possibilities and has a mechanism for explosion after penetrating the target which is known as “Behind Armor Effect.”

With this in mind, highly reactive materials have been considered as coating materials on the Cu liner in order to improve both the penetration depth and destructiveness of the liner. In this regard, the integrated work was done based on the following procedures. Pure aluminum coating material was manufactured via the kinetic cold spray process. We have checked the effect of ARM(arrested reactive milling) for reactive materials using DSC(Differential Scanning Calorimeter), which will be used for modeling and simulation of reactive reaction mechanism. The single impact of an Al particle onto an Al substrate with a high velocity was simulated by applying finite element modeling (FEM) using commercial explicit code (ABAQUS). The equivalent plastic strain and temperature distribution of the particle and substrate were obtained from the simulation results and were correlated to the bonding and microstructural analyses of the kinetic-sprayed Al particles. The strain rate effect on the mechanical properties were obtained by compression test and Split-Hopkinson Pressure Bar(from 1900, 3300 s-1)[1]. The double-layer shaped charge liner was used and numerical analysis was carried out

using the measured data for stress strain relations. In addition, modeling and numerical simulation for double-layer shaped charge liner were carried out and generation mechanism for jet formation and penetration will be discussed. In this study numerical computation was done using the commercial software, AUTODYN. Also for understand the highly reactive material behavior during penetration of jet and slug we have used the MPM(Material Point Method) method[4] and numerically simulated the behind armor effect by including chemical reaction. We have also numerically investigated the individual particle fragmentation and explosion using extracted chemical reaction kinetics analysis and the particle-based MPM program implemented including the chemical reaction. Chemical reaction kinetics analysis was carried out for the numerical parameter extraction using experimental data of DSC for Al/Ni material through the theoretical and numerical methods. Also, numerical simulation of the explosion behavior after penetration was done using MPM particle based source programs with the extraction data parameters.

Mason has recently conducted experimental testing of bimetallic and reactive shape to investigate small scale bimetallic and reactive liners and to record the target deformation characteristics of larger scale reactive liners [5]. In this talk we will also discuss detailed experimental procedures and results for our reactive double-layer liners

Acknowledgement

This work was supported by an Agency for Defense Development (ADD) grant funded by the Korean government (MOST) (No. 611155-911084002).

References

[1] K. Kim, C. Lee, H. Hun and K. Lee: *Materials Transactions*, 56(4), (2015) , pp605-609.

[2] D. Hasenberg: “Consequences of Coaxial Jet Penetration Performance and Shaped Charge Design Criteria,” Master Thesis, Naval Postgraduate School, (2010).

[3] S. Kim, S. Mun, K. Lee, C. Lee and S. Lee: *Materials Science Forum*, 767, (2014) pp52-59.

[4] YP Lian, X Zhang, X Zhou, S Ma, YL Zhao*: International Journal of Impact Engineering*, (2011), pp 238-246.

[5] J. S. Mason, “Experimental Testing of Bimetallic and Reactive Shape Charge,” Master Thesis, in Mechanical Engineering in the Graduate College of the University of Illinois at Urbana-Champaign, (2010).

ID139: Molecular-Dynamic Simulation of Nanocrystal Structure Evolution Under Shock Loading

L. A. Merzhievsky[1,a] , I.F. Golovnev [2], E.I. Golovneva [2]

[1]Lavrentiev Institute of Hydrodynamics SB RAS, Novosibirsk, 630090, Russia

[2]Khristianovich Institute of Theoretical and Applied Mechanics SB RAS, Novosibirsk, 630090, Russia

[a]merzh@hydro.nsc.ru

Methods of molecular dynamics occupied an important place in the investigation o microstructural mechanisms of deformation and fracture crystal materials. Using of these methods allows us to study microstructural mechanisms of irreversible deformation over time, which is impossible for available experimental methods. As is shown in [1, 2], this is the major advantage over the other methods and models of dynamic deformation. Particular attention is paid to nanocrystalline materials. It is known that conventional microstructural and nanostructural materials differ greatly in mechanical, physical, chemical and thermodynamic properties. Calculations show that this is due to the difference in the ratio of surface and bulk atoms.

In this paper we present the results of molecular dynamics simulations and studies of the peculiarities of the process of uniaxial shock (short - time) compression copper nanocrystals. The modified version of the commonly used Voter A.F. potential EAM [3] is used to describe the interatomic interaction. The calculations used velocity modification algorithm of the Verlet of the second-order accuracy, with the time pitch of 10^{-16} s. The energy calculation error in the closed system within 50 ps (500000 time pitches) did not exceed 10^{-5} %. The calculation results were analyzed by the method of meso-analysis of system developed by the authors[4].

The calculations include a detailed analysis of changes in density, velocity of the centers mass, temperature and potential energy of mesovolume at different times. In calculations are established intervals of shock wave amplitudes, which are different mechanisms of energy dissipation are realized. It is shown that there is a limit external load, above which in a nanocrystal with a perfect crystal lattice is an abrupt change in the energy absorption mechanism. In the calculation are established the formation of a plurality of structural defects, including similar dislocations.

The findings show that in plastic wave amorphization of structure occurs. The

process is accompanied by the emergence of a rotating component of the deformation. Calculations have allowed to determine the critical value of the loading pulse amplitude at which loss of stability the crystal lattice occurs.

It was further investigated the influence of the size of the nanostructures (nanocrystals) on the peculiarities of the process of uniaxial compression. In these calculations varied transverse dimensions of the crystal, which have determined the ratio of the surface and bulk atoms. The following cross-sectional dimensions were selected (the number of cells in the direction of crystal axes YZ): 5x5, 7x7, 10x10. In the compression direction along the X-axis the number of crystal cells were fixed at 50 or 200.

It was found that an increase in the transverse dimension changes the nature of the deformation (movement mesovolume) in the field of shock compression. There is a reduction of rotary components (vortex intensity, the angular momentum in the analysis of allocated cells) and the relative contribution of the rotational energy into internal energy of the nanocrystal. With the growing of the transverse dimension the temperature jump in a rotational wave is reduced. Thus, these results show that the shock wave structure essentially depends on the size of the nanocrystal. At the same time the total specific energy of rotational motion (energy per atom) is weakly dependent on the size of the nanocrystal.

The research was supported by the RFBR grant N 16-01-00468

References

[1] L.A. MerzhievCsky: *Materials Science Forum*, Vol. 767, (2014), pp 101–108.

[2] L. A. Merzhievskii: *Combustion, Explosion, and Shock Waves,* Vol. 51, No. 2, (2015), pp 69–283.

[3] A.F. Voter: *Los Alamos Unclassified Technical Report* # LA-UR-93-3901, (1993).

[4] Golovnev I.F., Golovneva E.I., Merzhievsky L.A., Fomin V.M., and Panin V.E.: *Phys. Mesomech.*, Vol. 17, No. 4, (2014), pp 41–48.

ID140: The Auxetic Cellular Structures in Impact Applications

Zoran Ren[1, a] , Nejc Novak[1, b] , Matej Vesenjak[1, c]

[1]University of Maribor, Faculty of Mechanical Engineering, Slovenia

[a]zoran.ren@um.si, [b]nejc.novak5@um.si, [c]matej.vesenjak@um.si

Materials with auxetic internal cellular structure are modern materials which have some unique and superior mechanical properties. As a consequence of the structural deformation of their internal cellular structure they exhibit a negative Poisson's ratio, i.e. they significantly increase in volume when stretched and vice versa, Fig. 1.

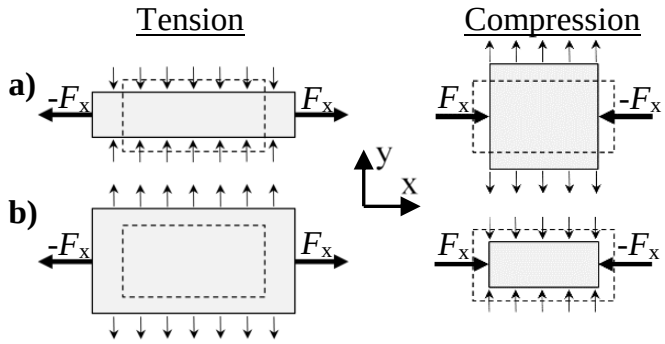

Fig.1 Non-auxetic a) and auxetic b) behaviour during tensile and compressive loading (dashed lines – undeformed geometry)

The auxetic materials have improved shear performance (increased shear modulus), stiffness, fracture toughness, damping, sound and energy absorption due to negative Poisson's ratio, which makes them particularly useful for many special applications [1]. These properties can be further tailored by using variable cell geometry and density distribution, which can be achieved with functionally graded porosity of the auxetic cellular structure.

In case of impact loading, the non-auxetic materials tend to move away from the impact area, while in case of auxetic materials they move towards the impact zone. This leads to densification of the auxetic materials in the impact zone and therefore raises their indentation resistance. For this reason they are being increasingly used in body and vehicle armor applications in sandwich plates for ballistic protection in combination with other materials [2].

New advanced additive manufacturing techniques provide means to fabricate the next generation of auxetic materials with functionally graded porosity, which can be

adapted to the requirements of a particular engineering application by computational simulations and topological optimization techniques. Such specifically designed internal cellular structure of auxetic materials would provide the best desired mechanical response to particular loading conditions. This response can for example result in constant deceleration of impacting projectile or constant reaction force on structures under impact, which is very useful for different applications in defense engineering and crashworthiness.

The auxetic cellular materials and structures show huge potential to become important light-weight structural materials of the future with further advances of additive manufacturing technologies and special designs of their internal cellular structure.

The presentation will first give some information on the known types of auxetic structures and their particularities and will then focus on some early research results of developing new and optimized auxetic structures for impact application by means of advanced computational simulations.

References

[1] Novak, N., Vesenjak, M., Ren, Z. (2016). Auxetic Cellular Materials - a Review. Journal of Mechanical Engineering, vol. 62, no. 9, pp. 485-493.

[2] Imbalzano, G., Tran, P., Ngo, T.D., Lee, P.V.S. (2015). A Numerical Study of Auxetic Composite Panels under Blast Loadings. *Composite Structures*, vol. 135, pp. 339-352.

ID141: The Technique of Magnetically Applied Pressure-shear and its Applications in Direct Measurement of Material Strength

Guiji Wang**, Binqiang Luo, Xuemiao Chen, Fuli Tan, Jianheng Zhao and Chengwei Sun

Institute of Fluid Physics, China Academy of Engineering Physics,64 Mianshan Road, Youxian Borough, Mianyang, Sichuan Province 621900, China

Strength of material is an important physics parameter to characterize the properties of materials, and it is used to describe the ability to resist deformation of matter under shear, which is one of the main factors affecting the dynamic behaviors of materials at high loading pressures and strain rates. Therefore, it is very significant in academy and engineering applications. In this paper, a technique of magnetically applied pressure-shear was developed to directly measure strength of materials under ramp wave loadings based on the compact pulsed power generator CQ-4 and 10 T quasi-static magnetic field generator.

In theoretical and numerical analyses, the relation of yield stress and deviatoric stress was obtained at uniaxial pressure and one dimensional transverse shear loadings and supposition of material yield behavior satisfying the Von-Mises criterion, which is $Y = \sqrt{3}S_{xy}$ when Sxy reaches yield surface and Sxx decreases to zero. Then a 3D LS-DYNA hydrodynamic software was used to simulate the dynamics response of alumina under ramp wave pressure-shear loading based on magnetically applied pressure-shear models. The calculated results verified those of theoretical analyses and both agreed very well.

In experiments, a multi-point transverse laser interferometer PDV (Photonic Doppler Velocimetry) was developed to measure longitudinal and transverse velocities of samples. Finally, three types of alumina and one polyethylene were tested on CQ-4. Their dynamic strength were obtained at different loading pressures up to 20GPa.

All theoretical and experimental results show that the technique of magnetically applied pressure-shear is a good tool to directly measure strength of materials under dynamic loadings. Some typically calculated and experimental data and results are presented in Figure 1 to Figure 4.

** Corresponding author: Guiji_wang@caep.cn .

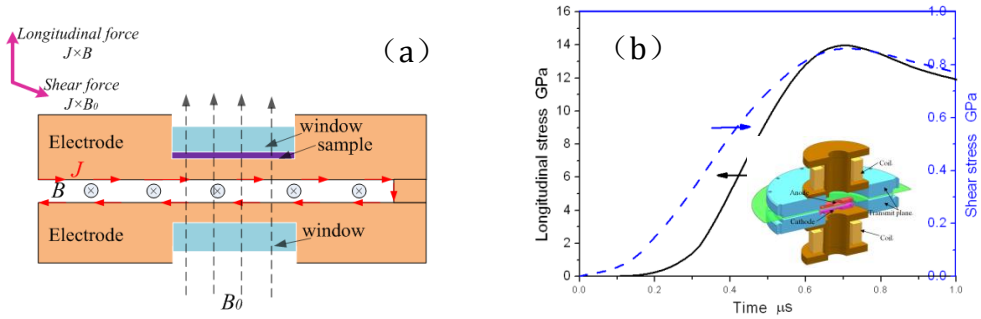

Figure 1. The working principle schematic of magnetically applied pressure-shear (a) and typical loading pressure histories on CQ-4 (b)

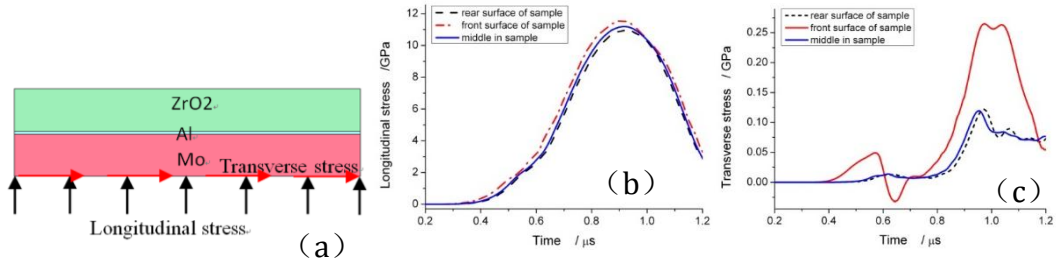

Figure 2. Calculated model (a), profiles of longitudinal stress at sample position(b) and profiles of transverse stress at sample position(c)

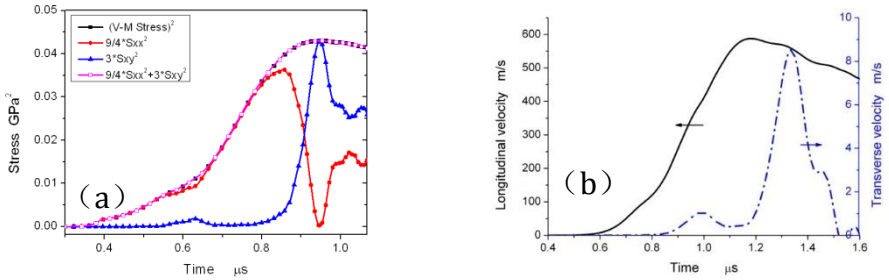

Figure 3. Relation of deviatonic stress and yield stress (a) and Longitudinal and transverse velocity at ZrO_2 window rear surface (b)

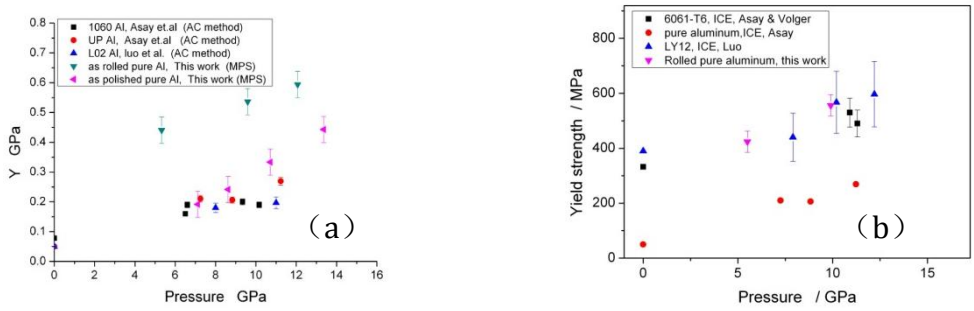

Figure 4. The experimental data of strength of pure alumina (a) and Ly12 alloy aluminum (b) measured by the technique magnetically applied pressure-shear on CQ-4

ID142: Study on Metal Forming Using the Underwater Shock Wave by Metal Wire Discharge

Kazuki Umeda[1, a] , Hirofumi Iyama[2, b], Masatoshi Nishi[2, c]

[1]Production Systems Engineering Course, National Institute of Technology, Kumamoto College, 2627 Hirayamashin-machi, Yatsushiro, Kumamoto 866-8501, Japan

[2]Department of Mechanical and Intelligent Systems Engineering, National Institute of Technology, Kumamoto College, 2627 Hirayamashin-machi, Yatsushiro, Kumamoto 866-8501, Japan

[a]ap5495umed@g.kumamoto-nct.ac.jp

[b]eyama@kumamoto-nct.ac.jp

[c]nishima@kumamoto-nct.ac.jp

The purpose of this study is to establish a technique free forming of the metal plate using underwater shock wave. In this research, the underwater shock wave is generated by applying high voltage to the metal thin wire in underwater, and the metal plate is transformed to a predetermined shape. The experimental device for metal forming is shown in Fig.1. Experimental device is constituted by the pressure vessel and the blank holder and the die, using a copper plate with a thickness of 0.5 mm, diameter of 140 mm. Numerical simulation were performed using ALE (Arbitrary Lagrangian Eulerian) method[1]. Numerical simulation model is shown in Fig.2. Explosive and water Euler area, the metal plate and the vessel was simulated as Lagrange area.

On simulation results, velocity vector of the metal plate is shown in Fig.3. The process propagation of the underwater shock wave and deformation process of the metal plate were confirmed. Forming shape of copper plate is shown in Fig.4. As a result of having performed shape measurement of the test pieces after the experiment, test pieces were formed as the shape of the curved surface that the height is maximum in the center. The whole test piece have become thinner. In addition, the thickness strain of the center was larger.

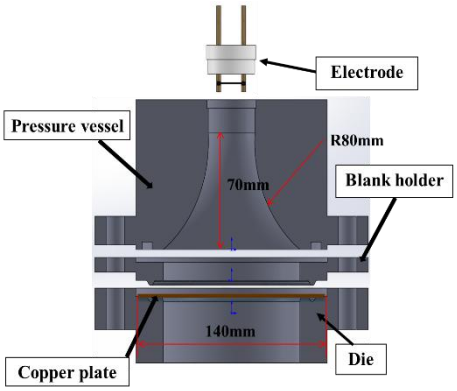

Fig.1 Experimental device.

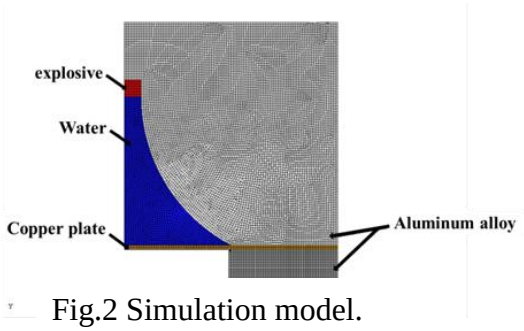

Fig.2 Simulation model.

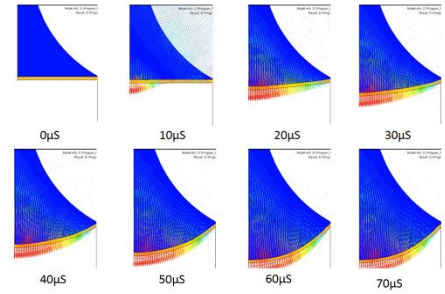

Fig.3 Velocity vector change.

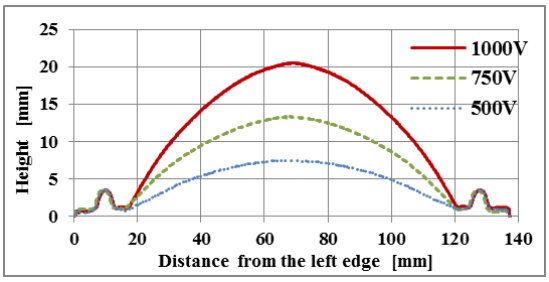

Fig.4 Forming results of the copper plates.

References

[1] N. Aquelet, et al.，Euler-Lagrange coupling with damping effects: Application to slamming problems，vol.195 (2006).

ID143: An Investigation on Explosive Forming of Magnesium Alloy Plate

Hiroko Sakaguchi[1,a], Masatoshi Nishi[2,b], Hirofumi Iyama[2,c], Masahiro Fujita[3], Liqun Ruan[3]

[1]Production Systems Engineering Course, National Institute of Technology, Kumamoto College, 2627 Hirayamashin-machi, Yatsushiroshi, Kumamoto 866-8501, JAPAN

[2]Department of Mechanical and Intelligent Systems Engineering, National Institute of Technology, Kumamoto College, 2627 Hirayamashin-machi, Yatsushiroshi, Kumamoto 866-8501, JAPAN

[3]Kumamoto University, 2-39-1 Kurokami, Chuo-ku, Kumamoto 860-8555, JAPAN

[a]ap5510saka@g.kumamoto-nct.ac.jp, [b]nishima@kumamoto-nct.ac.jp,

[c]eyama@kumamoto-nct.ac.jp

It is important to conserve energy in the transportation industry, such as aircraft and railroad [1]. One of the possibilities for energy saving is to use Magnesium alloys due to the advantages in terms of strength-to-weight ratio. Magnesium alloys, however, harden with any type of cold work and therefore it is not easy to perform the cold-worked with the usual plastic forming method.

Explosive forming method is one of the plastic forming methods with a specific forming mechanism. A specimen plate is accelerated by pressure of underwater shock wave generated by explosive and then it collides with a die at high velocity. The work pieces made by explosive forming method are very precious in shape and size of a die. Therefore, this study investigates plastic forming method of Magnesium alloys by using explosive forming method.

Since a concave die is often used in explosive forming method, the specimen plate which has a lower plastic limit often cracks at the center of the plate. Therefore, this study uses a convex die in the shape of a circular truncated cone shown in Fig. 1. The advantage of a convex die is the low elongation because the center of the plate is supported by the die during the high pressure generated by explosive.

Schematic drawing of experimental device is shown in Fig. 2. The cover plate (Al

plate with a thickness of 0.3mm and a diameter of 84mm) is set on the specimen plate (AZ31 plate with thickness of 0.3mm and a diameter of 50mm) to avoid cracks on the specimen plate and coated with Molybdenum (lubricant) to reduce joining of the two surfaces. It is necessary for explosive forming method to keep high vacuum between the die and the specimen plate because the presence of air results in adiabatic compression. Therefore, the vacuumed experimental device is covered by plastic tapes and then sunk in the water chamber. The experimental conditions are as follows: dimension of the dieφ = 20mm, h = 15mm,θ = 30deg, charge of SEP explosive W= 3~6g, distance between explosive and the cover plater d= 40~ 80 mm.

Figure 3 shows experimental results which represents the unsuccessful cases. Depending on the experimental conditions, there still remain problems such as the wrinkle at outer circumference and the cracks near the shoulder of die. This study further clarifies the optimal conditions by experimental and numerical simulations.

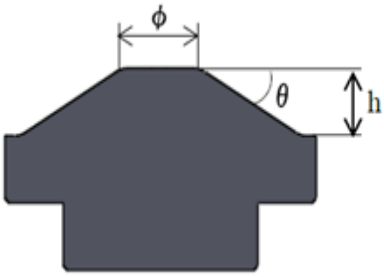

Fig.1 Schematic view of

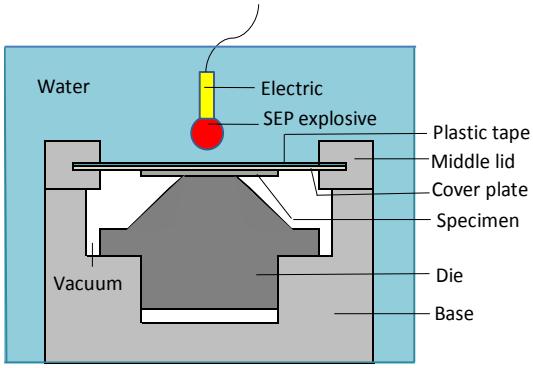

Fig.2 Schematic view of experimental

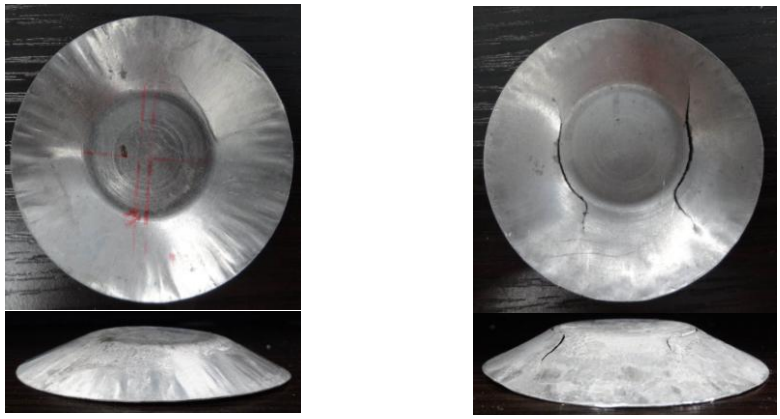

Fig.3 Experimental results.

Reference

[1] Yumi C.D., You B.S., Lee J.S., and Kim W.C.: *Mater.Trans.* 45 (2004) pp.3018-3022.

ID144: Experiment Study of Electrical Iron Wire Explosion Underwater

Xin Gao[1,a] , Naoaki Yokota[2], Hayato Oda[2], Shigeru Tanaka[2], Kazuyuki Hokamoto[2], Pengwan Chen[1,b]

[1]State Key Laboratory of Explosion Science and Technology, Beijing Institute of Technology, Beijing 100081, China

[2]Institute of Pulsed Power Science, Kumamoto University, Kumamoto, Japan

[a]Xin.Gao0522@gmail.com,

[b]pwchen@bit.edu.cn

Electrical wire explosion refers to the phenomenon that when a strong current produced by the discharge of a capacitor passes through a wire, the wire is evaporated in burst with bright flash by joule heating [1]. During this progress, the electrical wire explosion has strong mechanical, light, heat and electromagnetic effects. So it is widely used to synthesize nano particles, to provide shock wave, to study plasma physics, etc [2,3].

In this study, the pure iron wires with a diameter of 0.25 mm are exploded to study the iron wire explosion underwater and the relationship between the charging voltages and the products in the experiments. The charging voltages in the experiments are in the range of 8~20 kV. The current and voltage datum are recorded and the products are recovered and dried. The iron and different iron components ultra-fine particles are synthesized by electrical iron wire explosion underwater. As shown in Fig. 1a, the current peaks and voltage peaks are stronger with higher charging voltage. And the second current peak indicates a strong arc plasma is measured [1,4]. The strong arc plasma contributes to more active atoms and chemical reaction, which results in multiple iron components (as illustrated in Fig 1b).

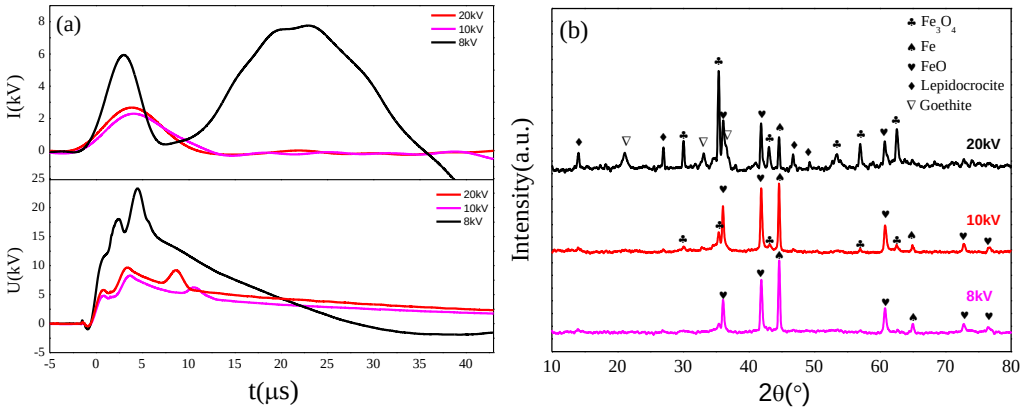

Fig.1 a) the typical current and voltage plots of the experiments, b) the XRD patterns of the different samples.

Acknowledgment: This study is funded by Internatioanl Graduate Exchange Program of Beijing Institute of Technology

References

[1] Y. A. Kotov: *J NANOPART RES* 5(2003), pp539-550.

[2] W. Kim, S. Lee, C. Suh, S. Cho, T. Ryu, J. Park, I. Shon: *Mater. Trans.* 51(2010), pp2125-2128.

[3] N. Wada, K. Akiyoshi, K. Morita, K. Hokamoto: *Ceram. Int.* 39(2013), pp7927-7933.

[4] C. S. Wong, B. Bora, S. L. Yap: *Current Applied Physics*, 12(2012), pp1345-1348.

ID146: Dynamic Mechanical Behavior of C/SiC Composites：Micro-structures and Fracture Mechanisms

T. Li[1], Y.L. Li[1]* , J.J. Mo[2] , S.N. Luo[3]

[1] Fundamental Science on Aircraft Structural Mechanics and Strength Laboratory, Northwestern Polytechnical University, Xian 710072, Shaanxi, P. R. China

[2] The Peac Institute of Multiscale Sciences, Chengdu, Sichuan 610207, P. R. China

[3] Institute of Fluid Physics, China Academy of Engineering Physics, Mianyang 621900, Sichuan, PR China

Abstract: Components of the carbon fiber-reinforced SiC-matrix composites, or C/SiC composites, are mapped with scanning electron microscope (SEM) and X-ray computed tomography, including C fibers and fiber bundles, SiC matrix, and inter- and intrabundle voids. Dynamic loading is applied by split Hopkinson pressure bar, gas gun and electrical gun at strain rates of 10^2 - 10^3 s^{-1}, and the recovered specimens are examined by SEM. A microstructure-based modeling is developed to simulate micro damage evolution with finite element method. For the in-plane compressive loading, two dynamic fracture modes illustrated by high-speed photography are actually induced by inhomogeneous micro-structures. One fracture mode promoting the toughness significantly (increase of 35%), mostly without strength decrease, provides a promising way for micro-structure optimization of C/SiC composites. For the out-of-plane tensile loading, failure involves delamination, fiber pullout and fiber breaking. In contrary to normal solids, dynamic tensile or spall strength decreases with increasing impact velocities, owing to compression-induced pre-damage before subsequent tensile loading. For hypervelocity impact loading, the distribution of debris clouds shows “three zones” mode, forming with different mechanisms, and demonstrates that there is a high-energy powdering column in the entre zone. Furthermore, the damage induced by hypervelocity impact significantly reduces the strength of C/SiC composites.

Key words: C/SiC composites, micro-structures, fracture mechanisms

ID147: High Resolution Numerical Simulation of Explosion and Impact Problems

Cheng Wang

State Key Laboratory of Explosion Science and Technology, Beijing Institute of Technology, Beijing 100871, P.R. China

Abstract: Explosion and impact are nonlinear problems where a variety of media, such as gas, solid and liquid, strongly interact under high speed, high temperature and high pressure conditions, formidable challenge is imposed on the theoretical and experimental research. Due to such advantages as security, confidentiality, design flexibility, environment and process controllability and high cost-effective ratio, numerical simulation becomes the main approach to investigate such problems. This paper introduces in detail the researches on high resolution computations of explosion and impact problems and multi-medium interface treatment conducted by the authors in recent years. Based on real ghost fluid method (RGFM) method and Level Set method, the computational method that can address high density and high pressure ratio is proposed. High order finite difference weighted essentially non-oscillatory (WENO) method are generalized to solve the explosion problems with chemical reaction source terms. Based on this, a high precision parallel computation code was developed for explosion and impact problems. The code can simulate problems such as gas detonation, initiation of condensed-phase explosives, detonation diffraction, shock wave interaction with bubbles, underwater explosion, jet formation and penetration. By constructing artificial solutions and comparison with experimental results, the accuracy and computation results of the computation method are validated and verified.

ID148: Three Dimensional High Order Numerical Investigation on Explosions

Tao Li, Cheng Wang

State Key Lab of Explosion Science and Technology, Beijing Institute of Technology
Beijing, 100081, China

Abstract: Based on the double shockwave approximation procedure, combining with RGFM and level-set method, local Riemann problem for strong nonlinear equations of state such as JWL equation of state was constructed and then solved to suppress successfully the numerical oscillation caused by high-density ratio and high-pressure ratio across the explosion product-water interface. A fifth order WENO finite difference scheme and the third-order TVD Runger-Kutta method were utilized for spatial discretization and time advance, respectively. A novel enclosed-type MPI-based parallel methodology for RGFM procedure on uniform structured meshes was presented to realize the parallelization of three dimensional RGFM code for air blast and underwater explosion, which had dramatically improved the practical scale of computing model. For air blast cases, the peak overpressure at same location and same proportional distance of gauge points for both TNT and aluminized explosives was monitored and analyzed for revealing the rule of peak pressure propagation and the influence of aluminum powder combustion on peak overpressure of explosion wave. The overall process of three dimensional bubble pulsation generated by underwater explosion of both explosives mentioned above was successfully simulated with high order numerical scheme. The numerical results obtained indicated that the attenuation of explosion wave formed by aluminized explosives is slower than that caused by TNT. The influence of aluminum powder combustion on bubble pulsation was also investigated by comparing TNT with aluminized explosives.

Keywords: underwater explosion, Air blast, WENO scheme, RGFM, parallel computation

ID149: Dynamic Response of Fiber-Composite-Reinforced Shell Structure Subjected to Internal Blast Loading

Yundan Gan, Renrong Long, Qingming Zhang*, Pengwan Chen, Shaolong Zhang

State Key Laboratory of Explosion Science and Technology, Beijing Institute of Technology, Beijing 100081, China

*Corresponding author:

E-mail: qmzhang@bit.edu.cn

Abstract: In this study, we report the analysis of a dynamic response process of a fiber-composite-reinforced shell when subjected to internal blast loading of different TNT equivalent by using a three-dimensional digital image correlation method. And it was compared with the dynamic response of the metal shell with the same TNT equivalent and the same surface density. We received the relationship between dynamic deformations and the sizes of the two shells under different TNT equivalence. Through comparison of the results, it was shown that the response process of the fiber-composite-reinforced shell was much more complex than that of the metal shell. Our experimental results suggest that the shock wave intensity, the material mechanical properties and the structure symmetry had important influences at different stages of the structural dynamic response. Fiber composites with high strength restricted the structural deformation extent and deformation rate. In addition, the interaction between fiber composite and metal liner reduced the probability of structural damage caused by the energy concentration. This work provides important insights for the design of cylindrical explosion vessels.

Keywords: Fiber-composite-reinforced shell, Blast load, Dynamic responses, Digital image correlation

ID150: Experiment Study on the Explosive Welding of Al/Cu Composite Plates

Yuan Yuan[1, a], Pengwan Chen[1, b], Qiang Zhou[1], Erfeng An[1], Jianrui Feng[1]

[1]State Key Laboratory of Explosion Science and Technology, Beijing Institute of Technology, Beijing 100081, China

[a]yuanyuan198406@163.com,

[b]pwchen@bit.edu.cn

Abstract: Explosive welding can be defined as the process of joining two or more material by the detonation of explosives. The most characteristic of explosive welding is that it can combine same, especially different metals tightly, simply and quickly. In this investigation Aluminum alloys 2024/Copper T2 composite plates were obtained successfully by the method of explosive welding. The effect of annealing on the interface microstructures of the composite plates was investigated under different temperatures. Optical microscopy (OM), scanning electron microscopy (SEM) and microhardness test were performed. The results demonstrated that the Al/Cu composite plates were bonding well. The bonding interface of the Al/Cu composite plates was almost straight. The intermetallic compound Al_2Cu was found near the interface of the composite plates. Microhardness measurements showed that the hardness of the composite plates near to the interface was higher than other parts and the hardness of the whole composite plates was lower after annealing.

ID151: Experiment Study on the Shock Consolidation of Ti+Si Powders

Naifu Cui [1, a] , Pengwan Chen[1, b] , Qiang Zhou[1]

[1]State Key Laboratory of Explosion Science and Technology, Beijing Institute of Technology, Beijing 100081, China

[a]naifuc@163.com, [b]pwchen@bit.edu.cn

Abstract: The research on the explosive compaction of reactive powders is a hot issue. In this work, unreacted Ti-Si block with high compactness has been successfully fabricated under explosive-driven compaction process. The precursors of Ti-Si powder with different stoichiometric ratios undergo pre-compaction shaping by hydraulic press and then shock loading treatment by using low-detonation-velocity explosives of varying loading conditions. The results show that the chemical reaction between Ti and Si powders are partly initiated even under low detonation pressures, indicating extremely low reaction threshold in the Ti-Si system. Meanwhile, optimal experimental conditions are displayed as the initial pressing compactness degree of 61%, and shock pressure of 11GPa. A compactness of 97% is achieved in the synthesized Ti-Si block with the lowest reactivity.

ID152: The Diagnostic in the Characteristic Parameter of Plasmas Produced by Shaped Charge Jet

Qiong Hou, Qingming Zhang, Yijiang Xue, Yangyu Lu, Cheng Shang

State Key Laboratory of Explosive Science and Technology, Beijing Institute of Technology, Beijing 100081, China

Abstract: Shaped charge jet, one of three experimental methods to obtain hypervelocity impact, has been widely used on the warhead in various of weapons. When the metallic material is under hypervelocity impact, the plasma is produced. In this paper, the optimized structure of triple Langmuir probe is adapted to diagnose the plasma which is generated while the shaped charge jet is penetrating on metal target. By changing the angle and the material kinds of shaped charge liner, the velocity of the shaped charge jet reaches to 3800m/s、5100m/s、6800m/s、7200m/s, respectively. The relation between the velocity of shaped charge jet and the comprehensive characteristic parameters of electron temperature and electron density of the plasmas is acquired. Multiple measuring points are arranged, at the same time, the velocity characteristics of plasmas are analyzed. The damage of the weapon system can be assessed by establishing the relationship between different velocities of shaped charge jet, or different materials of the shaped charge liner, and the characteristic parameters of plasmas.

Keywords: Plasma diagnostic, Damage assessment, Shaped charge jet, Characteristics parameter